Spring 4-17-2019

Physiological Effects of Climate Change on the American Lobster, Homarus americanus

Amalia M. Harrington
University of Maine

PHYSIOLOGICAL EFFECTS OF CLIMATE CHANGE

ON THE AMERICAN LOBSTER,

HOMARUS AMERICANUS

By

Amalia M. Harrington

B.A. University of San Diego, 2010

M.S. San Diego State University, 2014

A DISSERTATION

Submitted in Partial Fulfillment of the

Requirements for the Degree of

Doctor of Philosophy

(in Marine Biology)

The Graduate School

The University of Maine

May 2019

Advisory Committee:

    Heather Hamlin, Associate Professor of Marine Biology, Advisor

    Damian Brady, Assistant Professor of Oceanography

    Nisha Jayasundara, Assistant Professor of Marine Biology

    Paul Rawson, Associate Professor of Marine Biology

    Robert Bayer, Professor of Food and Agriculture

PHYSIOLOGICAL EFFECTS OF CLIMATE CHANGE

ON THE AMERICAN LOBSTER,

HOMARUS AMERICANUS

By Amalia M. Harrington

Dissertation Advisor: Dr. Heather Hamlin

An Abstract of the Dissertation Presented
in Partial Fulfillment of the Requirements for the
Degree of Doctor of Philosophy
(in Marine Biology)
May 2019

Increases in anthropogenic input of carbon dioxide into the atmosphere have caused widespread patterns of ocean warming and ocean acidification. Both processes will likely have major impacts on commercial fisheries and aquaculture, with acidification posing a particular threat to many marine calcifying invertebrates. In the State of Maine, commercial fisheries landings and a growing aquaculture industry have a combined value in excess of $600 million, 75% of which is sustained by marine calcifiers. Moreover, the American lobster (*Homarus americanus*) supports the most economically valuable fishery in the Gulf of Maine and Atlantic Canada. Previous research has documented a strong link between lobster biology and ocean temperature, but it is unclear how *H. americanus* will respond to a rapidly changing environment. Additionally, previous efforts have focused primarily on the direct effects of a changing climate on lobsters (i.e., changes in growth, survival, and calcification), with little emphasis placed on the potential for sublethal risk factors (e.g., sub-cellular changes) to impact the population.

In this dissertation, I explore the effects of increasing ocean temperatures and acidification on *H. americanus* to understand how environmental changes can alter the health and physiology in multiple life stages of marine calcifying invertebrates. In Chapter 1, I introduce the global patterns and effects of climate change on marine calcifiers and review the current state of knowledge of my study species. In

Chapter 2, I discuss how exposure to warming conditions impacts larval development, with a focus on potential trade-offs between enhanced growth and developmental instability. In Chapter 3, I continue to explore the sublethal impacts of warming on larval lobsters by examining changes in gene expression patterns in postlarvae exposed to varying temperatures during development. Chapter 4 explores how short-term exposure to acidified conditions impacts subadult (50 – 65 mm carapace length) lobster thermal physiology, hemolymph chemistry, and stress levels, a relatively understudied yet crucial life history stage. Finally, Chapter 5 summarizes the overarching themes of the dissertation, and concludes by providing suggestions for future research efforts.

ACKNOWLEDGEMENTS

TABLE OF CONTENTS

LIST OF TABLES

LIST OF FIGURES

CHAPTER 1

INTRODUCTION

1.1. Ocean Warming and Acidification

Increases in anthropogenic input of carbon dioxide into the atmosphere from the mid-20th century onward have resulted in global changes in climatic conditions, including widespread patterns of ocean warming and ocean acidification (IPCC, 2013). Global ocean surface temperatures have increased by 0.11°C per decade from 1971 – 2010, and the pH of surface ocean waters has decreased (i.e., become more acidic) by 0.1 units since the beginning of the Industrial Revolution (IPCC, 2013). Temperatures across the world's oceans are increasing rapidly (Reid and Beauguard, 2012), and some of the most accelerated rates of warming are occurring in the Northwest Atlantic (Sherman et al., 2009; Taboada and Anadón, 2012; Pershing et al., 2015). For example, the Gulf of Maine (GoM) region is warming at a rate of 0.4°C per decade (Thomas et al., 2017), which is faster than 99% of the global oceans (Pershing et al. 2015). Moreover, the frequency of occurrence of extreme temperature events has increased over the second half of the 20th century (Hansen et al., 2012; Smale et al., 2019). Most recently, the 2012 ocean heat wave was the largest and most intense warming event recorded over the last 30 years in the Northwest Atlantic (Mills et al., 2013). This heat wave resulted in sea surface temperatures that were at least 1.1°C above the 1950 – 2014 climatology for the Northwest Atlantic, and greater than 3°C above the climatological record for the GoM (Mills et al., 2013; Scannell et al., 2016). Bottom water (100 – 200 m) temperatures in the region were also elevated following the 2012 ocean heat wave, but it is unclear if this was an anomaly, or reflective of a more drastic warming trend, due to a paucity of deep-water sampling (Koopman et al., 2014).

Since many organisms native to the GoM are considered cold-water species, their growth, survival, and distribution are expected to be directly impacted by ocean warming. For instance, the GoM is the southern limit of the northern shrimp (*Pandalus borealis*), and warming conditions hinder pelagic larval development and subsequent recruitment into the GoM stock (Richards et al., 2012). Similarly,

hatching success of the dominant copepod of the GoM, *Calanus finmarchicus*, is significantly reduced at temperatures above 22°C, and eggs produced by GoM copepods are less heat tolerant than those collected from more southern latitudes (Preziosi and Runge, 2014). Ocean warming may also indirectly affect the species of the GoM by altering species distributions (Lucey and Nye, 2010; Kleisner et al., 2016). Species associated with deep-water habitats are moving deeper to track cooler bottom water temperatures, but shallow-water species are generally moving into shallower areas (Kleisner et al., 2016). Warming can therefore drastically alter the community composition of native species within the GoM, while allowing non-native warm-water species to expand into the region (e.g., black sea bass, tile fish, trigger fish: Nye et al., 2009; Lucey and Nye, 2010; Kleisner et al., 2016).

Underlying these drastic region-wide warming trends is a natural and steep latitudinal thermal gradient along coast of New England and Atlantic Canada that creates sharp along-shore environmental gradients in the coastal waters of the GoM (Longhurst, 1998). Research in other study systems suggests that species may compensate for stressors along similar environmental gradients through alterations in life history traits, behaviors, and/or physiological responses via co- or counter-gradient adaptation (Conover and Schultz, 1995). For instance, in the genera *Chlorostoma* (formerly *Tegula* – marine snails), *Petrolisthes* (porcelain crabs), and *Mytilus* (blue mussels), species that occupy more thermally stressful (warmer) environments generally exhibit a greater thermal tolerance compared to colder-water congeners (Tomanek and Somero, 1999; Stillman and Somero, 2000; Braby and Somero, 2006). Cold-water species also demonstrate less plasticity in their response to thermal stress compared to warm-water congeners (Tomanek, 2002), which may play a role in setting species' distribution limits. Counter-gradient variation and adaptation have been examined in some marine invertebrates of the GoM (e.g., the salt marsh fiddler crab, *Uca pugnax* – Sanford et al., 2006; the invasive green crab, *Carcinus maenas* – Tepolt and Somero, 2014), but the complexity associated with the abiotic environment in the region make it difficult to construct generalities. It is also unclear if the biota of the GoM will be able to use these adaptive means to effectively keep pace with the region's rapidly changing climate.

Coinciding with global ocean warming is the ongoing reduction in the pH of the world's oceans, ocean acidification (OA), which is caused primarily through the uptake of carbon dioxide from the atmosphere (IPCC, 2013). As carbon dioxide dissolves in the ocean, it reacts with water to form carbonic acid (H_2CO_3), which can then disassociate into bicarbonate (HCO_3^-), carbonate (CO_3^{2-}), and hydrogen (H^+) ions. The increase in the concentration of H^+ reduces pH, causing surface waters to become more acidic. OA also reduces the saturation state of seawater with respect to aragonite, high-magnesium calcite, and low-magnesium calcite, carbonate minerals used to construct hard parts in marine calcifying invertebrates, through the alteration in the concentration of carbonate ions (Ries et al., 2011). Decreases in both seawater pH and carbonate mineral saturation state play a role in reducing organismal calcification rates, although there is still much debate in the literature as to which process is the main driver (see Cryonak at al., 2016a, 2016b; Waldbusser et al., 2016). However, OA has been linked to direct negative effects on marine calcifying organisms, including reduced growth and calcification, and may also result in reduced reproductive output and ultimately death (Kroeker et al., 2010; Browman, 2016). OA may also disrupt olfaction (Kim et al., 2016), behavior (Dissanayake and Ishimatsu, 2011), internal chemistry (Dissanayake et al., 2010), immune response (Wang et al., 2016), and energy allocation (Pan et al., 2015) in a number of species. Waters off of New England and Nova Scotia are particularly at risk for acidification due to the region's low buffering capacity resulting from high freshwater input and low temperatures, which dilutes both alkalinity and dissolved inorganic carbon (Gledhill et al., 2015). Ongoing research by the Northeast Coastal Acidification Network (NECAN) has identified regions where high nutrient and freshwater inputs create corrosive plumes of water capable of not only reducing calcification rates and destroying shells of organisms, but also of producing high rates of productivity that result in a buildup of carbon dioxide (Gledhill et al., 2015). However, the full local and global consequences of acidification are as of yet unknown (Browman, 2016), and inconsistent trends across taxa (Hendriks et al., 2010; Whiteley, 2011; Kroeker et al., 2013; Wittmann and Pörtner, 2013; Przeslawski et al., 2015), as well as ontogeny (Ceballos-Osuna et al., 2013; Small et al., 2015, 2016; Davis et al., 2016, 2018), make it difficult to construct generalizations.

1.2. Life History of the American Lobster

The American lobster (*Homarus americanus*) is an omnivorous, nocturnal forager that inhabits the waters off the Atlantic Coast of North America from Newfoundland, Canada, in the north, to North Carolina, USA, in the south (Herrick, 1911). Although known to dwell in hard-bottom habitat ranging from the sublittoral to a depth of 480 m, *H. americanus* is most common at depths between 4 – 50 m (Holthius, 1991). Generally, *H. americanus* resides singly within shelters; however, cohabitation does occur during the act of mating (Karnofsky et al., 1989). During this process, a premolt female selects a male to mate with and performs a number of pheromone-mediated, ritualistic behaviors within his shelter to form a pair bond (Atema et al., 1979). Within a few hours (but up to days), the female molts and the male deposits a spermatophore into a receptacle on the female's soft body (Atema and Cobb, 1980). When ready to spawn, the female releases as many as 10,000 eggs from her ovaries, which are fertilized as they pass through the sperm receptacle before they are extruded onto her abdomen. She then carries her fertilized eggs using her pleopods for 10 – 11 months (Holthius, 1991). During this brooding period, females exhibit a seasonal migration from shallow (< 20 m depth) waters in the summer and fall, to deeper (> 200 m) waters in the winter and spring to maximize egg development (Campbell, 1986). Females then return to warm, shallow water to release their eggs where their offspring begin a complex life cycle comprised of various phases (further subdivided into stages: Lavalli and Lawton, 1996). The naupliar larval stage, a characteristic of crustaceans, is passed within the egg of a lobster and the form that is released is considered a prelarva. Hatching of eggs typically occurs at night in successive "batches" over the course of 15 – 31 days, with up to 1,950 prelarvae released per event (Ennis, 1975). The prelarval form quickly molts into the first of three pelagic larval stages (Stage I), all of which pass over a period of several weeks. All three larval stages are similar in morphology and behavior in that they are transparent with highly setose appendages; incapable of swimming with directed movements; and have a voracious appetite, preying upon larval forms of other species, fish eggs, and other lobster larvae (Herrick, 1911). It is not until a larva molts from the third stage (Stage III) to the postlarval (PL) phase that it resembles the adult lobster form, with the characteristic chelipeds and greenish-brown coloration.

In contrast to the larval phase, the PL phase is able to swim with clear direction and speed (Cobb et al., 1989). Postlarvae are negatively phototactic and spend less time at the surface as they swim down to the benthos (Herrick, 1911). As such, the PL phase marks the point of transition, or settlement, from the pelagic to the benthic realm in the life history of the American lobster (Lavalli and Lawton, 1996). Postlarvae are 4 – 5 mm carapace length (CL) in size (Lavalli and Lawton, 1996), making them vulnerable to intense predation pressure from crabs, shrimps, and fishes during and shortly after settlement (Wahle and Steneck, 1992; Sigurdsson and Rochette, 2013). Upon transitioning to the benthos, PL must find adequate shelter to enhance survival; however, not all habitat types provide sufficient protection. Although capable of burrowing into bare sediment (Herrick, 1911), settling in this habitat type only affords PL protection from non-burrowing predators (e.g., cunner *Tautogolabrus adspersus*). In contrast, rocky substrate with abundant crevices provides a refuge from both burrowing (e.g., mud crab *Neopanope texani*) and non-burrowing predators (Lavalli and Barshaw, 1986). Postlarvae are therefore highly substrate-specific, most often settling in cobble beds over bare sediment, a behavior that significantly reduces post-settlement mortality (Palma et al., 1998).

Once a PL settles and makes the transition to the benthos, it enters the juvenile phase. This phase is broken up into three stages, which are designated based on lobster size and behavior: 1) the shelter-restricted stage (5 – 14 mm CL, marked by a cryptic existence); 2) the emergent stage (15 – 25 mm CL, marked by limited movement outside of shelter); and 3) the vagile stage (25 – 50 mm CL, marked by aggressive behavior and increased foraging away from shelter; Wahle 1992; Wahle and Steneck, 1992; Lavalli and Lawton, 1996). Even up to its vagile juvenile stage, *H. americanus* is at risk of predation by a variety of demersal fishes and crabs (Wahle and Steneck 1992; Wahle et al. 2013). However, the risk of predation greatly decreases with increasing body size, and lobsters ≥ 60 mm CL are essentially immune to predators in areas where large-bodied fishes are rare (e.g., coastal, inshore locations – Wahle and Steneck, 1992). This size refuge from predators is obtained somewhere between the final two phases in the life history of the American lobster, the adolescent and adult phases (Lavalli and Lawton, 1996). The adolescent phase (or subadult; minimum size of 50 mm CL) is marked by physiological maturity (i.e.,

oogenesis and spermatogenesis occur in females and males, respectively), but not functional maturity. Functional maturity, or successful mating, marks the transition into the final, adult phase, which occurs when lobsters are > 50 mm CL (Lavalli and Lawton 1996). Subadult and adult lobsters have similar behavioral patterns, foraging at night and returning to shelter at dawn (Lavalli and Lawton 1996).

Today, only the smallest life stages are vulnerable to predators; however, historically, even adult lobsters were prey for a suite of demersal fishes, including cod *Gadus morhua*, pollock *Pollachius virens*, striped bass *Morone saxatalis*, sea bass *Centropristis striata*, and others. However, the extirpation of many groundfish released the larger size classes from predation pressure by demersal fishes, effectively restructuring the community composition. This relaxation in predation risk allowed lobster populations to greatly increase in abundance and resulted in drastic behavioral changes. Where groundfish have been depleted, the number of lobsters utilizing non-shelter providing habitat has increased (Hovel and Wahle, 2010; Wahle et al., 2013), and lobsters are able to obtain a size refuge from predators at a significantly smaller size (Wahle et al., 2013). Additionally, where lobster densities are high, cannibalism of small lobsters by larger conspecifics may act as a density-dependent population regulation mechanism (Oppenheim and Wahle, 2013).

1.3. Lobsters and Climate Change

The American lobster has a rich history as a fishery species. Total annual landings have fluctuated over time, but today *H. americanus* supports the most economically valuable fishery in the Gulf of Maine and Atlantic Canada (Steneck et al., 2011). Moreover, the fishery has managed to persist despite intense harvesting pressure over the last century, and it sustains higher landings today than ever before (Steneck and Wahle, 2013). Valued at >$400 million, more than 80% of all seafood harvested in the State of Maine comes from the lobster fishery, the perturbation of which could result in disastrous economic impacts (Steneck et al., 2011; Maine DMR, 2019). For example, the 2012 warming event induced earlier molting and migration of lobsters, triggering the onset of an early spring fishing season in the GoM. This resulted in an unexpected increase in lobster landings and a glut of USA lobster landings prior to the conclusion of the (typically) complementary Canadian winter lobster fishery, which

precipitated a historic drop in the price of lobster and caused an economic crisis in the fishery (Mills et al., 2013).

Homarus americanus has a preferred thermal niche of $16.5 \pm 4°C$ (Crossin et al., 1998), although waters spanning its geographic distribution vary along a 25°C gradient and result in variation in growth rate, age/size at maturity, morphology, and body size across the species' range (Factor, 1995; Wahle et al., 2013). Individuals may benefit from warmer temperatures via enhanced growth rates (Hadley, 1906), and those acclimated to temperatures > 20°C exhibit greater thermal tolerance, and thus greater survivability, at higher temperatures (Camacho et al., 2006). However, warm acclimation does not alter the maximum temperature lobsters can tolerate (Camacho et al., 2006), and prolonged exposure to temperatures outside of the preferred thermal range could lead to physiological stress, including erratic cardiac performance and gill ventilation rate (Mercaldo-Allen and Thurberg, 1987) and compromised function of the immune response (Dove et al., 2005). Moreover, warming events have been linked to mass mortality events and the spread of a shell disease epizootic across the southern extent of the species' range (Pearce and Balcom, 2005; Wahle et al., 2009).

Previous research exploring single-factor effects of climate change on the larval stages of *H. americanus* has demonstrated that exposure to acidified conditions reduces the growth rate, hinders development, and reduces survival (Keppel et al., 2012), and that exposure to warmer temperatures enhances development while increasing survival (MacKenzie, 1988; Barret et al., 2017). However, the combined effects of OA and warming produce drastically different results, suggesting no effect of OA on growth or survival, but significant reductions in survival while increasing oxygen demand under warming conditions (Waller et al., 2017). Due to its use of high-magnesium calcite, which is more soluble under acidified conditions, it is likely that OA will not negatively impact calcification rates in adult forms (Ries et al., 2009, 2011). However, previous efforts have failed to address the impacts of OA on the subadult (or adolescent) phase and have largely ignored potential sublethal risk factors of climate change in favor of addressing direct impacts. Therefore, to gain a better understanding of how ocean warming and acidification will impact this important species, this dissertation has two research objectives: 1) to

examine the effects of ocean warming on the physiology, developmental stability, and gene expression of larval lobsters; and 2) to explore how short-term exposure to acidified conditions affects subadult lobster thermal physiology, hemolymph chemistry, and overall stress level. By addressing multiple factors and their impacts across two distinct life history stages, the overarching goal of this dissertation is to utilize biological endpoints to evaluate climate change impacts on this commercially important species.

CHAPTER 2

EFFECTS OF TEMPERATURE ON LARVAL AMERICAN LOBSTER (*HOMARUS AMERICANUS*): IS THERE A TRADE-OFF BETWEEN GROWTH RATE AND DEVELOPMENTAL STABILITY?

2.1. Chapter Abstract

The American lobster supports the most economically valuable fishery in the Gulf of Maine and Atlantic Canada. Across much of its range, ocean temperatures have increased at rates faster than almost anywhere in the world. Studies of warming effects on larvae have largely focused on survival and development, but rarely have examined sublethal effects that could influence settlement and subsequent recruitment to the fishery. We explored how warming influences rate of development, survival, stress, and developmental stability of larval lobsters reared under four nominal temperatures: 14, 16, 18, and 22°C. Our study is the first to evaluate the use of fluctuating asymmetry as a biomarker for developmental instability in larval American lobster. We also recorded total hemocyte counts in postlarvae as an indicator of stress, a novel technique for work in larval lobster. Development proceeded significantly faster as temperature increased, and cumulative survival was significantly positively correlated with temperature. However, postlarvae reared under temperature extremes exhibited elevated hemocyte counts and had significantly lower levels of variance in midline asymmetry compared to intermediate temperature groups. Together, this suggests that warmer temperatures may facilitate faster growth at the expense of increased physiological stress and a loss of genetic diversity, potentially affecting the species' ability to adapt to changing environmental conditions. Fluctuating asymmetry could prove to be a useful bioindicator for population resilience.

2.2. Introduction

Temperatures in the world's oceans are increasing rapidly (Reid and Beauguard, 2012; IPCC, 2013), and some of the most accelerated rates of warming are occurring in the Northwest Atlantic (Sherman et al., 2009; Taboada and Anadón, 2012; Pershing et al., 2015). The Gulf of Maine region, for example, is warming at a rate of 0.4°C per decade (Thomas et al., 2017), which is faster than 99% of the global oceans (Pershing et al., 2015). American lobsters (*Homarus americanus*) occupy this region and

are a vital part of the marine ecosystem throughout the Northeastern United States and Canada (Holthuis, 1991). American lobsters have a preferred thermal niche of $16.5 \pm 4°C$ (Crossin et al., 1998), although waters spanning its geographic distribution vary along a 25°C gradient, producing variation in growth rate, age/size at maturity, morphology, and body size across the species' range (Factor, 1995; Wahle et al., 2013).

The American lobster sustains the most economically valuable fishery in the Gulf of Maine and Atlantic Canada (Steneck et al., 2011), and this industry is valued in excess of two billion dollars (FAO, 2017). Lobster populations in Southern New England experienced a collapse more than ten years ago, which was coincident with elevated ocean temperatures and the emergence of epizootic lobster shell disease (Pearce and Balcom, 2005; Wahle et al., 2009). The severity of the recent rate of temperature increase in the lobsters' geographical region has raised concern regarding the consequences of elevated temperatures, particularly sublethal effects that could contribute to stress and disease susceptibly. Previous research exploring the sublethal effects of temperature on American lobsters has focused primarily on benthic adults, and a number of these studies have explored changes in total hemocyte counts (THCs) and altered biochemical function as metrics of stress and immune health (Battison et al., 2003; Dove et al., 2005; Battison, 2006). Hemocytes are cells that are carried in the hemolymph and attack foreign invaders through phagocytosis and other mechanisms (Martin and Hose, 1995; Babcock et al., 2008). Studies on larval lobster stages have generally examined the direct effects of temperature on survival, rates of development, molting, and hatching success, but the effects of temperature on THCs have yet to be assessed in larvae (see Quinn, 2017 for recent review).

Although not yet explored in lobsters, fluctuating asymmetry (FA) is a metric that has been used in many taxa to assess developmental stability and is defined as random deviations of bilateral traits from perfect symmetry due to subtle variations in the developmental environment (Palmer and Strobeck, 2003). Both genetic and environmental stressors have been linked to elevated FA, including pesticides, parasitism, metals contamination, and suboptimal temperatures (see Polak, 2003 and Beasley et al., 2013 for comprehensive reviews). Exposure to elevated temperatures has also been linked to increased levels of

10

FA in developing larval fruit flies (*Drosophila melanogaster* and *D. buzzatii* – Imasheva et al., 1997), juvenile mussels (*Mytilus edulis* – Nishizaki et al., 2015), and adult isopods (*Asellus aquaticus* Linn. – Savage and Hogarth, 1999). Further, some studies have shown correlations between FA, parasitism, and disease susceptibility (Rantala et al., 2004; Møller, 2006; Thornhill and Gangestad, 2006; Morris et al., 2016). Although elevated temperatures may increase growth rate and survival in larval lobsters (e.g., MacKenzie, 1988; Barret et al., 2017), there may be consequences to rapid growth and FA could be a novel metric to highlight potential risks to this important species. This study seeks to examine the effects of temperature on survival, growth, hemocyte abundance, and FA to increase our understanding of the possible impacts of increasing temperatures on the health of larval lobsters.

2.3. Materials and Methods

2.3.1. Study Species

The American lobster inhabits hard-bottom substrate at depths commonly between 4 – 50 m along the Atlantic Coast of North America from Newfoundland, Canada, to North Carolina, USA (Herrick, 1911; Holthuis, 1991). Females can produce up to 10,000 eggs, which hatch in the shallows (< 20 m depth) during the summer months. Newly hatched lobsters proceed through three, pelagic larval stages (I-III) before molting into the final, postlarval (IV) stage. Unlike the three larval stages, postlarvae can swim with clear direction and speed (Cobb et al., 1989) and are negatively phototactic, spending less time at the surface as they swim down to the benthos (Herrick, 1911). As such, stage IV marks the point of transition, or settlement, from the pelagic to the benthic realm in the life history of the American lobster (Lavalli and Lawton, 1996).

2.3.2. Larval Rearing

In the summers of 2016 and 2017, egg-bearing females were collected by the Maine Department of Marine Resources (ME DMR) Ventless Trap Survey and delivered to the University of Maine's Aquaculture Research Center (ARC) in Orono, ME. Females were housed individually in bins (36 cm wide x 54 cm long x 28 cm deep) within several recirculating seawater systems. Artificial seawater was mixed to a salinity of 34 ppt and a pH of 8.1 using Kent Marine Superbuffer-dKH™, and temperature was

maintained at 16°C to provide the optimal egg-development environment (Factor, 1995). Females were observed every 10 hours for newly-hatched larvae. Upon hatch, larvae were carefully removed from bins and counted. Larvae were then evenly distributed among four temperature treatments selected to span the steep latitudinal thermal gradient encountered across the species' range (Factor, 1995): 14, 16, 18, and 22°C. Pilot efforts to rear larvae at colder temperatures (i.e., < 12°C) produced too few postlarvae for analyses, thus precluding them from subsequent experiments.

We used four recirculating seawater systems (one for each temperature treatment) that consisted of a 227 L header tank, four 75 L replicate experimental tanks, a 114 L sump, and a 65 L biofilter. We held between 10 – 12 females at a time, and experimental tanks were stocked with larvae from at least three different females. Importantly, we did not continue to stock any individual tank for more than 48 hours to reduce size differentiation among larvae, and larvae from each female were spread equally among the treatments to account for genetic differences. Depending on the number of larvae available during stocking, larval densities ranged from 3.5 – 14 larvae per L in experimental tanks. Larval tanks were highly aerated and lobsters were fed live *Artemia* spp. (Grade A Brine Shrimp Eggs, Brine Shrimp Direct, Inc., Ogden, Utah) twice a day at a density of 12 ml^{-1} to prevent cannibalism. Dissolved oxygen content, temperature, and salinity of the experimental tanks were monitored daily, and water quality was assessed weekly. The pH of each system was also assessed bi-weekly and maintained at 8.1 using Kent Marine Superbuffer-dKH^{TM}.

2.3.3. Biological Endpoints

To assess development, a subset of 20 individual larvae was carefully netted and removed from each tank daily and staged using a Unitron® Z850 Zoom Stereo Microscope. Stage II larvae were distinguished from stage I larvae by the presence of pleopods on the abdomen; stage III larvae were distinguished by the enlargement of the claws and the presence of uropods on either side of the telson; and stage IV (postlarvae) were identified by well-defined and extended claws and a more typical lobster morphology (Herrick, 1895; Factor, 1995). Progression through these stages was determined as the date when at least 50% of the animals in a tank metamorphosed into the subsequent stage. Excluding stage IV,

larvae were returned to experimental tanks following stage assessment. Cumulative survival was calculated as the proportion of stage I larvae initially stocked that successfully metamorphosed to stage IV.

2.3.4. Morphological Analyses

Upon reaching stage IV, postlarvae were removed from a given tank and assigned a unique identification number. Postlarvae were then placed in a clear Petri dish atop 6 mm x 6 mm grid paper and photographed using a Canon Rebel T5 camera. Photographs were taken on the "no flash" setting, and the lens was zoomed in so that lobsters could be seen in detail. Photographs from at least 20 postlarvae from each temperature treatment were blindly assessed using ImageJ2 software (Rueden et al., 2017). In triplicate, we measured the distance (in mm) from the middle of each eye to the midline of the body (Figure 2.1). Average values were then used to calculate metrics of asymmetry.
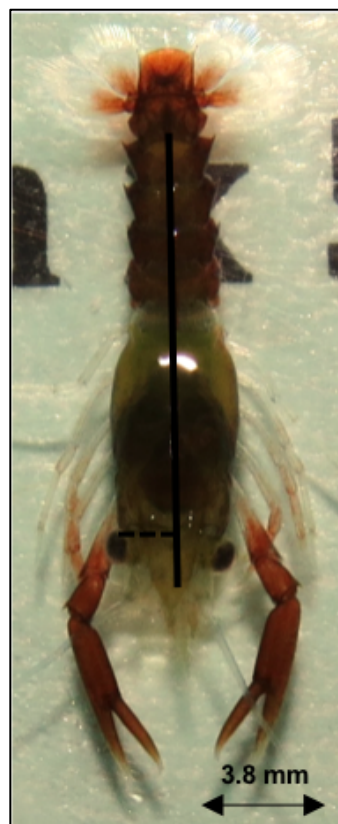
Figure 2.1. Example image used for morphometric analyses of a stage IV larva. The solid line indicates the midline of the body and the dotted line depicts the measured distance from the center of one eye to this midline (this measurement is not pictured but was conducted for the other eye as well).

2.3.5. Total Hemocyte Counts

Hemolymph was drawn from at least 12 postlarvae per temperature treatment to measure total hemocyte counts (THCs). Briefly, postlarvae were individually placed on a platform (a small crevice of a damp sponge) and viewed under a Unitron® Z850 Zoom Stereo Microscope. We used 6 mm BD® Insulin Syringes to draw as much of the animal's hemolymph as possible. Hemolymph was placed in pre-weighed glass vials containing 50 µl of fixative (10% buffered formalin in filtered, sterilized seawater) and the ratio of hemolymph to fixative was calculated using mass-differences. After aspirating the mixtures with a pipette, a 10 µl subsample was added to a hemocytometer (KOVA Glastic® Slide 10 with Grids). The total number of hemocytes was counted three times, and an average was calculated. This was repeated two more times, for a total of three subsamples per individual. Final counts were averaged and standardized to account for hemolymph : fixative dilutions among individuals (protocol modified from Dove et al., 2005).

2.3.6. Statistical Analyses

We used General Linear Models (GLMs) to determine the effects of temperature, year, and the interaction of year and temperature on the rate of development, cumulative survival, and THCs of postlarvae. We also explored whether stocking density had an effect on larval survival or rate of development using GLMs. We used Levene's Test to assess equal variance across groups and visually inspected data using histograms and q-q plots to assess normality. Time (in days) to stage II, stage III, and stage IV, as well as THC data, were log transformed, and cumulative survival data were square root transformed to meet test assumptions. Post hoc LSD tests were used to conduct pairwise comparisons across nominal temperature groups.

We calculated midline asymmetry (M_a) as the absolute difference between the distance from the middle of the right eye to the centerline of the body (R) and the middle of the left eye to the centerline of the body (L): $M_a = |R - L|$ (Palmer and Strobeck, 1986, 2003; Figure 2.1). We assessed temperature effects on midline asymmetry using a nonparametric Levene's Test because data did not meet test

assumptions of a GLM. We determined that measurement error was insignificant, found no effect of trait

size on fluctuating asymmetry, and conducted a series of preliminary tests to exclude other forms of

asymmetry (i.e., directional asymmetry and antisymmetry) following the protocols outlined in Palmer and

Strobeck (1986, 2003).

Finally, we performed bivariate correlation analyses between cumulative survival, time to stage

IV, and nominal temperature treatment. While the post hoc LSD tests illuminated treatment-specific

differences, this additional correlative approach allowed us to more fully understand the relationships

among these specific experimental variables. All tests were performed using IBM® SPSS® Statistics

Version 24.

2.4. Results

Development time was significantly faster in higher temperature treatments, particularly for time

to stage IV (Table 2.1; Figure 2.2), which was significantly negatively correlated with nominal

temperature ($R = -0.9$, $p < 0.01$). There was no significant year effect on time to stage II, but there was for

time to stages III and IV (Table 2.1). However, this was driven solely by the significantly greater values

observed in 2016 for the 14°C treatment as determined by comparing means using a t-test (stage III: $t =$

4.4, $p < 0.01$; stage IV: $t = 2.7$, $p = 0.05$). Pairwise comparisons found no significant differences in the

time to stage II between the 14 and 16°C and between the 16 and 18°C groups (LSD: $p > 0.1$); however,

all other temperature treatments were significantly different across all developmental stages (LSD: $p <$

0.05; Figure 2.2). We found no significant interactive effect between year and temperature treatment on

the time to any stage (Table 2.1). There was also no significant effect of stocking density on rate of

development for any stage (GLM, stage II: $F_{3,24} = 0.1$, $p = 0.9$; stage III: $F_{3,24} = 0.03$, $p = 0.9$; stage IV:

$F_{3,24} = 0.05$, $p = 0.9$), indicating no effect of density on the overall trends.

Table 2.1. Results of GLMs for the effects of year and nominal temperature on time to stage II (A), time to stage III (B), and time to stage IV (C). P values indicating strong evidence for effects are shown in bold.

Source	df	F	P
(A)			
Corrected model	7	9.2	**< 0.001**
Temperature	3	19.3	**< 0.001**
Year	1	3.7	0.069
Temperature * Year	3	2.2	0.121
(B)			
Corrected model	7	42.4	**< 0.001**
Temperature	3	97.9	**< 0.001**
Year	1	0.12	0.738
Temperature * Year	3	5.5	**0.006**
(C)			
Corrected model	7	75.4	**< 0.001**
Temperature	3	168.8	**< 0.001**
Year	1	8.5	**0.009**
Temperature * Year	3	2.8	0.069
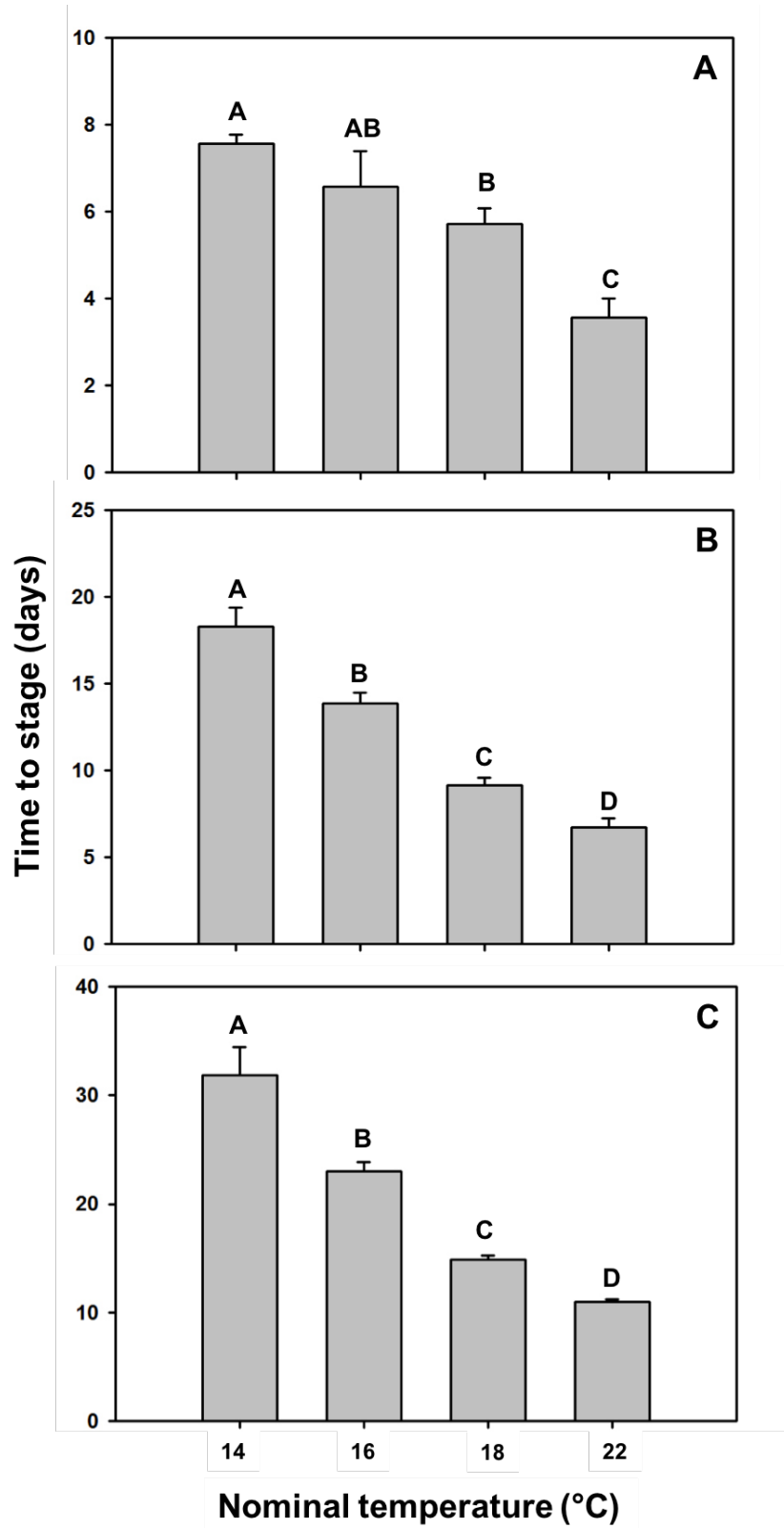
Figure 2.2. Mean (+ SE) time to stage II (A), stage III (B), and stage IV (C) for larvae reared under different nominal temperatures for 2016 and 2017 data combined. Letters indicate significant differences based on GLMs followed by post hoc LSD tests ($p < 0.01$).

Average cumulative survival was significantly affected by both year (GLM: $F_{1,20} = 4.8$, $p < 0.05$) and temperature (GLM: $F_{3,20} = 17.7$, $p < 0.001$) treatment, but there was no interactive effect (GLM: $F_{3,20} = 0.4$, $p = 0.73$; Figure 2.3). In both years, mean cumulative survival was significantly positively correlated with nominal temperature ($R = 0.6$, $p < 0.01$). However, pairwise comparisons found no significant difference in cumulative survival between the 14 and 16°C, 16 and 18°C, 16 and 22°C, and the 18 and 22°C treatments in 2016 (LSD: $p > 0.05$). Similarly, we observed no significant difference in cumulative survival values between the 14 and 16°C and the 18 and 22°C treatments in 2017 (Figure 2.3). Importantly, there was no significant difference in mean cumulative survival with each temperature treatment across years as observed using Student's t-tests (14°C: $t = 0.13$, $p = 0.90$; 16°C: $t = 1.71$, $p = 0.19$; 18°C: $t = 1.09$, $p = 0.07$; 22°C: $t = 1.41$, $p = 0.69$). There was also no significant effect of stocking density on cumulative survival (GLM: $F_{3,24} = 0.4$, $p = 0.8$), again suggesting variable stocking density did not impact our results.
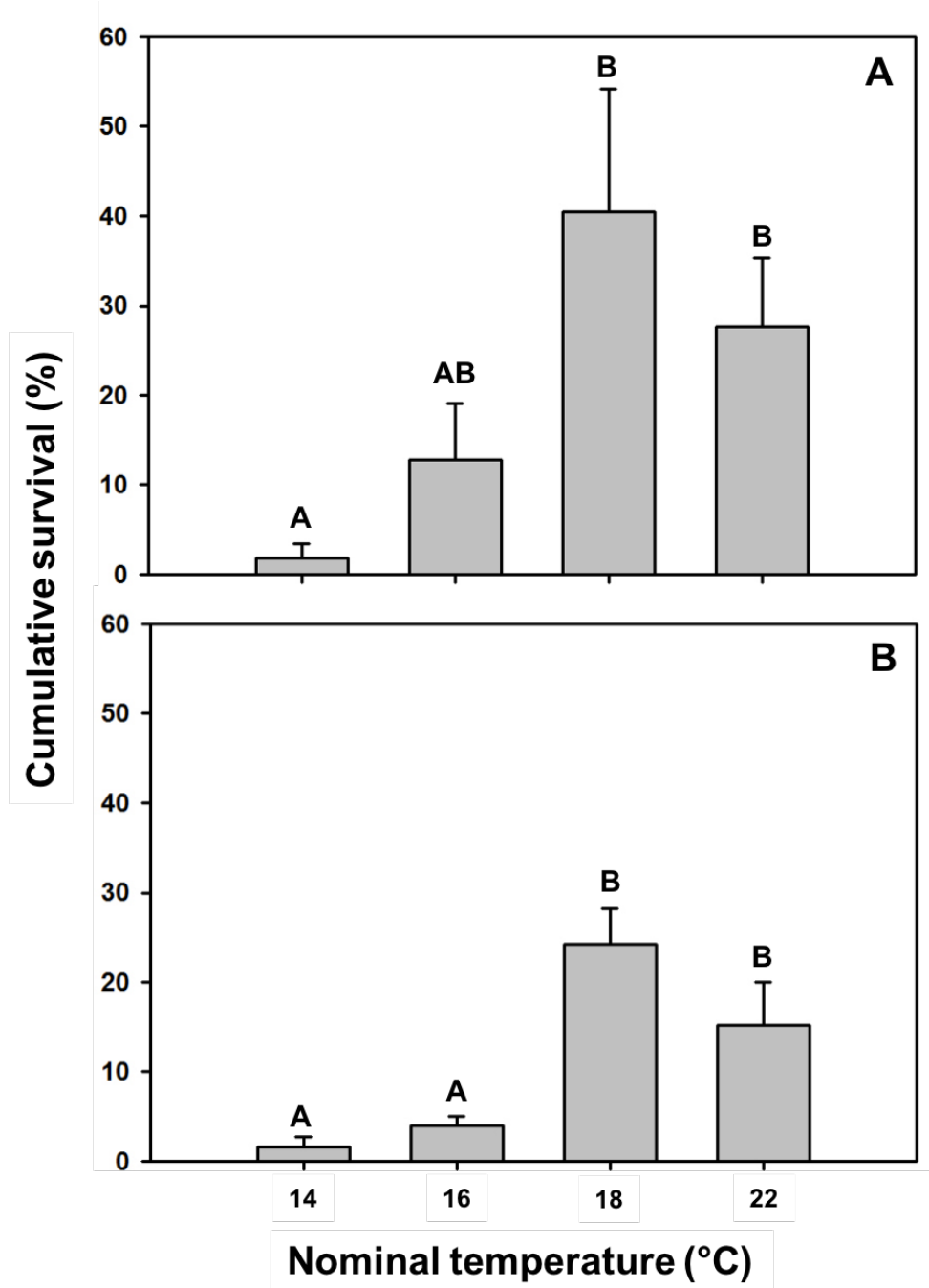
Figure 2.3. Mean (+ SE) cumulative survival for larvae reared under different nominal temperatures in 2016 (A) and 2017 (B). In 2016, mean (±SE) survival was 1.9 ± 1.5, 12.8 ± 6.2, 40.4 ± 13.7, and 27.6 ± 7.7% at 14, 16, 18, and 22°C, respectively. In 2017, mean (±SE) survival was 1.5 ± 1.2, 4.0 ± 1.0, 24.2 ± 4.0, and 15.3 ± 4.8% at 14, 16, 18, and 22°C, respectively. Letters indicate significant differences based on GLMs followed by post hoc LSD tests ($p < 0.01$).

THCs of postlarvae were significantly affected by temperature (GLM: $F_{3, 64} = 9.8$, $p < 0.001$; Figure 2.4). Mean THCs for postlarvae reared at the extremes (14 and 22°C) were not significantly different from one another but were significantly greater than mean THCs in postlarvae reared at both 16 and 18°C (which were not significantly different from one another; Figure 2.4).
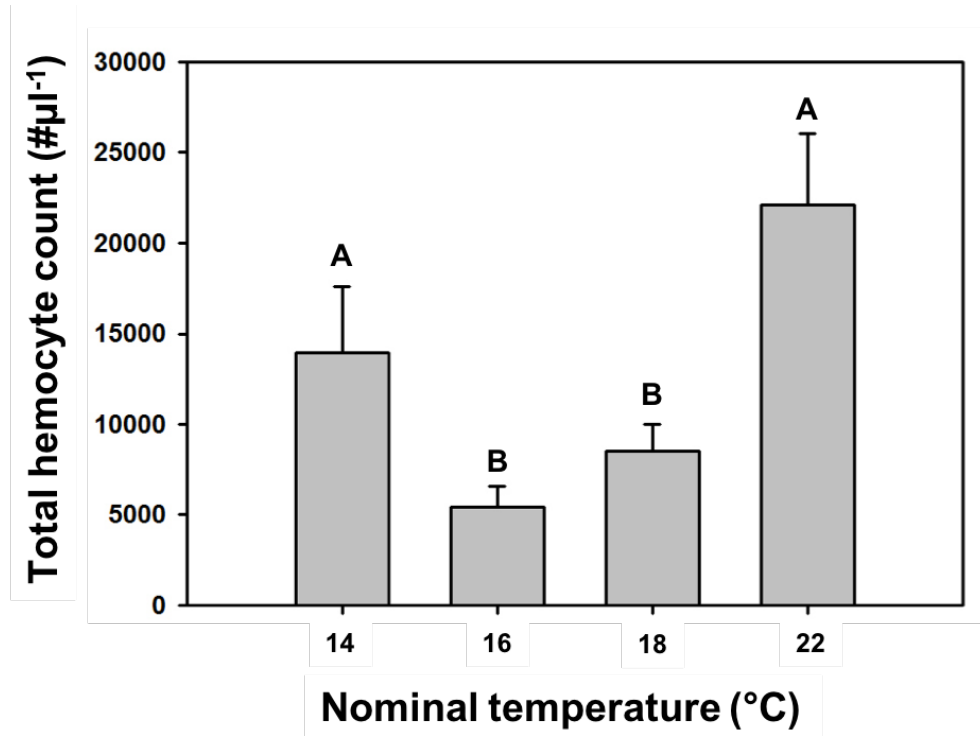
Figure 2.4. Mean (+ SE) total hemocyte count (THC) for larvae reared under different nominal temperatures in 2017. Letters indicate significant differences based on GLMs followed by post hoc LSD tests ($p < 0.01$).

We found a significant effect of temperature on the variance in midline asymmetry (Nonparametric Levene's Test: $F_{3,222} = 4.8$, $p < 0.01$; Figure 2.5). Variance in midline asymmetry was higher for postlarvae reared at 16 and 18°C compared to postlarvae reared at 14 and 22°C, with pairwise comparisons demonstrating significant differences between postlarvae reared at 14 and 16°C, 14 and 18°C, and between those reared at 16 and 22°C (LSD: $p < 0.05$; Figure 2.5).
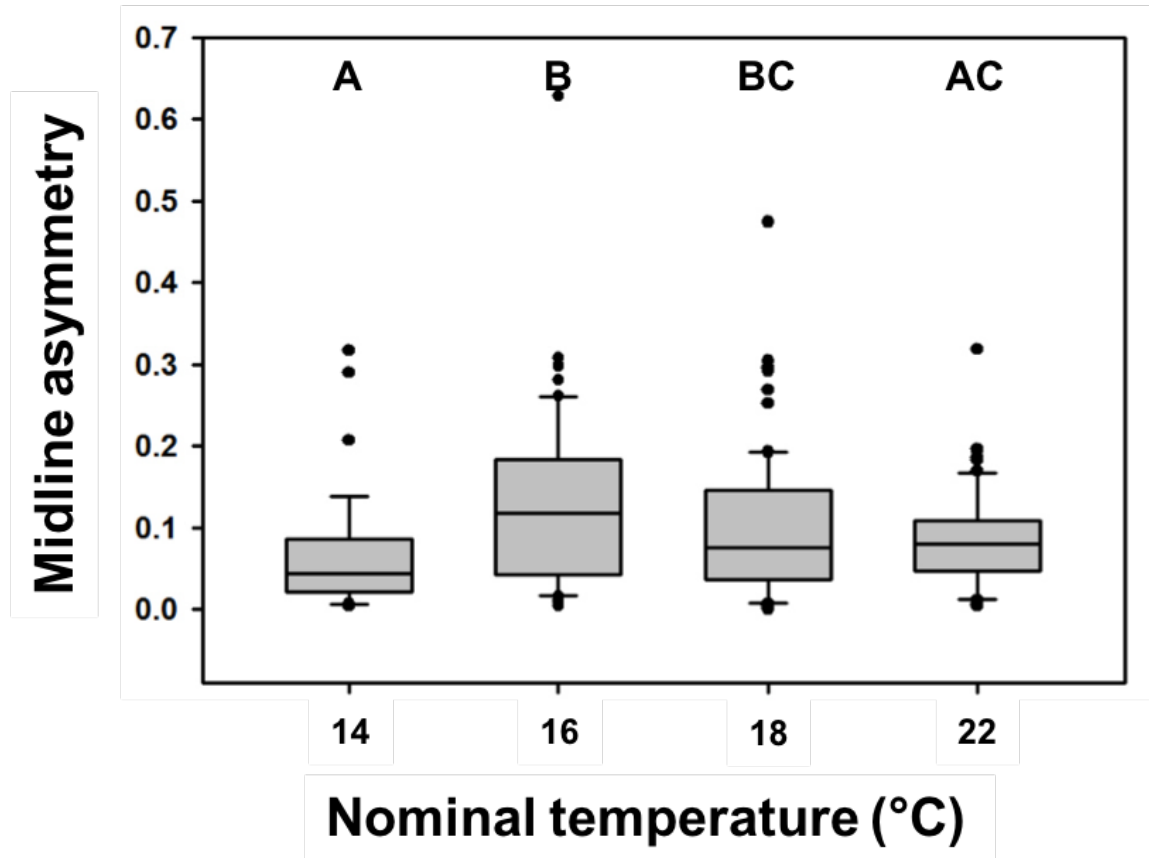
Figure 2.5. Boxplots depicting the midline asymmetry for 2016 and 2017 data combined. Letters indicate significant differences in variance via a nonparametric Levene's Test followed by post hoc LSD tests ($p <$ 0.01). The upper and lower quartiles are represented as the top and bottom ends of each box, respectively, and the median is marked by the horizontal line within each box. Lines extending vertically above and below the box indicate the variability outside of the upper and lower quartiles, and outliers are represented by individual points.

2.5. Discussion

Our work is the first to evaluate the use of FA as a biomarker for developmental instability in response to stress in larval *H. americanus*. We expected postlarvae reared under temperature extremes to exhibit greater levels of midline FA, but we found that postlarvae reared at 14 and 22°C had significantly lower levels of variance in midline FA compared to the intermediate temperature groups (Figure 2.5). There has been much debate about the utility of FA as an indicator of developmental instability (Palmer and Strobeck, 1986; Leung and Forbes, 1996). Although recent meta-analyses suggest that it is a reliable biomarker (Beasley et al., 2013), expression of FA in response to environmental stress is both species-

and trait-specific (Lazić et al., 2013; Klisarić et al., 2014). Elevated FA has been linked to elevated levels of pollution, including exposure to heavy metals in brown trout (*Salmo trutta* fario – Monna et al., 2011), tributyltin in surf crabs (*Ovalipes trimaculatus* – Lezcano et al., 2014), Roundup Original® in tadpoles (*Physalaemus cuvieri* – Costa and Nomura, 2016), and urbanization in lizards (*Podarcis muralis* – Lazić et al., 2013). Exposure to sub-optimal temperatures also produced increased levels of FA in developing larval fruit flies (*Drosophila melanogaster* and *D. buzzatii* – Imasheva et al., 1997), juvenile mussels (*Mytilus edulis* – Nishizaki et al., 2015), and adult isopods (*Asellus aquaticus* Linn. – Savage and Hogarth, 1999). This previous research has demonstrated a link between increased variance in traits of populations exposed to novel environments or pollutants, suggesting that elevated variance arises as populations struggle to adapt to a changing environment (see references within Orlando and Guillette, 2001); however, research also suggests that human-induced stress produces a loss of genetic diversity in populations via genetic erosion (van Straalen and Timmermans, 2002). Genetic erosion can be caused by genetic bottlenecks, mutations, altered migration patterns, and directional selection of tolerant genotypes in response to stress, and it can lead to the loss of alleles, reduced population growth, and increased susceptibility to further genetic erosion (van Straalen and Timmermans, 2002; Ribeiro and Lopes, 2013). For example, scientists observed reduced genetic diversity in populations exposed to trace metal pollution (e.g., amphibians – Fasola et al., 2015; cladocerans *Daphnia longispina* – Venâncio et al., 2016; tiger prawn *Penaeus monodon* – Rumisha et al., 2017), climate-induced habitat loss and fragmentation (e.g., chipmunk *Tamias alpinus* – Rubidge et al., 2012; tree frogs *Litoria ewingii* and *L. raniformis* – Potvin et al., 2017), and human-induced habitat destruction (snails *Littoraria subvitatta* – Nehemia et al., 2017). At first glance, our results might appear to indicate lower levels of developmental instability of postlarvae reared under extreme temperatures compared to the intermediate temperature treatments. However, we suggest that only those individuals with genotypes tolerant of the extreme temperature treatments were able to survive this thermal stress, potentially altering morphological development that manifested as reduced variability in midline FA. Moreover, this observed decline in variation of FA suggests that postlarval populations reared under our warmest temperature treatment may have lower adaptive

capacities to deal with additional stressors (van Straalen and Timmermans, 2002). This is particularly

important in the context of climate change, in which postlarvae will have to deal with numerous other

stressors in addition to warming temperatures. Individuals (and thus populations) that are tolerant of one

stressor may be sensitive to a second stressor, potentially enhancing genetic erosion in a population via a

second round of gene loss (van Straalen and Timmermans, 2002; Venâncio et al., 2016). Future efforts

should continue to explore the utility of FA as an indicator of developmental instability in larval lobsters,

particularly in response to multiple stressors.

We assessed physiological stress levels by quantifying total hemocyte counts (THCs), a common

measure of stress that has not been previously implemented in work on larval lobsters. Invertebrates lack

an adaptive immune system, and as such hemocytes play a critical role in the innate immune response

(Cerenius and Soderhall, 2011; Adamo, 2012). Free hemocytes rapidly circulate within the hemolymph,

surveying for areas of damage and identifying self from non-self (Babcock et al., 2008). In *H.

americanus*, hemocytes assist in wound healing via clotting, harden the exoskeleton, and remove foreign

material and pathogens via phagocytosis (Martin and Hose, 1995; Battison et al., 2003; Mori and Stewart,

2006). Most previous work on hemocytes in invertebrates has focused on understanding changes in THCs

in the context of pathogen exposure (e.g., white shrimp *Litopenaeus vannamei* – Cheng et al., 2006; giant

prawn *Macrobranchium rosenbergii* – Chang et al., 2011; mud crab *Scylla paramamosain* – Zhou et al.,

2018). However, as the innate immune response and the stress response are intimately tied in

invertebrates (Adamo, 2012), THCs have also been measured in the context of other stressors. For

example, researchers linked elevated THCs to acute stress events in crickets (*Gryllus texensis* – Adamo,

2010) and western rock lobster (*Panulirus cygnus* – Jussila et al., 2001). Additionally, researchers

observed a decline in THCs in white shrimp (*Litopenaeus vannamei*) in response to cold shock,

suggesting a depressed immune response relative to preferred thermal conditions (Chang et al., 2009).

Previous work on adult *H. americanus* found an increase in THCs in response to elevated

temperatures (Dove et al., 2005). Moreover, this increase was accompanied by a 60% reduction of

phagocytotic activity of hemocytes within just two weeks of exposure to stressfully warm conditions, as

well as severe pH acidosis, suggesting deleterious effects of warming temperatures on lobster physiology (Dove et al., 2005). Similarly, we observed elevated THCs in postlarvae reared under 22°C compared to those reared under 16 and 18°C, suggesting an elevated stress response in these treatments. One might expect physiological responses to increase in lobsters as their external environmental temperature increases because they are ectotherms; however, the fact that we did not observe a linear increase in THCs with temperature treatment points to a more regulated stress response independent of temperature. We also found an increase in THCs in postlarvae reared at 14°C that was not statistically different from that of the 22°C group, suggesting that these larvae also experienced stressful thermal conditions during development. A similar pattern was found in the freshwater amphipod (*Gammarus pulex*) when exposed to a range of environmentally-relevant temperatures (9 – 17°C), whereby THCs were reduced in individuals reared at intermediate temperatures compared to both the warm and cool extreme temperatures tested (Labaude et al., 2017). Amphipods reared at the extremes also exhibited a reduction in their ability to clear an *Escherichia coli* infection, suggesting a potential breakdown in the immune response as a consequence of temperature-induced stress (Labaude et al., 2017). Since some crustaceans exhibit greater levels of tissue damage at extreme temperatures (Madeira et al., 2015), it is possible that the elevated THCs observed in our study are related to wound healing and the breakdown of damaged cells (as suggested for *G. pulex* – Labaude et al., 2017). Continued warming conditions could increase disease susceptibility in recently settled American lobster if they are allocating more energy toward fixing damaged cells, potentially increasing post-settlement mortality. However, it is important to note that THCs are just one metric of stress, and future efforts should explore other indicators (e.g., levels of glucose, crustacean hyperglycemic hormone, or L-lactate – Basti et al., 2010). Additionally, future efforts should focus on not only measuring other parameters of hemolymph chemistry (e.g., phagocytotic activity and pH), but also understanding the potential interactions between temperature stress and immune function in postlarvae.

Development rate was significantly enhanced under warming conditions, which aligns with previous work on larval *H. americanus* (Hadley, 1906; Templeman, 1936; MacKenzie, 1988; Waller et

al., 2017; Barret et al., 2017). Mean cumulative survival was also significantly elevated by rearing temperature, which increased up to 18°C (24 – 40%) with an insignificant reduction in survival at 22°C (15 – 27%) (Figure 2.3). This finding is consistent with previous studies showing increased survival in larval *H. americanus* at elevated temperatures (MacKenzie, 1988; Barret et al., 2017). Although Waller et al. (2017) described significant reductions in survival of larvae reared at elevated temperatures, that study reports considerably lower cumulative survival (< 2.0%). This may have been due to cannibalism (Waller et al., 2017), which could be expected to increase at higher temperatures to compensate for increased feeding and growth rates. In our study, vigorous aeration was necessary to reduce agonistic interactions and limit the incidence of cannibalism. However, Quinn et al. (2013) also found low cumulative survival (< 4.0%) in larvae reared individually at 20°C, eliminating the possibility of cannibalism-induced mortality. Rearing larval lobsters can be technically challenging, and numerous factors including system design, diet, and water quality can play a substantial role in survival outcomes. Notably, survival was lowest in our 14°C treatment, and pilot efforts to rear larvae at colder temperatures (10 – 12°C) produced too few larvae for meaningful analyses. This is consistent with Barret et al. (2017) and MacKenzie (1998) which generally found < 5.0% survival at 10°C. Variation in larval development is dependent upon both larval origin (i.e., cold- vs. warm-water maternal origin – Quinn et al., 2013), and the thermal variability encountered in the natural environment (Quinn and Rochette, 2015). Females used in this study were collected from southern Maine waters, so it is possible that their larvae perform better under warmer conditions compared to those from females of waters near colder portions of the species' range. More work is needed to understand the geographical variation in responses to warming temperatures, particularly in the context of a changing climate.

Overall, this work adds to our understanding of the indirect risk factors of rising temperatures on larval *H. americanus*, providing insight into the potential sublethal effects of ocean warming that could assist modeling efforts to link larval settlement to subsequent recruitment into the fishery (e.g., Barret et al., 2017; Quinn et al., 2017). Our findings suggest that larvae reared under warming conditions exhibit enhanced rates of development and higher rates of survival, but these benefits are potentially outweighed

by the increase in stress level as indicated by elevated THCs. We also suggest that reduced variation in midline FA may indicate a reduced capacity to deal with additional stressors, although more work is needed to understand long-term consequences. Taken together, these data indicate a potential trade-off between enhanced growth and sublethal impacts on larval physiology under warming conditions. This is the first study to explore the utility of FA as an indicator of developmental stability in *H. americanus*, and future efforts should explore additional morphometric traits, as well as the potential for geographic variation in these metrics. Future research should also focus on understanding more downstream effects of both FA and THCs in the context of post-settlement survival, particularly as these parameters relate to interspecific interactions and foraging behaviors. Finally, it is important to acknowledge that ocean warming is not occurring in isolation, and future efforts should examine the potential interactive effects of temperature, ocean acidification, and salinity on *H. americanus* larval survival, development, and fitness post-settlement.

CHAPTER 3

EFFECTS OF TEMPERATURE ON THE POSTLARVAL AMERICAN LOBSTER TRANSCRIPTOME

3.1. Chapter Abstract

The American lobster (*Homarus americanus*) is one of the most iconic and economically valuable fisheries species in the Northwestern Atlantic. Temperature heavily influences lobster biology and distribution, and the ocean is rapidly warming across much of the species' range. Warmer temperatures accelerate rates of larval development and enhance survival to the postlarval stage, but the potential effects of warming at the cellular level have rarely been addressed. We explored how exposure to current summer temperatures (16°C) or elevated temperature regimes (18°C and 22°C) during development influences the postlarval lobster transcriptome. We *de novo* assembled the larval lobster transcriptome and identified 2,542 differentially expressed (DE; adjusted $p < 0.05$) transcripts in postlarvae exposed to 16°C vs. 22°C and 422 DE transcripts in postlarvae reared at 16°C vs. 18°C. Lobsters reared at 16°C significantly over-expressed transcripts annotated to proteins related to cuticle formation and the immune response up to 14.4- and 8.5-fold, respectively, relative to those reared at both 18°C and 22°C. However, as treatment temperature increased the expression of transcripts annotated to proteins affiliated with metabolic turnover increased up to 7.1- fold. These results suggest that postlarvae exposed to increasingly warmer temperatures during development experience a shift in the transcriptome that reflects a potential trade-off between maintaining immune defenses and meeting the energetic demands associated with increased physiological rates under ocean warming. This could have major implications for post-settlement survival through increased risk of mortality due to disease and/or starvation if energetic demands cannot be met.

3.2. Introduction

Increased input of anthropogenic carbon dioxide (CO_2) into the atmosphere has caused widespread changes in climatic conditions, including increased rates of ocean warming and acidification. Global ocean surface temperatures have increased by 0.11°C per decade from 1971 – 2010 (IPCC, 2013),

and recent modeling efforts suggest that the oceans are likely warming at a rate faster than previously projected (Cheng et al., 2019). The Northwestern Atlantic Ocean is experiencing some of the most rapid rates of warming (Pershing et al., 2015). Specifically, the Gulf of Maine region is warming four times the average global rate (i.e., 0.4°C per decade – Thomas et al., 2017), which has had considerable impacts on the regions' commercial finfish (Pershing et al., 2015) and shellfish (Richards et al., 2012; Arnberg et al, 2013) fisheries. Moreover, warming ocean temperatures have been linked to mass mortality events and disease outbreaks in the southern portion of the American lobster (*Homarus americanus*) population (Pearce and Balcolm, 2005), raising concerns of increased disease susceptibility for northern portions of the population as the Gulf of Maine continues to warm.

Underlying the overt impacts of warming on Gulf of Maine species is the effect of temperature on physiological processes (i.e., Q_{10} effects), and the increase in oxygen demand associated with these effects on metabolism (Somero et al., 2015, 2017). Although manipulative experiments have helped determine general patterns in organismal responses to various environmental stressors, they often do not identify the cellular mechanisms driving observations. However, as bioinformatics tools continue to advance, next-generation sequencing efforts and gene expression studies have provided a much greater understanding of how organisms respond to environmental stress (Conesa et al., 2016). Transcriptomics, the study of transcriptomes and their functions through RNA-sequencing (RNA-seq; Lesk, 2013), has been implemented in a variety of research efforts and study systems in the aquatic environment, particularly in the context of understanding cellular responses to climate change (e.g., blue mussels *Mytilus* spp. – Lockwood et al., 2010; corals *Acropora millepora* – Moya et al., 2012; Sydney rock oysters *Saccostrea glomerata* – Goncalves et al., 2017; purple urchins *Strongylocentrotus purpuratus*– Evans et al., 2017; Wong et al., 2018). Transcriptomics is a particularly useful tool to explore gene expression patterns as it does not require that the genome or the transcriptome of a species of interest be fully known (Clark and Greenwood, 2016). Sophisticated software packages allow a user to *de novo* assemble a transcriptome (e.g., Trinity – Grabherr et al., 2011; Haas et al., 2013), which can then serve as a reference for subsequent analyses.

We explored how elevated temperatures influence the transcriptome of postlarval American lobster. *Homarus americanus* inhabits waters off the Atlantic Coast of North America from North Carolina, USA, to Newfoundland, Canada (Herrick, 1911; Holthuis, 1991). During the summer months, newly hatched lobsters proceed three pelagic larval stages (I-III) prior to metamorphosing into the final, postlarval stage (IV) that resembles the adult form. As the postlarval stage marks the point of transition, or settlement, from the pelagic to the benthic realm in the life history of *H. americanus*, how the environment impacts this stage may have huge implications for post-settlement survival and thus recruitment to the population. Although development time varies with larval origin (Quinn et al., 2013) and environmental conditions (Quinn and Rochette, 2015), previous research suggests that exposure to warmer temperatures significantly accelerates larval development time (Hadley, 1906; Templeman, 1936; MacKenzie, 1988; Waller et al., 2017; Barret et al., 2017; Harrington et al., 2019), and increases survival to stage IV (MacKenzie, 1988; Barret et al., 2017; Harrington et al., 2019). However, these potential benefits of ocean warming may be outweighed by increased oxygen demand due to elevated metabolic rates (Waller et al., 2017) and elevated levels of cellular stress (Harrington et al., 2019), which could lead to reduced post-settlement survival and a potential loss of diversity. Previous genetic analyses of developing *H. americanus* indicate that the constitutive expression of immune-related genes increases and is maximized upon reaching the postlarval stage (Hines et al., 2014), and transcriptomic efforts have identified numerous putative immune-related genes in larval *H. americanus* that remain to be validated (Clark and Greenwood, 2016). However, transcriptomic analyses have primarily focused on adult lobsters, particularly in the context of pathogen- and tissue-specific immune responses (Clark et al. 2013a, 2013b, 2013c; Clark et al. 2015), as well as tissue-specific expression patterns of genes related to biological neural circuits (McGrath et al., 2016), with few exploring the impacts of environmental change on the larval transcriptome.

To our knowledge, this is the first study to address how exposure to warming conditions during development influences the postlarval *H. americanus* transcriptome. As *H. americanus* lacks a fully sequenced reference genome, our first goal was to *de novo* assemble a postlarval lobster transcriptome.

We then characterized the transcriptional profiles across postlarvae exposed to three temperature treatments during development. Finally, we compared transcriptome-wide differences across these temperature groups, focusing on transcripts annotated to genes associated with innate immunity and metabolic turnover. These data attempt to address the potential downstream effects of ocean warming on this important species and provide a better understanding of the cellular mechanisms involved in potential trade-offs between accelerated growth and overall fitness in a warming ocean.

3.3. Materials and Methods

3.3.1. Larval Rearing

Egg-bearing female lobsters were collected by the Maine Department of Marine Resources (ME DMR) Ventless Trap Survey in summer 2017 from the waters off of the mid-coast Maine region. Females were transported to the University of Maine's Aquaculture Research Center (ARC) in Orono, ME, and housed individually in recirculating seawater systems as previously described (Harrington et al., 2019). Briefly, females were observed at least every 10 hours for newly-hatched larvae, which were evenly distributed among four temperature treatments: 14, 16, 18, and 22°C. These temperatures were selected because they represent the environmentally relevant range of temperatures encountered by *H. americanus* across its distribution (Factor, 1995), with 16°C representing current average summer temperatures experienced by larval *H. americanus* in the collection area (The Northeastern Regional Association of Coastal Ocean Observing Systems, NERACOOS, Past X-Band MODIS Satellite Sea Surface Temperature Data; neracoos.org). We used four recirculating seawater systems that consisted of four replicate 75 L tanks each. Experimental tanks were stocked evenly with larvae from at least three different females over no longer than 48 hours to limit size variation among larvae, resulting in stocking densities that ranged from 3.5 – 14 larvae per L depending on the number of individuals available during stocking events. Tanks were heavily aerated, and live *Artemia* spp. (Grade A Brine Shrimp Eggs, Brine Shrimp Direct, Inc., Ogden, Utah) were added at a density of 12 ml^{-1} to reduce cannibalism. We conducted daily assessments of water quality and animal husbandry as described in Harrington et al. (2019).

3.3.2. Sample Preservation and RNA Extraction

Larval development was assessed daily using a Unitron® Z850 Zoom Stereo Microscope to examine morphological characteristics (see Harrington et al., 2019). Upon reaching stage IV, postlarvae were removed from the experimental tanks. A subset of individuals was immediately placed in DNA/RNA-free microcentrifuge tubes containing 1 ml of RNALater for preservation and were stored at -20°C until homogenization. Whole animals were homogenized in 1 ml of TRIzol® reagent using a Tissue Tearor (Biospec Products, Inc). Following Clark et al. (2013a), 200 µl of chloroform was added to each sample vial and inverted prior to incubating at room temperature (~20°C) for three minutes. Samples were then centrifuged at 4,000 g at 4°C for 15 minutes. Approximately 600 µl of the supernatant of each sample was carefully removed and combined with an equal volume of 70% ethanol (Molecular Biology Grade). RNA was then isolated using the Qiagen RNeasy® Mini Kit following the manufacturer's protocols, including the optional DNase I treatment. RNA was quantified spectrophotometrically using a Thermo Scientific NanoDrop^{TM} Spectrophotometer. Samples were stored at -80°C, and material from five replicate animals reared at 16, 18, and 22°C were sent to the Genomic Services Lab (GSL) at the HudsonAlpha Institute for Biotechnology (Huntsville, AL) for library preparation and sequencing. Low survival at 14°C precluded us from using postlarvae for RNA extraction and as such have been omitted in the analyses that follow.

3.3.3. Library Preparation and *de novo* Transcriptome Assembly

Libraries were prepared for all samples by the GSL following internal quality control assays: initial quantification via a Quibit® fluorometer (Life Technologies), bioanalysis via the Agilent 2100 Bioanalyzer (Agilent Technologies, CA), and final quantification using a KAPA Library Quantification Kit (KAPABiosystems, MA). RNA-Seq libraries were prepared using poly(A) enrichment and sequenced on an Illumina HiSeq v4 sequencer (paired end, 50 bp, 50M reads). Raw sequence reads were uploaded to the Galaxy Server (Afgan et al., 2018; Galaxy Version 18.09). Read quality was assessed using FastQC (Andrews, 2010; Galaxy Verions 0.72), and reads were trimmed using Trim Galore! (Babraham

Bioinformatics; Galaxy Version 0.4.3.1). A *de novo* transcriptome was assembled using the Trinity

bioinformatics suite (Grabherr et al., 2011; Haas et al., 2013; Galaxy Version 0.0.1). Following the data

analysis pipeline of Pertea et al. (2016), reads were aligned to the transcriptome using HiSAT2 (Kim et

al., 2015; Galaxy Version 2.1.0+galaxy3) and assembled into full and partial transcripts using StringTie

(Pertea et al., 2015; Galaxy Version 1.3.4). StringTie Merge was used to create a set of consistent

transcripts across samples (Pertea et al., 2015; Galaxy Version 1.3.4), and featureCounts was used to

count reads and normalize these data (Liao et al., 2013; Galaxy Version 1.6.2).

We used both DESeq2 (Love et al., 2013; Galaxy Version 2.11.40.2) and edgeR (Robinson et al.,

2010; Liu et al., 2015; Galaxy Version 3.20.7.2) to assess differential transcript expression. With both

statistical approaches, *p*-values were adjusted for multiple testing with the Benjamini-Hochberg

procedure, which controls false discovery rate (FDR). For the DESeq2 analysis, factor levels 1, 2, and 3

corresponded to postlarvae reared at 16°C, 18°C, and 22°C, respectively, resulting in three pairwise

comparisons across treatments: 16°C vs. 22°C, 16°C vs. 18°C, and 18°C vs. 22°C. As such, fold change

(FC) was calculated for each transcript as a ratio of expression in postlarvae reared at 16°C relative to

22°C, 16°C relative to 18°C, and 18°C relative to 22°C in each comparison, respectively. Similar pairwise

comparisons were set up for the edgeR analysis. All data were graphically represented as $\log_2$FC for ease

of visualization, where positive and negative values correspond to transcripts over- and under-expressed,

respectively, in postlarvae reared at 16°C relative to 22°C, 16°C relative to 18°C, and 18°C relative to

22°C in each comparison. Importantly, because FC is a ratio of expression, negative $\log_2$FC values can

also be interpreted as transcripts over-expressed in postlarvae reared at 22°C relative to 16°C, 18°C

relative to 16°C, and 22°C relative to 18°C in each temperature comparison, whereby FC values were

calculated as the inverse of those reported by DESeq2 and edgeR.

3.3.4. Annotation and Pathway Analysis

We used the NCBI BLAST+ blastx routine (Galaxy Version 0.3.0) to annotate our transcriptome

using NCBI non-redundant (nr) protein databases (E-value ≤ 1e – 10; downloaded in July 2018). We

assigned protein domain information using InterProScan (IPS) and Gene Ontology (GO) functional terms

to these annotations using Blast2GO (Götz et al., 2008; Version 5.2.5). We used the KEGG Automatic

Annotation Server (KAAS; Moriya et al., 2007) for ortholog assignment and pathway analysis of the top

100 differentially expressed (DE) and annotated transcripts that were over- and under-expressed in all

treatment comparisons from both the edgeR and DESeq2 analyses. We also identified transcripts

annotated to genes of interest (GOI) related to immunity, cuticle formation, and metabolism for further

discussion.

3.4. Results

3.4.1. Transcriptome Assembly and Annotation

The *de novo* assembly of the postlarval lobster transcriptome via Trinity produced 138,833

sequences resulting in 66,962 contigs across samples following the StringTie Merge analysis. Of these,

16,170 (24.2% of assembled contigs) were successfully annotated against NCBI nr protein databases.

Mapping these gene IDs to GO annotations identified 1,711 unique GO categories represented in our

transcriptome: 335 attributed to cellular components, 458 attributed to molecular function, and 918

attributed to biological processes. Of these, the top ten GO terms attributed to the greatest number of

transcripts (in descending order) were integral component of membrane, oxidation-reduction process,

membrane, transmembrane transport, nucleus, proteolysis, zinc ion binding, regulation of transcription

(DNA-templated), protein phosphorylation, and transmembrane transporter activity (Table 3.1).

Table 3.1. Top twenty Gene Ontology (GO) terms affiliated with the greatest number of transcripts. The letters "C", "P", and "F" refer to GO terms attributed to cellular functions, biological processes, and molecular functions, respectively.

Count	GO Term	GO Name
651	C:GO:0016021	Integral component of membrane
352	P:GO:0055114	Oxidation-reduction process
350	C:GO:0016020	Membrane
295	P:GO:0055085	Transmembrane transport
278	C:GO:0005634	Nucleus
262	P:GO:0006508	Proteolysis
259	F:GO:0008270	Zinc ion binding
193	P:GO:0006355	Regulation of transcription, DNA templated
193	P:GO:0006468	Protein phosphorylation
151	F:GO:0022857	Transmembrane transporter activity
139	C:GO:0005576	Extracellular region
137	F:GO:0042302	Structural constituent of cuticle
127	P:GO:0005975	Carbohydrate metabolic process
126	P:GO:0006412	Translation
117	F:GO:0016491	Oxidoreductase activity
108	F:GO:0046872	Metal ion binding
106	C:GO:0005840	Ribosome
97	P:GO:0006030	Chitin metabolic process
96	P:GO:0007165	Signal transduction
95	C:GO:0005737	Cytoplasm

3.4.2. Differential Expression

Using DESeq2 analysis, we observed a total of 2,542 differentially expressed (DE; adjusted $p <$ 0.05) transcripts in the 16°C vs. 22°C treatment comparison, 422 DE transcripts in the 16°C vs. 18°C treatment comparison, and 33 DE transcripts in the 18°C vs. 22°C treatment comparison (Table 3.2; Figure 3.1). Of these DE transcripts, none were shared across all three treatment comparisons, but 375 were shared between the 16°C vs. 22°C and 16°C vs. 18°C treatment comparisons (Figure 3.2). Results of the edgeR analysis identified 805, three, and zero DE transcripts in the 16°C vs. 22°C, 16°C vs. 18°C, and 18°C vs. 22°C treatment comparisons, respectively (Table 3.2). All three of the DE transcripts identified in the 16°C vs. 18°C treatment using edgeR were also identified by DESeq2, and we omit the edgeR results from subsequent analyses. However, edgeR identified 14 DE transcripts in the 16°C vs. 22°C that were not identified by DESeq2 (Figure 3.3), and as such we include both analyses for this treatment comparison in the following sections.

Table 3.2. Number of differentially expressed (DE; adjusted p-value ≤ 0.05) transcripts over- and under-expressed in each temperature comparison using both DESeq2 (A) and edgeR (B) analyses. For each comparison, the number of over- and under-expressed transcripts are expressed as the first temperature treatment relative to the second temperature treatment (e.g., in the 16°C vs. 22°C comparison, transcripts are over- or under-expressed in postlarvae reared at 16°C relative to those reared at 22°C).

Comparison	Total DE (#)	Over-expressed (#)	Under-expressed (#)
(A)			
16°C vs. 22°C	2,542	1,354	1,188
16°C vs. 18°C	422	326	96
18°C vs. 22°C	33	16	17
(B)			
16°C vs. 22°C	805	468	337
16°C vs. 18°C	3	1	2
18°C vs. 22°C	0	-	-
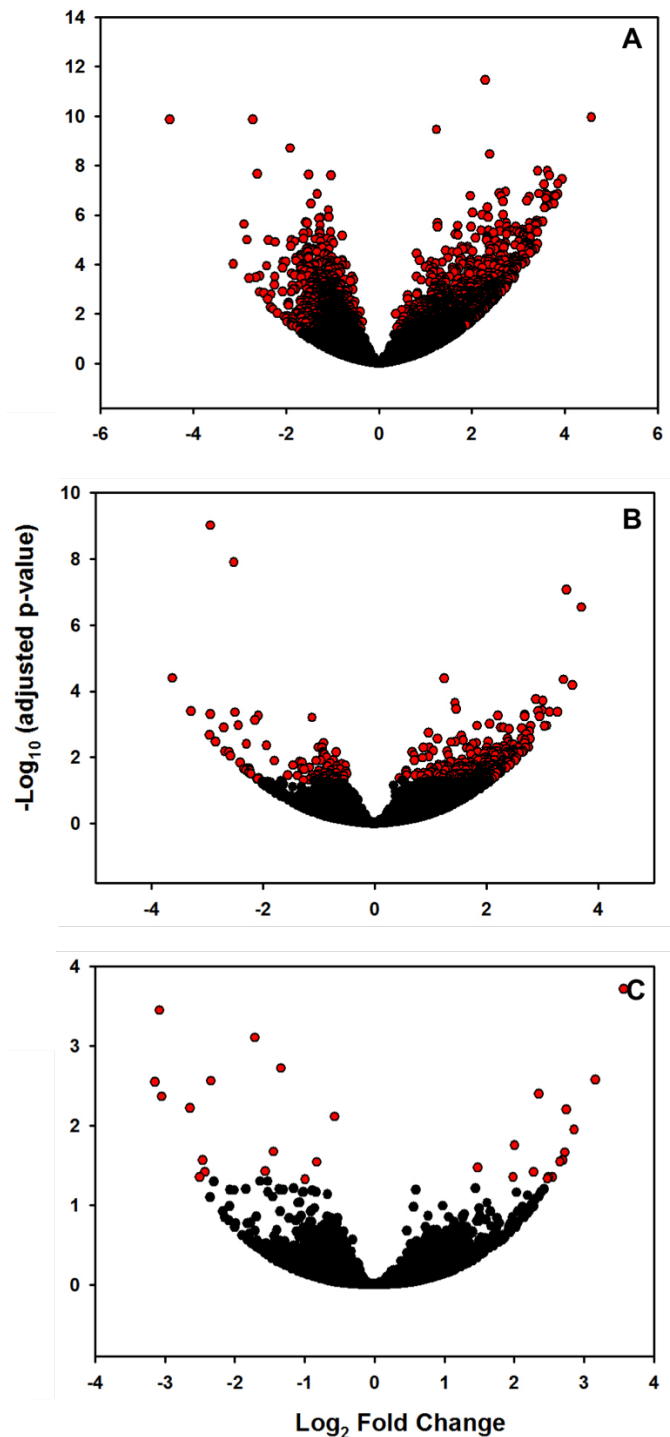
Figure 3.1. Volcano plots for expression of transcripts identified using DESeq2 in the 16°C vs. 22°C (A), the 16°C vs. 18°C (B), and the 18°C vs. 22°C (C) comparisons. For each comparison, $\log_2$ Fold Change values are expressed as the first temperature relative to the second temperature listed (e.g., in the 16°C vs. 22°C comparison, transcripts are over- or under-expressed in postlarvae reared at 16°C relative to those reared at 22°C). All differentially expressed (DE) transcripts with adjusted p-values ≤ 0.05 are indicated by the red circles. Over-expressed transcripts have $+\log_2$ Fold Change values, whereas under-expressed transcripts have $-\log_2$ Fold Change values.
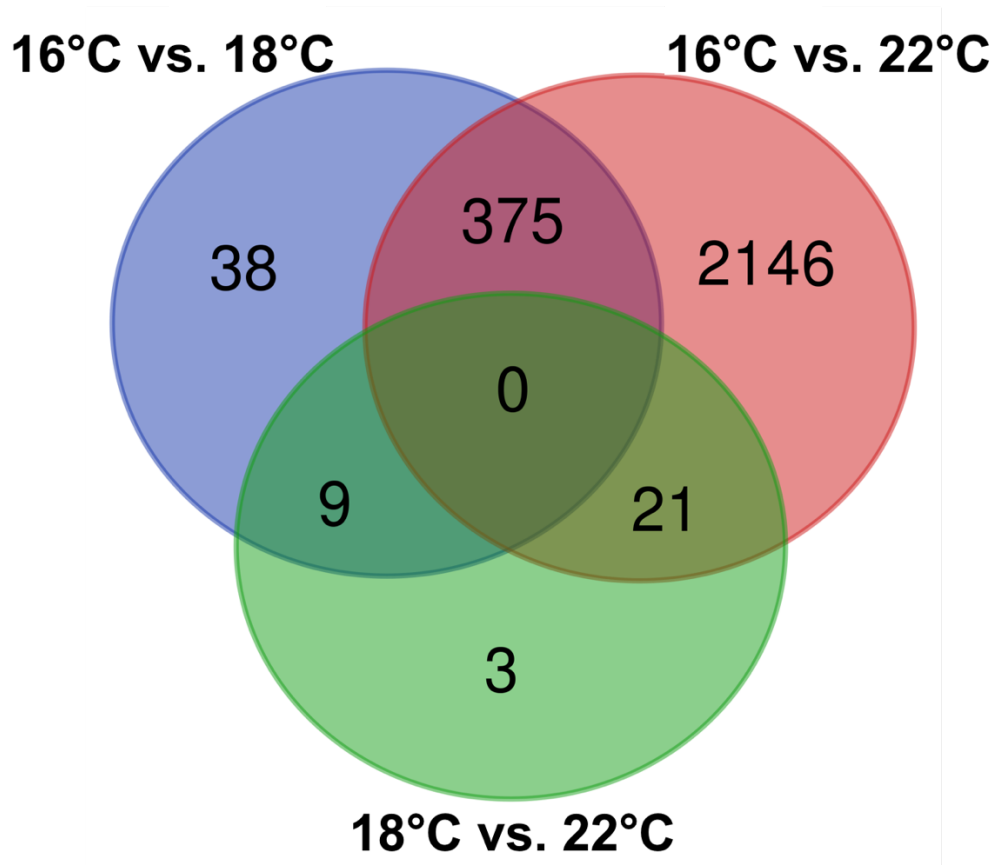
Figure 3.2. Venn diagram of all differentially expressed (DE; adjusted *p*-value ≤ 0.05) transcripts identified by DESeq2 in the various temperature treatment comparisons. Source: http://bioinformatics.psb.ugent.be/webtools/Venn/.
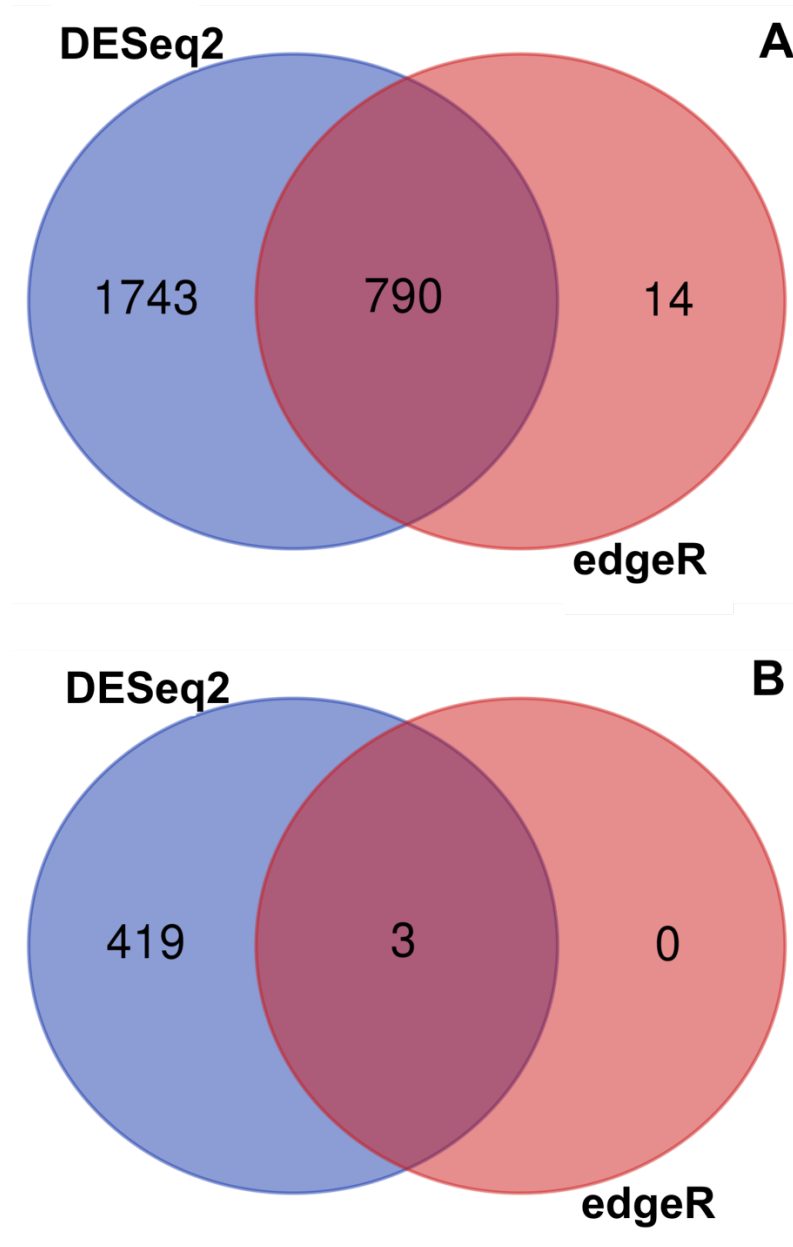
Figure 3.3. Venn diagrams of all differentially expressed (DE; adjusted *p*-value ≤ 0.05) transcripts identified by DESeq2 and edgeR for the 16°C vs. 22°C comparison (A) and 16°C vs. 18°C comparison (B). Source: http://bioinformatics.psb.ugent.be/webtools/Venn/.

3.4.3. Top 100 DE Transcripts

3.4.3.1. Comparison of Postlarvae Reared at 16°C vs. 22°C. Of the 2,542 DE transcripts identified in

the DESeq2 analysis, 53.3% and 46.7% were over- and under-expressed in postlarvae reared at 16°C

relative to 22°C, respectively (Table 3.2). Similarly, of the 805 DE transcripts identified in the edgeR

analysis, 58.1% and 41.9% were over- and under-expressed in postlarvae reared at 16°C relative to 22°C,

respectively (Table 3.2). From both statistical analyses, the top 10 GO terms affiliated with biological

processes in the significantly over-expressed ($+\log_2$FC) transcripts in postlarvae reared at 16°C relative to

22°C were related to the regulation of transcription (DNA-templated), transmembrane transport, cell

communication, and cellular processes (Table 3.3; Figure 3.4). The top 10 GO terms attributed to

molecular function included catalytic activity, structural constituent of the cuticle, and various "binding"-

related terms (Table 3.3; Figure 3.4). In contrast, the top 10 GO terms attributed to biological processes in

the significantly over-expressed transcripts in postlarvae reared at 22°C (i.e., under-expressed in

postlarvae reared at 16°C; $-\log_2$FC) included a number of terms affiliated with metabolism (e.g.,

metabolic process, biosynthetic process, and DNA metabolic process) and DNA replication (Table 3.3;

Figure 3.4), whereas the top 10 GO terms attributed to molecular function included catalytic activity,

oxidoreductase activity, aminoacyl-tRNA ligase activity, and several terms related to "binding" (Table

3.3; Figure 3.4).

Table 3.3. Top ten Gene Ontology (GO) terms affiliated with the greatest number of differentially expressed (DE; adjusted p-value ≤ 0.05) transcripts by treatment comparison. GO terms were generated for DE transcripts indicated by both DESeq2 and edgeR analyses for the 16°C vs. 22°C, (A) and (B), respectively, and from DESeq2 analysis for the 16°C vs. 18°C (C) and 18°C vs. 22°C (D) comparisons. The letters "C", "P", and "F" refer to GO terms attributed to cellular functions, biological processes, and molecular functions, respectively.

	Count	GO Term	GO Name
(A)			
	236	F:GO:0005515	Protein binding
	126	C:GO:0016021	Integral component of membrane
	126	F:GO:0005524	ATP binding
	102	F:GO:0042302	Structural constituent of cuticle
	100	F:GO:0003676	Nucleic acid binding
	75	P:GO:0055114	Oxidation-reduction process
	72	C:GO:0005634	Nucleus
	66	P:GO:0055085	Transmembrane transport
	63	C:GO:0016020	Membrane
	61	P:GO:0006508	Proteolysis
(B)			
	70	F:GO:0005515	Protein binding
	56	F:GO:0042302	Structural constituent of cuticle
	46	C:GO:0016021	Integral component of membrane
	34	F:GO:0005524	ATP binding
	28	P:GO:0055085	Transmembrane transport
	26	C:GO:0005634	Nucleus
	26	P:GO:0055114	Oxidation-reduction process
	21	F:GO:0003676	Nucleic acid binding

Table 3.3. Continued

21	F:GO:0003677	DNA binding
18	C:GO:0016020	Membrane

(C)

44	F:GO:0042302	Structural constituent of cuticle
26	F:GO:0005515	Protein binding
14	P:GO:0055114	Oxidation-reduction process
12	C:GO:0016021	Integral component of membrane
11	C:GO:0005576	Extracellular region
11	C:GO:0005634	Nucleus
11	F:GO:0003676	Nucleic acid binding
11	F:GO:0005524	ATP binding
11	P:GO:0006508	Proteolysis
10	P:GO:0006355	Regulation of transcription, DNA-templated

(D)

3	F:GO:0005515	Protein binding
2	C:GO:0005576	Extracellular region
2	C:GO:0016021	Integral component of membrane
2	F:GO:0008061	Chitin binding
2	F:GO:0022857	Transmembrane transporter activity
2	P:GO:0006030	Chitin metabolic process
2	P:GO:0055085	Transmembrane transport
1	C:GO:0005622	Intracellular
1	F:GO:0003713	Transcription coactivator activity
1	F:GO:0004198	Calcium-dependent cysteine-type endopeptidase activity
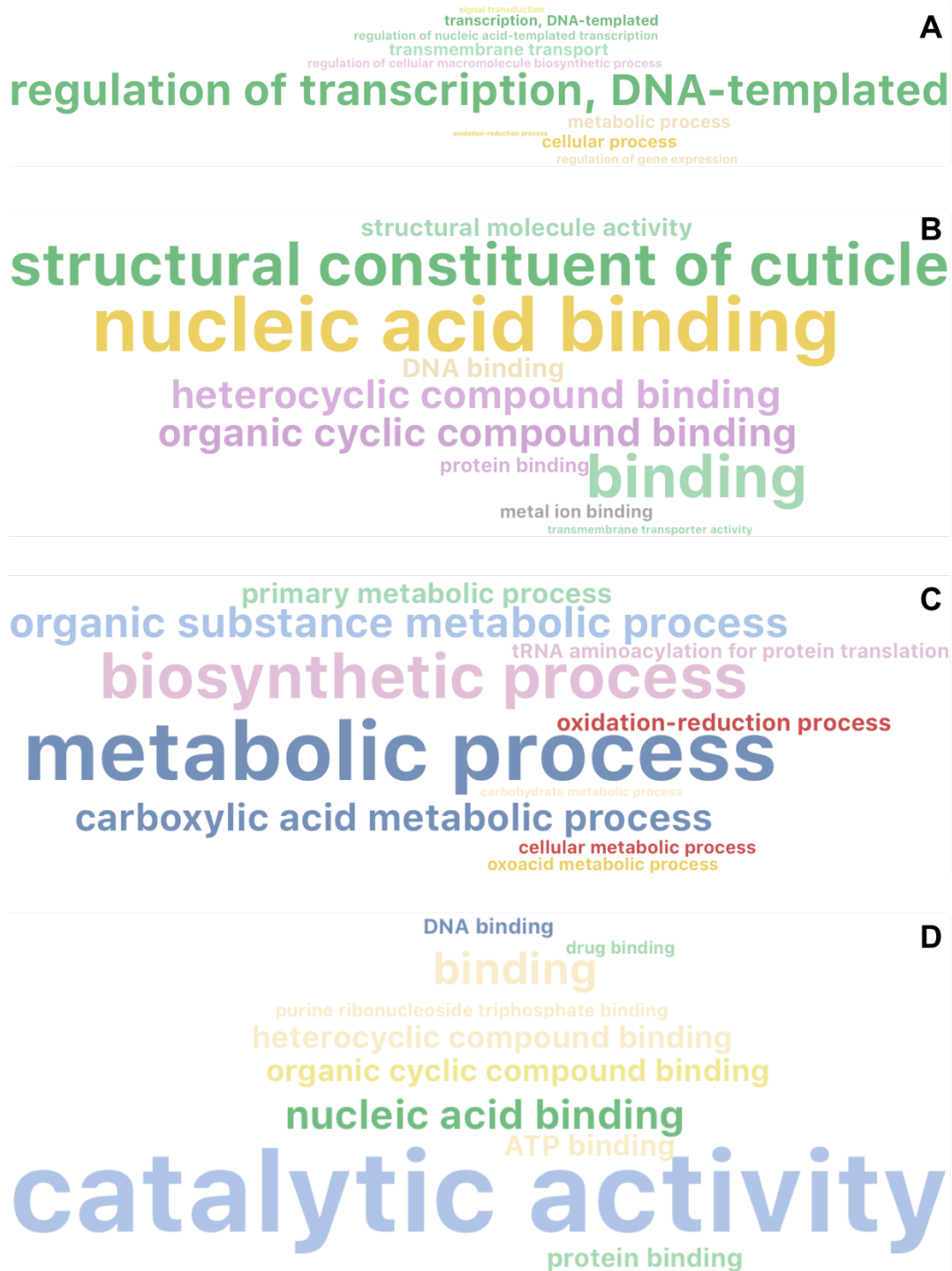
Figure 3.4. Word clouds of top 10 GO terms generated by Blast2GO for the 16°C vs. 22°C comparison. Panels (A) and (B) represent GO terms attributed to biological processes and molecular functions, respectively, for transcripts that were over-expressed in postlarvae reared at 16°C relative to 22°C. Panels (C) and (D) represent GO terms attributed to biological processes and molecular functions, respectively, for transcripts that were under-expressed in postlarvae reared at 16°C relative to 22°C. Importance of GO terms (i.e., frequency of occurrence) is represented by font size, and coloring is random. Figures were generated using a trial version of Blast2GO PRO.

KAAS pathway analysis indicated that over-expressed transcripts in the 16°C treatment included proteins involved in signaling and cellular processes, transcription, and the complement and coagulation cascade (Table A.1). Moreover, common IPS protein domains associated with these transcripts included those involved in transcription (e.g., Ets domain, pointed domain, and the orange domain), chitin-binding, immunity (e.g., Späetzle and the Alpha-2 macroglobulin bait domain), and cellular signaling (e.g., PDZ domain and the Roc domain; Figure 3.5). In contrast, KAAS pathway analysis indicated that the top 100 over-expressed transcripts in the 22°C treatment (i.e., under-expressed in postlarvae reared at 16°C) included proteins involved in a variety of metabolic processes (e.g., amino acid metabolism, carbohydrate metabolism, TCA cycle, glycolysis/gluconeogenesis, pyruvate metabolism, and lipid metabolism), DNA repair and replication processes, calcium ion signaling, the cell cycle (cell growth and death), ribosome biogenesis, and tRNA biogenesis (Table A.1). Similarly, these transcripts included IPS domains related to metabolism (e.g., the aldehyde dehydrogenase domain, the dihydrooroate dehydrogenase domain, the TauD/TfdA-like domain, and the transkelotase-like, pyrimidine-binding domain), as well as DNA replication and repair (e.g., MCM N-terminal, MCM domain, MCM AAA-lid domain; MCM OB domain; AAA+ ATPase domain, and the Ku70/Ku80 β barrel domain; Figure 3.5).
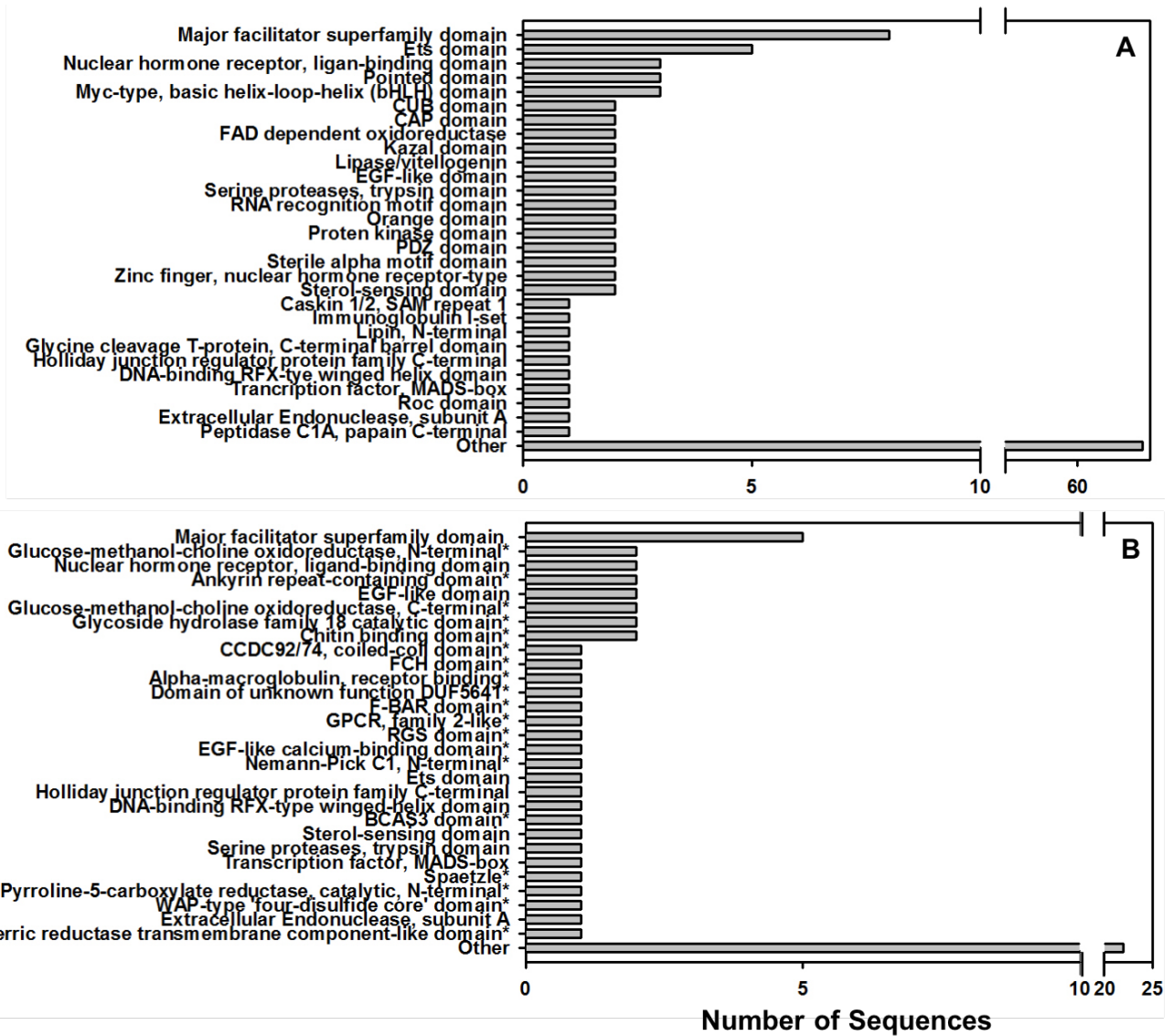
Figure 3.5. InterProScan protein domains associated with differentially expressed transcripts of the 16°C vs. 22°C comparison. Panels depict domains associated with transcripts that were over-expressed in postlarvae reared at 16°C relative to 22°C as identified by DESeq2 (A) and edgeR (B) analysis, and domains associated with transcripts that were under-expressed in postlarvae reared at 16°C relative to 22°C as identified by DESeq2 (C) and edgeR (D). Asterisks (*) indicate protein domains uniquely identified via edgeR analysis.

Figure 3.5. continued
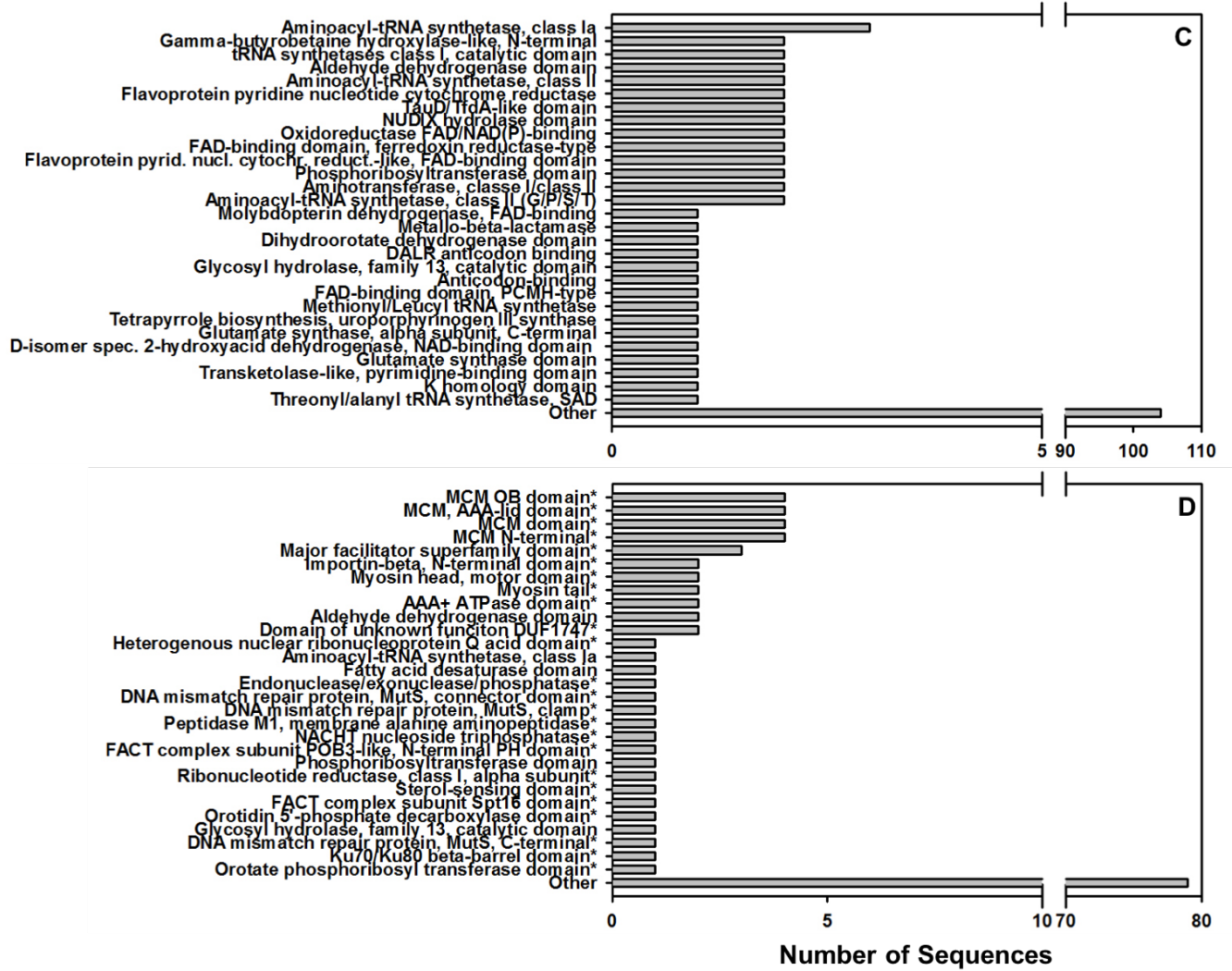
We identified a total of 38 genes of interest (GOIs) affiliated with significantly DE expressed transcripts in postlarvae reared at 16°C vs. 22°C, 26 of which were uniquely identified in this treatment comparison (Table 3.4; Figure 3.6). Twenty-six GOIs were annotated to transcripts over-expressed in postlarvae reared at 16°C, including 16 annotated to genes involved in cuticle formation or chitin degradation (e.g., chitinase, gastrolith protein 18.2, and early cuticle proteins 2, 5, and 6), and 10 annotated to proteins involved in the innate immune response (e.g., antimicrobial peptide type 2 precursor, crustin, Spätzle 4, Alpha 2-macroglobulin isoform 2, and hormone receptor; Table 3.4; Figure 3.6). In contrast, we identified 12 GOIs affiliated with transcripts over-expressed in postlarvae reared at 22°C, including eight annotated to proteins involved in cell division and DNA replication (e.g., DNA replication licensing factors MCM2, MCM3, MCM5, and MCM7) and five annotated to proteins affiliated with metabolism or energy demanding processes (e.g., acyl-CoA Δ-9 desaturase and Δ-9 desaturase; Table 3.4; Figure 3.6).

Table 3.4. List of genes of interest (GOIs) that correspond to transcripts that were over- (A) or under-expressed (B) in all treatment comparisons. GOI descriptions were determined by annotation against NCBI nr protein databases. GOIs with an asterisk (*) were common across both the 16°C vs. 22°C and the 16°C vs. 18°C treatment comparisons. For the 16°C vs. 22°C comparison, additional GOIs identified by edgeR are indicated by an obelisk (†).

	Comparison	GOI Description	Function of GOI
(A)	16°C vs. 22°C	Strongly chitin-binding protein*	Structural constituent of cuticle
		Chitin-binding protein*	Structural constituent of cuticle
		Cuticle protein 19.8*	Structural constituent of cuticle
		Gastrolith protein 18.2	Formation of chitin-based gastrolith matrix
		Chitinase	Breaks down glycosidic bonds in chitin
		Chitinase 2, partial	Chitin binding; Hydrolase activity; Carbohydrate metabolic process
		Calcification-associated soluble matrix protein 2 (Casp-2)	Chitin binding domain; Calcification of the cuticle
		Peritrophin*	Chitin binding; Chitin metabolic processes
		Peritrophin 44-like protein	Chitin binding; Involved in antibacterial innate immunity via peritrophic membrane formation
		Early cuticle protein 2	Structural constituent of cuticle
		Early cuticle protein 5	Structural constituent of cuticle
		Early cuticle protein 6	Structural constituent of cuticle
		Cuticle protein*	Structural constituent of cuticle

47

Table 3.4 continued

	Cuticle-like protein*	Structural constituent of cuticle
	Cuticle 7-like protein	Structural constituent of cuticle
	Cuticle protein 7†	Structural constituent of cuticle
	Antimicrobial peptide type 2 precursor	Peptidase inhibitor activity; Involved in innate immunity
	Crustin	Antimicrobial peptide; Involved in innate immunity
	Spätzle 1 (Spz1)*	Spätzle-like protein 1; Involved in innate immunity
	Spätzle 3 (Spz3)*	Spätzle-like protein 3; Involved in innate immunity
	Spätzle 4†	Spätzle-like protein 4; Involved in innate immunity
	Alpha 2-macroglobulin (A2M)*	Non-specific protease inhibitor; Involved in innate immunity
	Octopamine receptor β-2R†	Adrenergic receptor activity; Neuromodulator and neurotransmitter
	Alpha 2-macroglobulin isoform 2†	Non-specific protease inhibitor; Involved in innate immunity
	Hormone receptor, partial†	Anti-apoptosis and anti-inflammatory roles in innate immunity
16°C vs. 18°C	Chitin-binding protein, partial	Structural constituent of cuticle
	Cuticle protein AMP13.4	Structural constituent of cuticle; Antimicrobial peptide; Involved in innate immunity
	Spätzle	Spätzle-like protein; Involved in innate immunity
	Crustin 2	Antimicrobial peptide; Involved in innate immunity
	Arrestin	Regulates signal transduction at G-protein coupled receptors

Table 3.4 continued

	Glutamate-gated chloride channel, partial	Extracellular ligand-gated ion channel activity; Transmembrane signaling receptor activity
	Juvenile hormone esterase-like carboxylesterase 1	Hydrolase activity
	DNA/RNA non-specific endonuclease	Nucleic acid and metal ion binding; Cleaves phosphodiester bonds within polynucleotide chains
	Vrille	DNA-binding transcription factor activity
18°C vs. 22°C	Obstructor F	Chitin binding; Chitin metabolic processes
	Spondin 2-like	May bind to bacteria and act as an opsonin

(B)

16°C vs. 22°C	Acyl-CoA Δ-9 desaturase	Fatty acid metabolism; Cell membrane fluidity regulation; Oxidoreductase activity
	Δ-9 desaturase†	Lipid metabolism; Fatty acid biosynthetic process
	L-fucose kinase	ATP binding, kinase activity
	NADH dehydrogenase subunit 2*	Core subunit of mitochondrial membrane respiratory chain NADH dehydrogenase; Electron transport chain
	Sarco-endoplasmic reticulum Ca^{2+}-ATPase pump (SERCA)*	Calcium-transporting ATPase activity; ATP binding; Calcium ion transmembrane transport
	DNA primase-like protein	Involved in DNA replication; Synthesizes small RNA primers for Okazaki fragments
	p53 protein	DNA-binding transcription factor activity; Apoptotic processes

Table 3.4 continued

	DNA replication licensing factor MCM2†	DNA replication initiation; Negative regulation of DNA helicase activity
	DNA replication licensing factor MCM3†	DNA binding; DNA replication initiation
	DNA replication licensing factor MCM5†	DNA replication initiation
	DNA replication licensing factor MCM7†	DNA replication initiation
	FACT complex subunit SPT16†	Heterodimeric protein complex that impacts RNA polymerase II transcription elongation
16°C vs. 18°C	Calmodulin	Binds to Ca^{2+}; Regulates enzymes, ion channels, and aquaporins
	Calcium-activated chloride channel regulator 2, partial	Modulates chloride current across plasma membrane in Ca^{2+}-dependent manner
	Calcium/calmodulin-dependent protein kinase type 1 isoform X2	Cell cycle regulation; Calmodulin binding
	Alpha 2-macroglobulin (A2M)	Non-specific protease inhibitor; Involved in innate immunity
18°C vs. 22°C	Clottable protein 2	Lipid transporter activity; Lipid transport
	Calpain-B-like protein, partial	Calcium-dependent cysteine-type endopeptidase activity; Ca^{2+} binding; Proteolysis
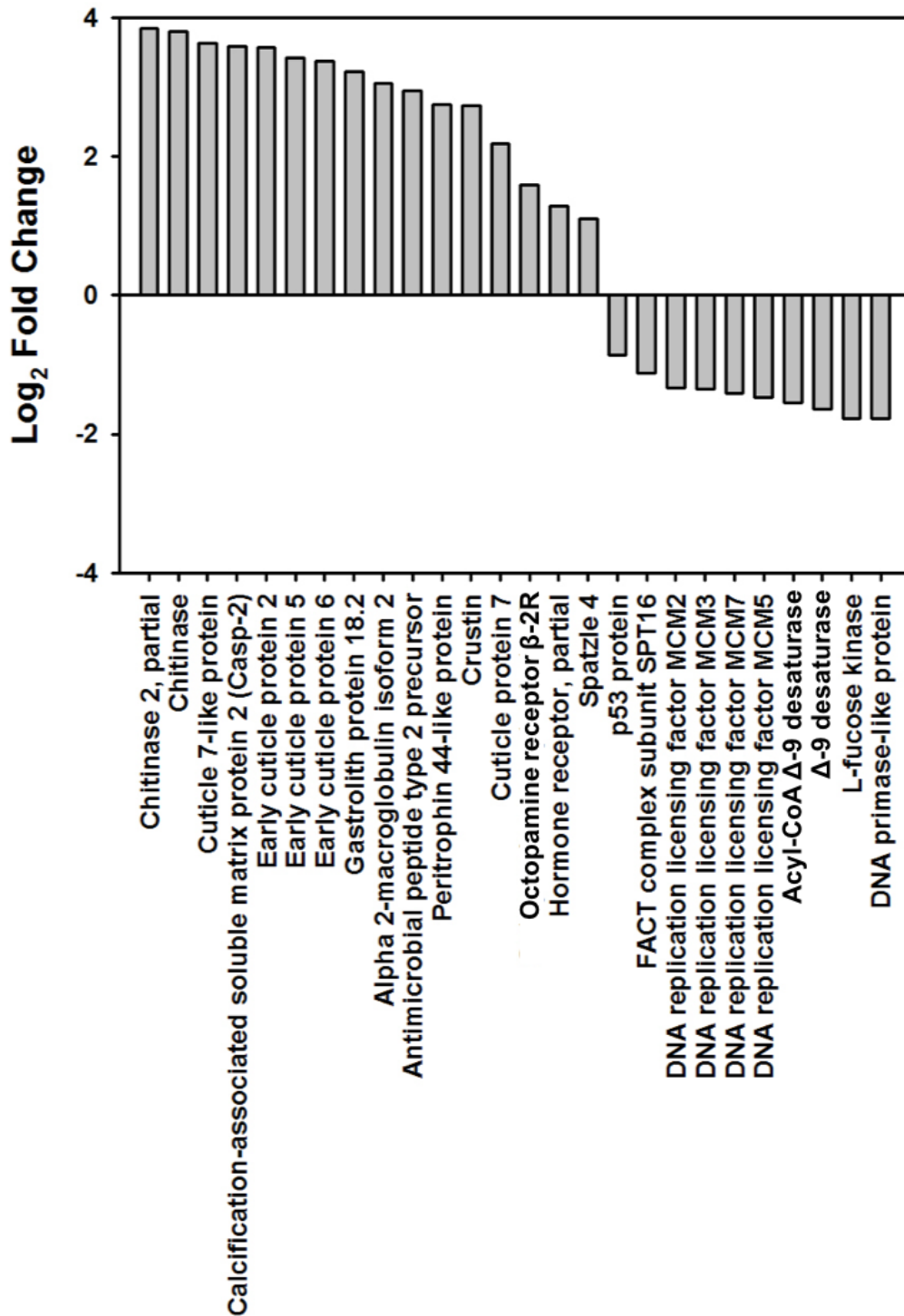
Figure 3.6. Expression levels (log$_2$ Fold Change) of genes of interest unique to the 16°C vs. 22°C treatment comparison. Positive and negative log$_2$FC values indicate over- and under-expressed transcripts, respectively, in postlarvae reared at 16°C relative to those reared at 22°C. Labels refer to Blast2GO descriptions.

3.4.3.2. Comparison of Postlarvae Reared at 16°C vs. 18°C. Of the total 422 DE transcripts identified in the DESeq2 analysis, 58.1% were over-expressed (+log_2FC) and 41.9% were under-expressed (-log_2FC) in postlarvae reared at 16°C relative to 18°C (Table 3.2). The top 10 GO terms in all categories were similar to those observed in the 16°C vs. 22°C comparison (Table 3.3), and proteins annotated to DE transcripts in this treatment comparison were generally involved in similar pathways identified via KAAS for the 16°C vs. 22°C comparison (Table A.1). IPS domains associated with the top 100 over- and under-expressed transcripts in the 16°C relative to the 18°C treatment included similar domains identified in 16°C vs. 22°C comparison. However, transcripts over-expressed in postlarvae reared at 16°C relative to 18°C included some additional domains associated with cellular signaling (e.g., the arrestin-like N-terminal and the neurotransmitter-gated ion-channel ligand binding domain) and transcription (e.g., the basic-leucine zipper domain and the La-type HTH domain; Figure 3.7).

We identified 25 GOIs in this treatment comparison, 13 that were uniquely detected in postlarvae exposed to 16°C vs. 18°C during development (Table 3.4; Figure 3.8). Nineteen GOIs were affiliated with transcripts over-expressed in postlarvae reared at 16°C compared to 18°C, including eight annotated proteins involved in cuticle formation (e.g., cuticle protein AMP 13.4), six annotated to proteins involved in innate immunity (e.g., Spätzle and crusin 2), and three annotated to proteins affiliated with developmental processes (e.g., arrestin and vrille; Table 3.4; Figure 3.8). In contrast, eight GOIs were affiliated with transcripts over-expressed in postlarvae reared at 18°C relative to 16°C, including four annotated to proteins related to or dependent upon calcium ion binding (e.g., calmodulin and calcium-activated chloride ion channel regulator 2; Table 3.4; Figure 3.8).
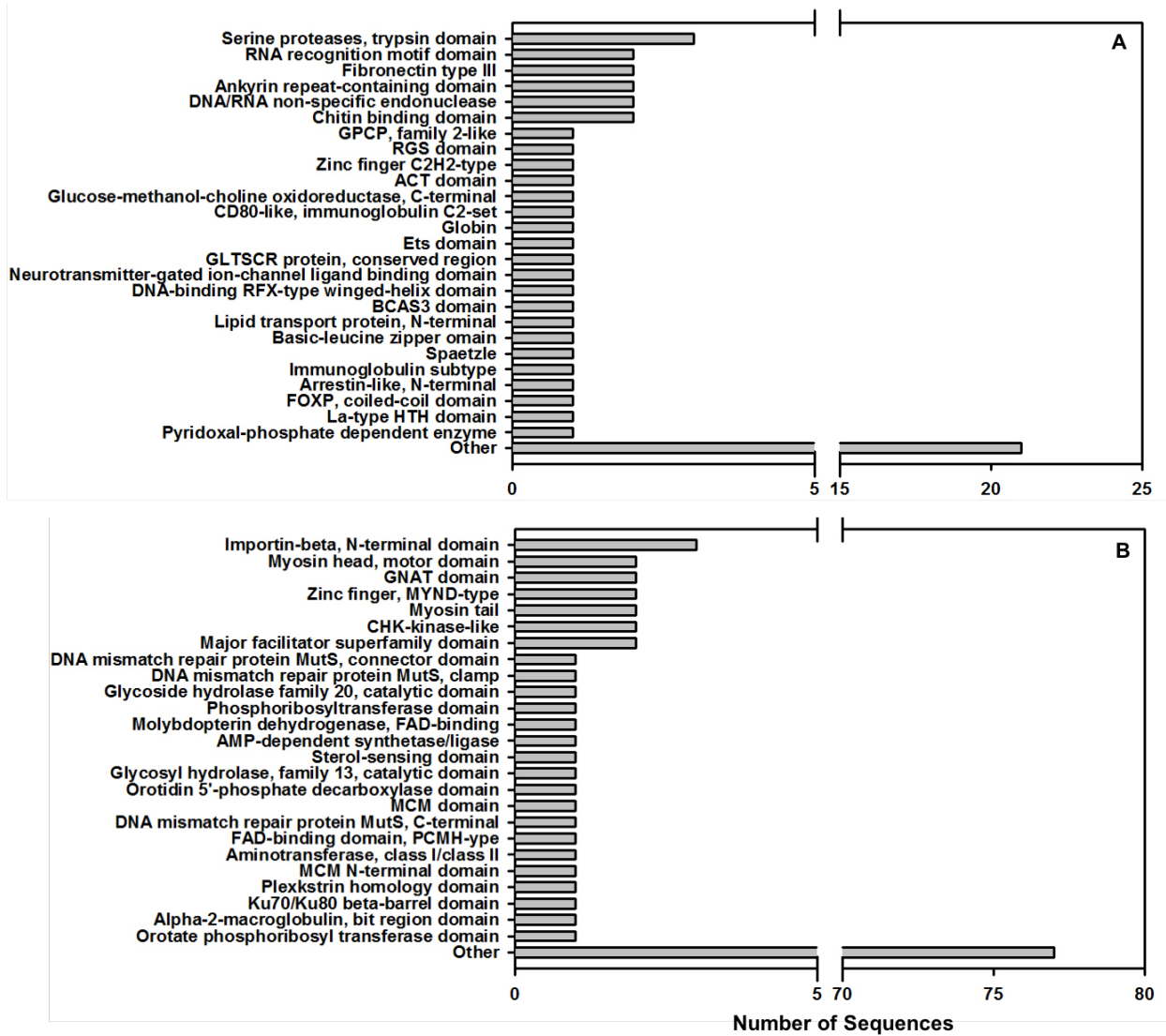
Figure 3.7. InterProScan protein domains associated with transcripts that were over-expressed (A) and under-expressed (B) in postlarvae reared at 16°C relative to 18°C.
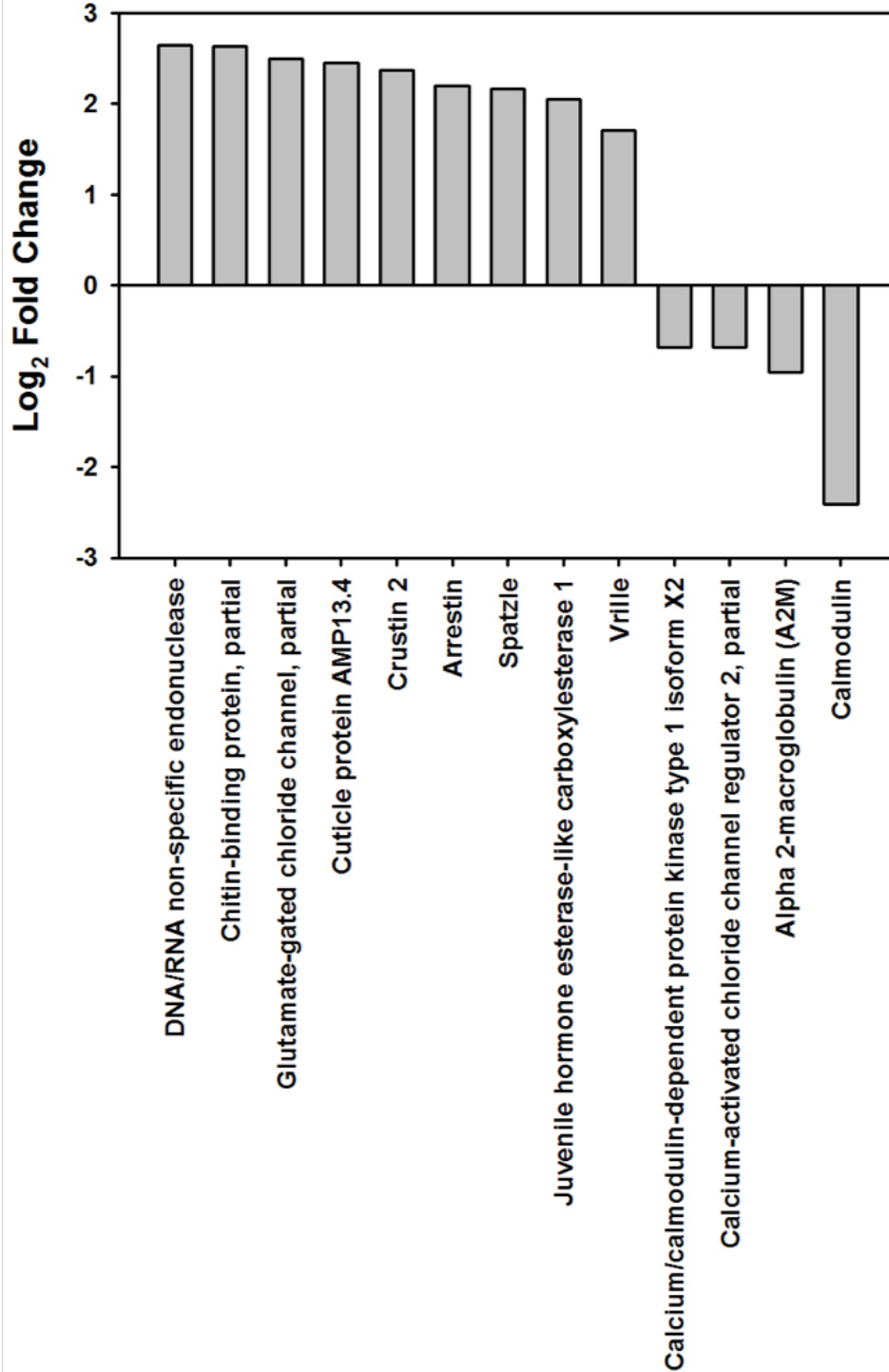
Figure 3.8. Expression levels (log$_2$ Fold Change) of genes of interest unique to the 16°C vs. 18°C treatment comparison. Positive and negative log$_2$FC values indicate over- and under-expressed transcripts, respectively, in postlarvae reared at 16°C relative to those reared at 18°C. Labels refer to Blast2GO descriptions.

3.4.3.3. Comparison of Postlarvae Reared at 18°C vs. 22°C. Due to the lack of DE transcripts in the 18°C vs. 22°C comparison, most of the GO terms affiliated with either over- or under-expressed transcripts occurred only once (Table 3.3). Transcripts that were both over- and under-expressed in postlarvae reared at 18°C relative to 22°C were affiliated with proteins involved in metabolism and the ubiquitin system according to KAAS pathway analysis (Table A.1). However, IPS protein domains associated with or regulated by calcium ions and protein domains associated with oxygen transport (e.g., hemocyanin-related domains) were more prominent in transcripts that were over-expressed in postlarvae reared at 22°C compared to 18°C (Figure 3.9). We also identified a total of four GOIs associated with the DE transcripts that were unique to this treatment comparison (Table 3.4; Figure 3.10). Transcripts over-expressed in postlarvae reared at 18°C were annotated to proteins involved in chitin binding, whereas transcripts over-expressed in postlarvae reared at 22°C annotated to proteins affiliated with lipid transport and calcium-dependent activity (Table 3.4; Figure 3.10).
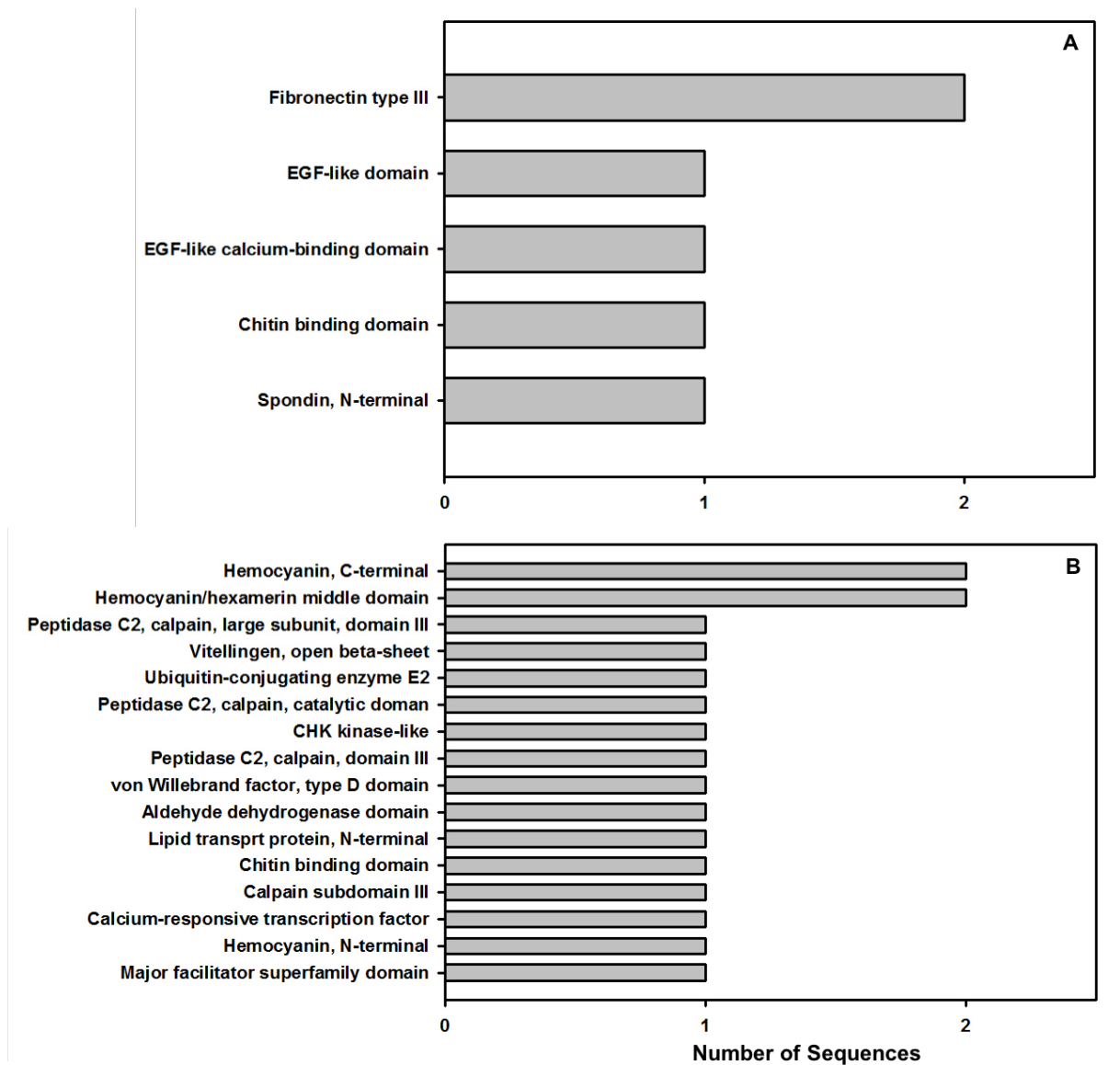
Figure 3.9. InterProScan protein domains associated with transcripts that were over-expressed (A) and under-expressed (B) in postlarvae reared at 18°C relative to 22°C.
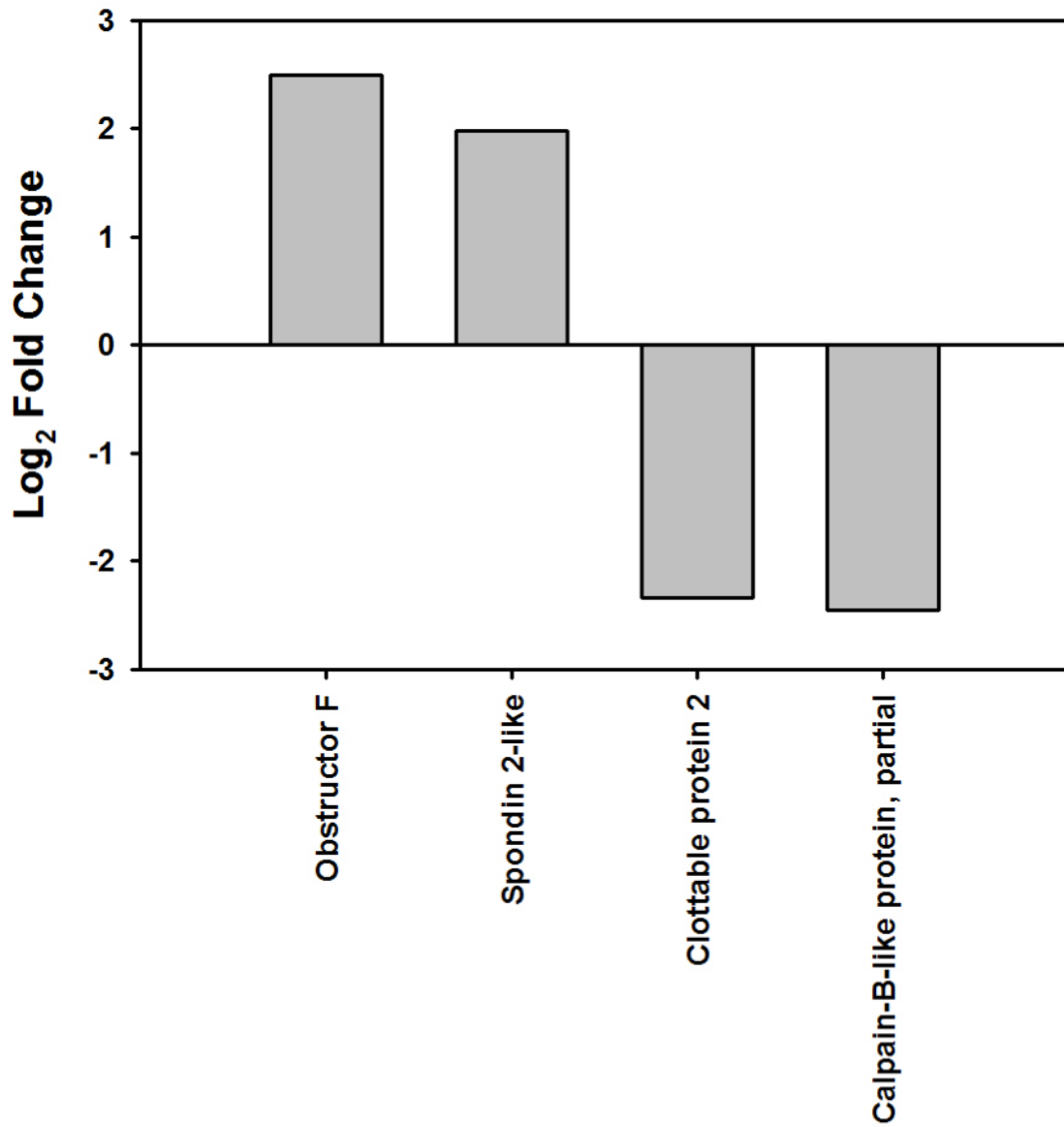
Figure 3.10. Expression levels (log$_2$ Fold Change) of genes of interest identified the 18°C vs. 22°C treatment comparison. Positive and negative log$_2$FC values indicated over- and under-expressed transcripts, respectively, in postlarvae reared at 18°C relative to those reared at 22°C. Labels refer to Blast2GO descriptions.

3.5. Discussion

Transcriptomics has proven a useful approach for understanding changes in cellular processes due to environmental stressors in a variety of species (Lockwood et al., 2010; Moya et al., 2012; Evans et al., 2017; Goncalves et al., 2017; Wong et al., 2018). We explored how exposure to temperatures mimicking projected ocean warming during development alters the postlarval American lobster transcriptome. Postlarvae reared under current average summer temperatures (16°C) of the mid-coast Maine region exhibited a significant over-expression of transcripts likely associated with the immune response and cuticle formation compared to lobsters exposed to either 18°C or 22°C (Table 3.4; Figures 3.6, 3.8). In contrast, as exposure temperature increased, postlarvae exhibited a significant over-expression of transcripts associated with metabolic turnover and DNA replication and repair relative to those exposed to cooler temperatures. This suggests a major shift in the transcriptome that reflects a strong emphasis on oxygen- and energy-demanding processes at the potential cost of reduced immunity and development as a consequence of warming. We therefore focus on the potential risks to *H. americanus* due to this trade-off and how survival post-settlement may be impacted under a changing climate.

3.5.1. Compromised Innate Immunity

Although invertebrates lack adaptive immunity, they possess a complex innate immune system that is capable of distinguishing self from non-self, eliminating pathogens, and healing wounds while repairing cellular damage using both humoral and cellular mechanisms (Hoffman, 2003; Royet, 2004; Cerenius and Soderhall, 2011). In *H. americanus*, this system consists of a variety of pattern recognition receptors (PRRs) and effector cells that recognize and bind to pathogen associated molecular patterns (PAMPs; highly conserved molecular structures common and unique to microorganisms – Ghosh et al., 2012); antimicrobial peptides (AMPs), which are small, cationic, amphipathic molecules that are active against Gram-negative and Gram-positive bacteria, yeasts, fungi, various parasites, and enveloped viruses (Zasloff et al., 2002); coagulation and melanization pathways; and PRRs similar to the vertebrate complement system (Clark and Greenwood, 2016; Bowden, 2017). Postlarvae reared under 16°C significantly over-expressed transcripts associated with the innate immune response 2.2- to 8.3-fold (log$_2$

FC values of 1.1 – 3.0) when compared to postlarvae reared under warmer temperatures. These included transcripts annotated to proteins that exhibit peptidase inhibitor activity (AMP type 2 precursor, crustin, crustin 2 – Rosa et al., 2007; Pisuttharachai et al., 2009; Kim et al., 2013); Toll-like receptors (TLR), which are essential components of the TLR-mediated NF-kB pathway that induces an immune response via immune gene expression regulation (Spätzle 1, 3, and 4 – Wang et al., 2012; Clark and Greenwood, 2016); non-specific protease inhibitors that bind to and neutralize pathogenic proteases (A2M and A2M isoform 2 – Lin et al, 2008; Ma et al., 2010); and an anti-apoptosis and anti-inflammatory factor (hormone receptor – Wang et al., 2018; Tables 3.4, A.1; Figures 3.6, 3.8). This indicates that ocean warming reduces the expression of components involved in a variety of immune pathways, potentially increasing disease susceptibility under warming. Postlarvae are at risk for a variety of microbial diseases (Fisher et al., 1978), the spread of which could be impacted by increasing temperature. In adult *H. americanus*, warming events have been linked to mass die offs and an increased incidence of epizootic shell disease (ESD) across the southern extent of the species range (Pearce and Balcolm, 2005; Wahle et al., 2009). While ESD prevalence has remained < 2% in lobsters sampled along the Maine coast (relative to 20 – 30 % in Southern New England), the highest levels of disease prevalence occurred in 2013 and 2017, which followed the two warmest years in the region since 2005 (ME DMR 2017). Progression of ESD is accelerated under warmer temperatures (Barris et al., 2018), and estimates predict that population-level impacts of ESD may increase as ocean temperatures continue to rise (Groner et al., 2018). Although much of the research on ESD in *H. americanus* has focused on adults, postlarvae may be vulnerable to this disease due to the relatively thin exoskeleton at this stage (Fisher et al., 1976, 1978). This may be particularly important in the context of ocean warming as we found that postlarvae reared under 16°C also expressed transcripts involved in cuticle formation and chitin metabolism at levels 4.5 – 14.4 ($\log_2$ FC values of 2.2 – 3.9) times greater than those reared at 18°C and 22°C (Tables 3.4, A.1; Figures 3.6, 3.8). These transcripts were annotated to proteins involved in the mineralization of the pre-exuvial cuticle (early cuticle proteins 2, 5, and 6 – Shafer et al., 2009), calcification of the exoskeleton (calcification-associated soluble matrix protein 2 – Inoue et al., 2008), ecdysis (chitinase and chitinase 2 – Fujitani et

al., 2014), and chitin-binding processes (cuticle protein and cuticle-like protein – Anderson, 1999; Inoue et al., 2003), suggesting that multiple aspects of proper exoskeletal formation may be compromised under warming conditions. Although postlarvae have a much higher molt frequency, and presumably greater chance of removing ESD than adults, they may encounter difficulties during molting due to adhesion of tissues to the cuticle (Fisher et al., 1978), which could be compounded by improper cuticle development and potentially lead to molt death syndrome.

Together, these data indicate that postlarval *H. americanus* exposed to both moderate (18°C) and severe (22°C) warming scenarios during development may be at a greater risk to pathogens due to compromisation of both the primary defense against pathogens (the exoskeleton) and multiple components of the innate immune system. Previous molecular studies of adult *H. americanus* have demonstrated the ability of lobsters to mount both pathogen- and tissue-specific immune responses (Clark et al., 2013a, 2013b, 2013c; Clark et al., 2015). To our knowledge, similar studies have not been conducted on the postlarval stage, especially in the context of environmental change. Future research would therefore benefit from assessing changes to the larval transcriptome following an immune challenge to more fully understand how a changing climate might impact disease susceptibility.

3.5.2. Elevated Energetic Demands

Physiological processes are highly dependent on temperature, and an increase in temperature by just 1°C may increase metabolic rates by 5 – 10%, greatly increasing oxygen and energy demands (Somero et al., 2015, 2017). In order to meet these energetic demands, organisms must generate ATP by either substrate-level phosphorylation (via glycolysis and TCA cycle) or oxidative phosphorylation (via the ATP synthase complex; Sokolova et al, 2012; Somero et al., 2017), as well as produce the reducing equivalents (NADH, NADPH, and $FADH_2$) needed to deliver electrons to the electron transport chain to drive oxidative phosphorylation (Somero et al., 2017). Postlarvae reared under 22°C significantly over-expressed transcripts related to amino acid metabolism, carbohydrate metabolism, the TCA cycle, glycolysis/gluconeogenesis, pyruvate metabolism, and lipid metabolism (as indicated via KAAS pathway analysis; Table A.1). We also found that lobsters reared under 22°C expressed transcripts annotated to

acyl-CoA Δ-9 desaturase and Δ-9 desaturase, proteins involved in fatty-acid metabolism (Guo et al., 2013), at levels that were 2.9 and 3.1 times greater, respectively, than postlarvae reared at 16°C (Figure 3.6). Furthermore, expression of transcripts annotated to NADH-dehydrogenase subunit 2 (also termed NADH-ubiquinone oxidoreductase chain 2, ND2) was 7.1- and 4.9-fold higher in postlarvae reared at 22°C and 18°C, respectively, relative to those at 16°C. ND2 functions as the core subunit of Complex I in the electron transport chain, and is responsible for the initial transfer of electrons from NADH to the immediate receptor, ubiquinone (Kim et al., 2011; Somero et al. 2017), which suggests an increase in electron transport under warming. Similarly, purple urchins (*S. purpuratus*) collected from southern portions of its distribution along the West Coast of the USA exhibited higher expression levels of genes related to metabolism, electron transport, and protein translation termination relative to urchins collected from northern sites that were 5 – 8°C cooler in temperature when reared under common garden conditions (Pespeni et al., 2013). Moreover, Pespeni et al. (2013) demonstrated that southern *S. purpuratus* likely possess a greater scope for growth (the difference between energy input as food and output as respiratory metabolism) based on these genetic differences, which was corroborated by a 10% increase in the rate of re-growth of urchin spines relative to northern urchins. Larval development time in *H. americanus* is significantly reduced in lobsters reared under 22°C relative to 16°C (Harrington et al., 2019), and postlarvae reared at 22°C significantly over-expressed transcripts affiliated with DNA repair and replication processes, cell cycle (cell growth and death), and tRNA biogenesis (KAAS pathway analysis; Table A.1). Additionally, postlarvae reared at 22°C expressed transcripts annotated to genes involved in DNA replication initiation and elongation (DNA primase-like protein and DNA replication licensing factors MCM2, MCM3, MCM5, and MCM7) and transcription elongation (FACT complex subunit SPT16) at levels that were 2.2 – 3.4 times greater than those reared at 16°C (Figure 3.6). These data suggest that postlarvae were likely able to meet the ATP demands associated with development and growth under warming conditions in a laboratory setting. However, elevated aerobic metabolism cannot be maintained if ATP supply (i.e., food availability) does not match ATP demand (Sokolova et al., 2012). Here, developing lobsters were fed live *Artemia* spp. to satiation and were thus not food limited up to

stage IV; however, recent research suggests a potential mismatch between the natural timing of *H. americanus* settlement and the peak abundance of a major food source, *Calanus finmarchicus*, under warming conditions (Carloni et al., 2018). It is therefore possible that postlarval *H. americanus* will be unable to meet the increasing energy demands associated with ocean warming due to declines in prey availability, which could result in reduced post-settlement survival in the face of future change.

3.5.3. Caveats

One major caveat associated with transcriptomics is that concentrations of mRNAs and corresponding proteins cannot be considered proportional without validation due to the differential lifetimes and translation rates of mRNAs (Lesk, 2013; Evans, 2015). Additional challenges arise for non-model organisms that lack a completely sequenced genome, as the amount of functionally annotated genetic information available on searchable databases is generally lacking and restricted to highly conserved pathways (Conesa et al., 2016). This presents challenges in discovering novel genetic adaptations that are unique to groups found in challenging environments (Clark and Greenwood, 2016). Other challenges include determining the appropriate sample size, accounting for alternative splicing, and integration with other types of data (e.g., DNA sequencing, DNA methylation, microRNAs – Conesa et al., 2016). These and additional challenges affiliated with pathway analyses continue to be addressed through the advent of new technological approaches (Grabherr et al., 2011; Khatri, 2012). However, transcriptomic approaches alone may not always indicate physiological changes in response to a changing environment. Transcriptomics focuses primarily on differentially expressed genes with large fold changes; however, these genes are often considered dispensable and redundant in function and may contribute only marginally to overall fitness levels relative to constitutively expressed "hub" genes that exhibit stable expression levels but have huge impacts on the expression or post-translational modifications of downstream genes in response to environmental stressors (Evans, 2015). Moreover, understanding protein activity and changes in energy allocation provides a more robust assessment of fitness during environmental stress (Evans, 2015; Pan et al., 2015), demonstrating the importance of supplementing transcriptomic data with other metrics of physiology in order to understand the full

organismal response to a changing environment. Finally, it is important to acknowledge the potential for contaminating eukaryotes (e.g., ciliates that may occur on or in the species of interest) to influence the results of transcriptomic analyses. Exercising caution while reviewing blastX hits during the annotation process can help eliminate suspect annotations prior to analyses, particularly in non-model species.

3.5.4. Concluding Remarks

We observed a shift in the postlarval lobster transcriptome as a result of exposure to warming conditions during development. Postlarvae reared under current summer conditions in the mid-coast Maine region over-expressed transcripts related to immunity and cuticle formation relative to those reared under temperatures that were 2°C and 6°C warmer. However, as rearing temperature increased, the abundance of significantly over-expressed transcripts affiliated with metabolic turnover increased, suggesting a cellular focus on meeting the demands of increased metabolic rates under warming at the potential expense of the immune response. Postlarval lobsters are at risk to a number of pathogens upon settlement, the spread of which may be enhanced under warming ocean temperatures. Postlarvae may also be particularly vulnerable to disease when experiencing dietary deficiencies (Fisher et al., 1976), which may already be contributing to post-settlement mortality in *H. americanus* as the zooplankton assemblage shifts as a consequence of warming (Carloni et al., 2018). Insufficient resources may also increase post-settlement mortality if lobsters are unable to meet the energetic and oxygen demands of a warming environment due to Q_{10} effects. Future efforts should focus on validating the findings presented here via RT-qPCR, as well as conducting subsequent physiological and behavioral assays to determine the additional downstream impacts of the observed changes in the transcriptome of *H. americanus* post-settlement. We also acknowledge that postlarval lobsters will not face ocean warming in isolation and suggest that future research should also explore changes in the transcriptome in the context of multiple environmental factors (e.g., warming, acidification, and reduced oxygen availability).

CHAPTER 4

OCEAN ACIDIFICATION ALTERS THERMAL CARDIAC PERFORMANCE, HEMOCYTE ABUNDANCE, AND HEMOLYMPH CHEMISTRY IN SUBADULT AMERICAN LOBSTERS *HOMARUS AMERICANUS* H. MILNE EDWARDS, 1837 (DECAPODA: MALCOSTRACA: NEPHROPIDAE)

4.1. Chapter Abstract

Increased anthropogenic input of carbon dioxide into the atmosphere has caused widespread patterns of ocean acidification (OA) and increased the frequency of extreme warming events. We explored the sublethal effects of OA on the hemolymph chemistry and physiological response to acute thermal stress in the American lobster (*Homarus americanus* H. Milne Edwards, 1837). We exposed subadult lobsters to current or predicted end-century pH conditions (8.0 and 7.6, respectively) for 60 days. Following exposure, we assessed hemolymph L-lactate and calcium concentrations (as indicators of oxygen carrying capacity), ecdysterone concentrations, total protein content, and total hemocyte counts (THCs) as an indicator of immune response. We also assessed cardiac performance in the context of an acute warming event using impedance pneumography. Calcium, total protein, and ecdysterone concentrations were not significantly altered ($P \geq 0.10$) by OA exposure. Control lobsters, however, had significantly higher levels of L-lactate concentrations compared to acidified lobsters, suggesting reduced oxygen carrying capacity under OA. THCs were also 61% lower in acidified vs. control lobsters, suggesting immunosuppression under chronic OA. Lobsters exposed to acidified conditions exhibited reduced cardiac performance under acute warming as indicated by significantly lower ($P = 0.040$) Arrhenius Break Temperatures compared to control lobsters. These results suggest that although some physiological endpoints of American lobster are not impacted by OA, the stress of OA will likely be compounded by acute heat shock and may present additional physiological challenges for this species in the face of future change.

4.2. Introduction

Increases in anthropogenic carbon dioxide (CO_2) into the atmosphere from the mid-20th century onward have resulted in widespread patterns of ocean acidification (IPCC, 2013). The pH of surface

ocean waters has decreased (i.e., become more acidic) by 0.1 units since the beginning of the Industrial Revolution (IPCC, 2013), which will likely pose a particular threat to marine calcifying invertebrates. Ocean acidification (OA) alters the concentration of carbonate ions, reducing the saturation state of seawater with respect to the carbonate minerals marine calcifiers use to construct hard parts (i.e., aragonite and high- and low-magnesium calcite; Ries et al., 2009, 2011). OA has been linked to direct negative effects on marine calcifying organisms, including reduced growth, development, and calcification, and could also result in reduced reproductive output and ultimately death (Kroeker et al., 2010, 2013; Browman, 2016). OA may also disrupt olfaction (Kim et al., 2016), behavior (Dissanayake and Ishimatsu, 2011), internal chemistry (Dissanayake et al., 2010), and energy allocation (Pan et al., 2015) in a number of species. Although there is a general lack of data on the impact of environmental factors on crustacean immunity (Le Moullac and Haffner, 2000), research suggests the potential for OA and warming to be immunosuppressive (Hernroth et al., 2012; Wang et al., 2016). The full consequences of OA, however, are as of yet unknown (Browman, 2016), and there are inconsistent trends across taxa (Hendriks et al., 2010; Whiteley, 2011; Kroeker et al., 2013; Wittmann and Pörtner, 2015; Przeslawski et al., 2015), as well as ontogeny (Ceballos-Osuna et al., 2013; Small et al., 2015, 2016; Davis et al., 2016, 2018), which makes it difficult to construct generalizations.

Crustaceans can adjust the acid-base balance within the hemolymph in response to environmental perturbations (Whiteley and Taylor, 2015). Hemolymph pH is regulated through the passive buffering of CO_2 via alterations in the carbonate system, mainly through the exchange of H^+ and HCO_3^- ions across the gills, and through changes in the concentrations of non-carbonate species, such as proteins. There is likely a threshold for compensation in buffering capacity that is both species- and stage-specific, and chronic exposure to acidified conditions can disrupt the capacity of this buffering and cause an internal acidosis (Spicer et al., 2007; Pörtner, 2008; Whiteley, 2011; Whiteley and Taylor, 2015). This build-up of H^+ ions further lowers hemolymph pH, which reduces the ability of hemocyanin to successfully bind to oxygen (Truchot, 1975; Olianas et al., 2009) and leads to a disruption in oxygen delivery (Whiteley and Taylor, 2015). During low-oxygen conditions (hypoxia), crustaceans employ both organic (e.g., L-lactate,

urate, sulfide) and inorganic (e.g., H^+, Ca^{2+}, Mg^{2+}, Cl^-) molecular modulators to maintain hemocyanin's oxygen affinity, thus assisting in oxygen delivery (Bridges, 2001). However, little work has been dedicated to understanding how the concentrations of these molecular modulators change in the context of OA. Limited research suggests these modulators increase in concentration as a result of acute exposure to acidified conditions but may decline in the face of chronic exposure (Knapp et al., 2015, 2016).

Elevated levels of atmospheric CO_2 have also been implicated in widespread patterns of ocean warming, as well as an increase in the frequency of occurrence of extreme warming events (Hansen et al., 2012; IPCC, 2013; Smale et al., 2019). Physiological processes are heavily influenced by environmental temperature, and aerobic performance has an optimal temperature range marked by upper and lower thermal limits that are characterized using the oxygen- and capacity-limited thermal tolerance (OCLTT) concept (Pörtner and Farrell, 2008; Pörtner et al., 2017; Somero et al., 2017). As organisms encounter thermal limits, the ability to supply oxygen to tissues to meet demands becomes constrained and performance declines (Pörtner et al., 2017). Thermal performance windows can shift through acclimatization and evolutionary processes, resulting in greater tolerance thresholds based on environmental exposure (Pörtner, 2010). The unpredictable occurrence and duration of abrupt and extreme warming events, however, may preclude organisms from acquiring effective responses to a rapidly changing environment. Moreover, exposure to additional stressors, like acidification, further compresses an organism's performance curve and narrows thermal limits (Pörtner, 2008, 2010; Sokolova et al., 2012). For example, spider crabs (*Hyas araneus*) exposed to temperature extremes have reduced aerobic scope in performance that is made worse under concomitant exposure to elevated pCO_2 (Zittier et al., 2013). Similarly, exposure to acidified conditions causes increased sensitivity to thermal stress in the edible crab (*Cancer pagurus* – Metzger et al., 2007) and the intertidal limpet (*Cellana toreuma* – Wang et al., 2018).

We explored the sublethal effects of OA on the American lobster (*Homarus americanus* H. Milne Edwards, 1837). Distributed from North Carolina, USA, to Newfoundland, Canada, the American lobster sustains the most economically valuable fisheries species in the Northeastern United States and Atlantic

Canada (Steneck et al., 2011). Across much of its range off New England, *H. americanus* may encounter waters that are particularly at risk for acidification due to the region's low buffering capacity resulting from high freshwater input and low temperatures, which dilutes both alkalinity and dissolved inorganic carbon (Gledhill et al., 2015). Lobsters may also encounter areas where high nutrient and freshwater inputs create corrosive plumes of water capable of not only reducing calcification rates and destroying shells of organisms, but also of producing high rates of productivity that result in a subsequent buildup of carbon dioxide (Gledhill et al., 2015). In addition to warming at some of the most accelerated rates on the planet, the Northwest Atlantic has also experienced an increase in abrupt warming events in the last decade (Sherman et al., 2009; Taboada and Anadón, 2012; Pershing et al., 2015; Smale et al., 2019). For example, the 2012 ocean heat wave in the Northwest Atlantic was the largest and most intense warming event recorded over the last 30 years in the region (Mills et al., 2013), and it produced sea surface temperatures that were at least 1.1°C above the 1950 – 2014 climatology for the region (Scannell et al., 2016). We therefore examined how exposure to reduced pH impacts the hemolymph chemistry of subadult *H. americanus* (50 – 65 mm carapace length (CL)) and their ability to maintain aerobic performance under an additional acute thermal stress. Specifically, we explored if exposure to acidified conditions alters the concentrations of L-lactate and calcium (Ca^{2+}), molecular modulators known to affect the oxygen carrying capacity of hemocyanin in other crustaceans (Ahearn et al., 2004; Small et al., 2010; Knapp et al., 2015, 2016). We also used total hemocyte counts (THCs) as indicators of immunity as a first step to understanding if OA exposure is immunosuppressive, as has been demonstrated in the Norway lobster (*Nephrops norvegicus* – Hernroth et al., 2012). We subsequently conducted an acute thermal challenge post-exposure to test the hypothesis that exposure to acidified conditions increases thermal sensitivity and reduces aerobic performance in lobsters. These data provide the first attempt to explore the potential sublethal effects of OA on subadult lobsters, a relatively understudied life history stage, and is the first study to address how exposure to acidified conditions alters the physiological response of lobsters to an acute and extreme warming event. This work also serves as the foundation upon

which to build future studies exploring the combined effects of OA and warming on this important species.

4.3. Materials and Methods

4.3.1. Experimental Setup

We constructed four identical 708 l recirculating seawater systems at the Aquaculture Research Center (ARC), Orono, ME, each consisting of four replicate and sealed 75 l tanks, for a total of 16 experimental tanks. Systems were filled with pre-mixed seawater (Tropic Marin® Pro Reef salt, salinity 35 ppt, pH 8.1; Tropic Marin USA, Montague, MA, USA) and the temperature was maintained at 12 – 13°C across all systems. Two systems were designated control systems where the pH was maintained at a target level of 8.0 across the eight replicate tanks (four tanks per system; see Table 4.1), and the other two were designated the acidified systems where the pH was lowered to 7.6 through the diffusion of beverage-grade carbon dioxide. Prior to entering the systems, carbon dioxide was removed from the incoming air source using a CAS1-11 CO_2 adsorber/dryer (dual desiccant tower) (PUREGAS, Broomfield, CO, USA). We used Durafet pH sensors (Honeywell, Morris Plains, NJ, USA) calibrated twice weekly using NBS buffers (Thermo Fisher Scientific, Waltham, MA, USA) and verified twice monthly via spectrophotometry (see Riebesell et al., 2011) and a Pentair Point Four™ RIU (Pentair Aquatic Eco-Systems, Cary, NC, USA) to monitor and maintain the desired pH levels in our systems, and a LI-COR® LI-840A CO_2/H_2O gas analyzer (LI-COR, Lincoln, NE, USA) to monitor pCO_2 in the head space of each tank, the experimental room, and atmospheric conditions. Pure nitrogen gas was used to zero the LI-840A prior to each use.

Female, subadult lobsters (50 – 65 mm CL) were obtained from the Ventless Trap Survey of the Maine Department of Marine Resources (ME DMR) in August 2017. Lobsters within this size range are in transition from adolescence, which is marked by physiological maturity (i.e., oogenesis and spermatogenesis) but not functional maturity, to adulthood, which is marked by successful mating (Lavalli and Lawton, 1996). As such, any negative effects of environmental stressors on the fitness of this stage may have major downstream impacts on the population as a whole. We focused specifically on

68

female subadults to control for the potential of sex-specific responses to OA (Ellis et al., 2014). Lobsters were held at the ARC for four months prior to use in the trial, and as such were acclimated from summer to winter water temperatures (18°C and 12°C, respectively) following the seasonal temperature change occurring in nature. Three lobsters were randomly assigned to each tank of the four experimental systems in December 2017 *(N = 24 per pH treatment)* and allowed to acclimate for one week prior to the initiation of the experiment. Lobsters were exposed to experimental pH conditions for 60 d. We conducted daily measurements of temperature, dissolved oxygen, salinity, pH, and pCO_2; observed lobsters for overall health twice-daily and fed them twice-weekly; and assessed water quality twice-weekly using a Hach® DR1900 portable spectrophotometer (Hach, Loveland, CO, USA). We also collected additional water samples for total alkalinity (A_T) via titration twice-weekly (Riebesell et al., 2011). A subset of these measurements was then used in the program CO2SYS to calculate carbonate chemistry (Pierrot et al., 2006), with constants from Mehrbach (1973) and refit by Dickson and Millero (1987), KHSO4 from Dickson (1990), and [B]T from Uppström (1974) (see Table 4.1 for a summary of data).

Table 4.1. Water chemistry in tanks over the course of the experiment (mean ± SE). Parameters calculated using CO2SYS are indicated by an asterisk *.

Parameter	Acidified	Control
Salinity ppt	35 ± 0.001	35 ± 0.002
Dissolved oxygen mgL^{-1}	10.07 ± 0.03	10.26 ± 0.02
Oxygen saturation (%)	93.4	95.1
Temperature °C	12.5 ± 0.003	12.3 ± 0.03
pH_{NBS}	7.60 ± 0.002	7.95 ± 0.002
A_T $\mu molkg^{-1}$	2140.7 ± 15.8	2138.9 ± 18.0
*HCO_3^- $\mu molkg^{-1}$	2033.07 ± 15	1931.79 ± 15
*CO_3^{2-} $\mu molkg^{-1}$	41.64 ± 0.4	83.18 ± 0.9
*$\Omega_{calcite}$	0.99 ± 0.01	1.99 ± 0.02
*$\Omega_{aragonite}$	0.63 ± 0.01	1.25 ± 0.01
*pCO_2 ppm	850.45 ± 11	486.4 ± 5

4.3.2. Biological Assays

Approximately 1.5 ml of hemolymph was collected from each lobster after 60 d. Briefly, the dorsal side of the abdomen was disinfected using 70% ethanol and hemolymph was collected from the abdominal sinus using a 26-gauge needle and a sterile 2.0 ml syringe. Samples were centrifuged at 10,000 g for 10 min at 4°C to obtain cell-free hemolymph. From this, 500 μl was deproteinated with 500 μl of cold 0.5 M metaphosphoric acid and centrifuged at 10,000 g for 5 min before neutralizing the supernatant with 50 μl potassium carbonate. This mixture was centrifuged again at 10,000 g for 5 min to remove precipitated salts, and the resulting supernatant was removed and stored at –80°C until assayed for L-lactate concentration using a spectrofluorometric assay kit (Cayman Chemical, Ann Arbor, MI, USA). The remaining plasma was aliquoted and stored at –80 °C until analysis for protein, calcium, and

ecdysterone. Although we had intended to assay hemolymph samples from all 48 lobsters in all tests described below, we were often limited to a smaller subset due to sample coagulation. As such, the sample size for each assay is reflected below.

We measured total protein content as an indicator of stress (Taylor et al., 1997; Lorenzon et al., 2007; Bernardi et al., 2015) using the microplate procedure of the Pierce[TM] BCA Protein Assay Kit (Thermo Fisher Scientific) and bovine serum albumin as our standard. Standards and samples (at a 1:9 dilution with ultrapure water) were pipetted in duplicate into the wells of a 96-well plate (N = 14 lobsters per pH treatment). Absorbance at 562 nm was read using a BioTek® Synergy[TM]2 Microplate Reader (BioTek Instruments, Winooski, VT, USA).

We selected calcium and L-lactate as focal molecular modulators as they have been the target of previous efforts exploring oxygen carrying capacity of hemocyanin in other species of lobster, e.g., *Homarus gammarus* (Zeis et al., 1992 and Nies et al., 1992 – cited as *H. vulgaris*), *Palinurus gilchristi* (Olianas et al., 2009), and *Jasus lalandii* (Knapp et al., 2015, 2016). We measured total calcium content using the Cayman Chemical Calcium Assay Kit (Cayman Chemical, Ann Arbor, MI, USA) according to kit instructions. Aliquots were thawed and diluted 1:10 with 10X Assay Buffer (100 mM Tris-HCl, pH 7.0). Samples and standards were pipetted in duplicate and absorbance was read at 575 nm using a BioTek® Synergy[TM]2 Microplate Reader (N = 16 lobsters per pH treatment). L-lactate concentration was measured using a Cayman Chemical L-lactate Assay Kit according to kit instructions. Aliquots were thawed and diluted 1:2 with Assay Buffer (50 mM potassium phosphate, pH 7.5). The fluorescence was read on a BioTek® Synergy[TM]2 Microplate Reader using an excitation wavelength of 540 nm and an emission wavelength of 590 nm (N = 16 lobsters per pH treatment).

We used the 20-Hydroxyecdysone (ecdysterone, 20E) Enzyme Immunoassay (EIA) kit (Bertin Bioreagent, Montigny le Bretonneux, France) to explore if OA influences the concentration of the primary molting hormone in crustaceans (Chang and Mykles, 2011). Following kit instructions, hemolymph was extracted twice using ether and pipetted in duplicate to the wells of a 96-well plate at a

71

1:20 dilution with EIA buffer. Absorbance was read at 405 nm on a BioTek® ELx808™ Absorbance Microplate Reader (BioTek Instruments; $N = 12$ lobsters per pH treatment).

4.3.3. Total Hemocyte Counts

We measured THCs as an indicator of total immune response (Battison et al., 2003; Dove et al., 2005; Battison, 2006). A 200 μl aliquot of hemolymph was drawn from each lobster as stated above and placed in a pre-weighed glass vial containing 800 μl of fixative (10% buffered formalin in filtered, sterilized seawater). The ratio of hemolymph to fixative was calculated using mass-differences. Samples were aspirated with a pipette, and three independent 10 μl subsamples were added to a separate KOVA Glasstic® Slide 10 with Grids hemocytometer (Kova International, Garden Grove, CA, USA). For each subsample, the total number of hemocytes was counted three times, and an average was calculated. Final THCs for each individual were averaged from the subsamples and standardized to account for hemolymph : fixative dilutions among individuals (Basti et al., 2010; Harrington et al., 2019). All samples were stored for no more than four days at 4°C prior cell counting ($N = 18$ lobsters per pH treatment).

4.3.4. Cardiac Performance

To determine if chronic exposure to OA influences the thermal physiology of subadult lobsters, we conducted a post-exposure acute thermal stress experiment in which cardiac performance was assessed using impedance pneumography (Braby and Somero, 2006; Camacho et al., 2006). Lobsters ($N = 18$ per pH treatment) were given a recovery period of at least 32 h following hemolymph sampling, after which a pin vice was used to hand drill (part-way) through the lobster carapace on either side of the pericardial space. A sterile dissecting needle was used to finish each hole to prevent extensive damage to the animal. Electrodes made of 36 – 38-gauge magnetic wire were inserted into the holes and secured to the carapace using cyanoacrylate glue. Once the glue was dry, lobsters were place into a water bath (12°C) for a 25 min acclimation period. Following the acclimation period, lobsters were moved into the experimental arena where water temperature was increased from 12°C to 28°C over the course of 2 hr 30

min using a Fisher Scientific™ Isotemp™ refrigerated/heated bath circulator. Temperature was recorded using a T-type Thermocouple Probe and T-type Pod (ADInstruments, Colorado Springs, CO, USA), and lobster heart rate was recorded using a PowerLab® Data Acquisition System (ADInstruments).

4.3.5. Statistical Analyses

We used an independent-samples t-test to first determine the effect of system (i.e., within treatment differences) on total protein content, THC, and the concentrations of calcium, L-lactate, and ecdysterone. With the exception of calcium concentration, we found no significant differences across systems within treatments. As such, data were pooled across systems and we report here only on the across-treatment (i.e., pH) differences. We nevertheless used a General Liner Model (GLM) followed by post hoc LSD tests to determine the effect of system and treatment on calcium concentrations (Zar, 2010). We used a two-way mixed ANOVA to determine if there were differences in lobster heart rate between the acidified and control pH treatments over the course of the temperature ramp. We chose this approach over a two-way repeated measures ANOVA (e.g., Camacho et al., 2006) as we had an unequal sample size across our pH treatments. Heart-rate data were then transformed and fit with a piece-wise regression to determine the Arrhenius Break Temperatures (ABTs; the temperature at which heart rate begins to decrease with increasing temperature; Stenseng et al., 2005; Camacho et al., 2006) as an indicator of the thermal limit of capacity. We used Levene's test to assess equal variance across groups ($P > 0.05$) and Shapiro-Wilk's test to assess normality ($P > 0.05$). THC and ABT data were log transformed to meet test assumptions. L-lactate data failed to meet the assumption of equal variance, and these data were analyzed using a Welch's t-test to determine if there were differences in concentrations between acidified vs. control lobsters. All tests were performed using IBM® SPSS® Statistics Version 24.

4.4. Results

Mean total protein content was not significantly different across treatments ($t = 0.32$, $df = 28$, $P = 0.76$; Figure 4.1A). Similarly, mean 20E concentration was not significantly different across treatments, but values were more variable in control vs. acidified lobsters ($t = 1.04$, $df = 28$, $P = 0.31$; Figure 4.1B). Overall, mean calcium concentration was slightly higher in acidified vs. control lobsters, although this

was not statistically significant (GLM: $F_{3,35} = 2.09$, $P = 0.12$; Figure 4.1C). This general trend was primarily driven by a significantly lower mean concentration in lobsters from one of the replicate control systems (post hoc LSD $P < 0.05$). Mean hemolymph L-lactate concentration was significantly reduced in acidified vs. control lobsters (Welch's $t = 2.93$, $df = 24.3$, $P < 0.01$; Figure 4.1D). Mean THCs were 61% lower in acidified vs. control lobsters, demonstrating a strong trend for reduced hemocyte abundance ($t = 1.91$, $df = 39$, $P = 0.06$; Figure 4.1E).

The two-way mixed ANOVA failed to meet the assumption of sphericity (Mauchly's test of sphericity: $\chi^2 = 747.6$, $P < 0.001$); as such, we used the Greenhouse-Geisser correction when interpreting our results (Maxwell and Delaney, 2004). We found no significant interaction between pH treatment and temperature on lobster heart rate ($F_{3.25,104.07} = 0.44$, $P = 0.74$, $\eta^2 = 0.013$). There was nevertheless a significant increase in heart rate for all lobsters as temperature increased throughout the acute exposure period ($F_{3.25,104.07} = 190.56$, $P < 0.001$, $\eta^2 = 0.86$; Figure 4.2). Over the course of the 2 hr 30 min acute warming exposure, control lobsters had higher mean heart rates compared to lobsters in the acidified group, especially between $18 - 24°C$ (Figure 4.2). Moreover, mean ABT was significantly higher in control vs. acidified lobsters ($t = 2.09$, $df = 35$, $P = 0.04$; Figure 4.2) at $26.3 \pm 0.4°C$ and $25.2 \pm 0.4°C$, respectively. It should be noted that this test was not physiologically stressful enough to induce mortality, and although heart rate was not measured again to ensure cardiac performance returned to baseline function, all lobsters exhibited normal behaviors within 24 hr post-experiment and survived 5 d until euthanization.
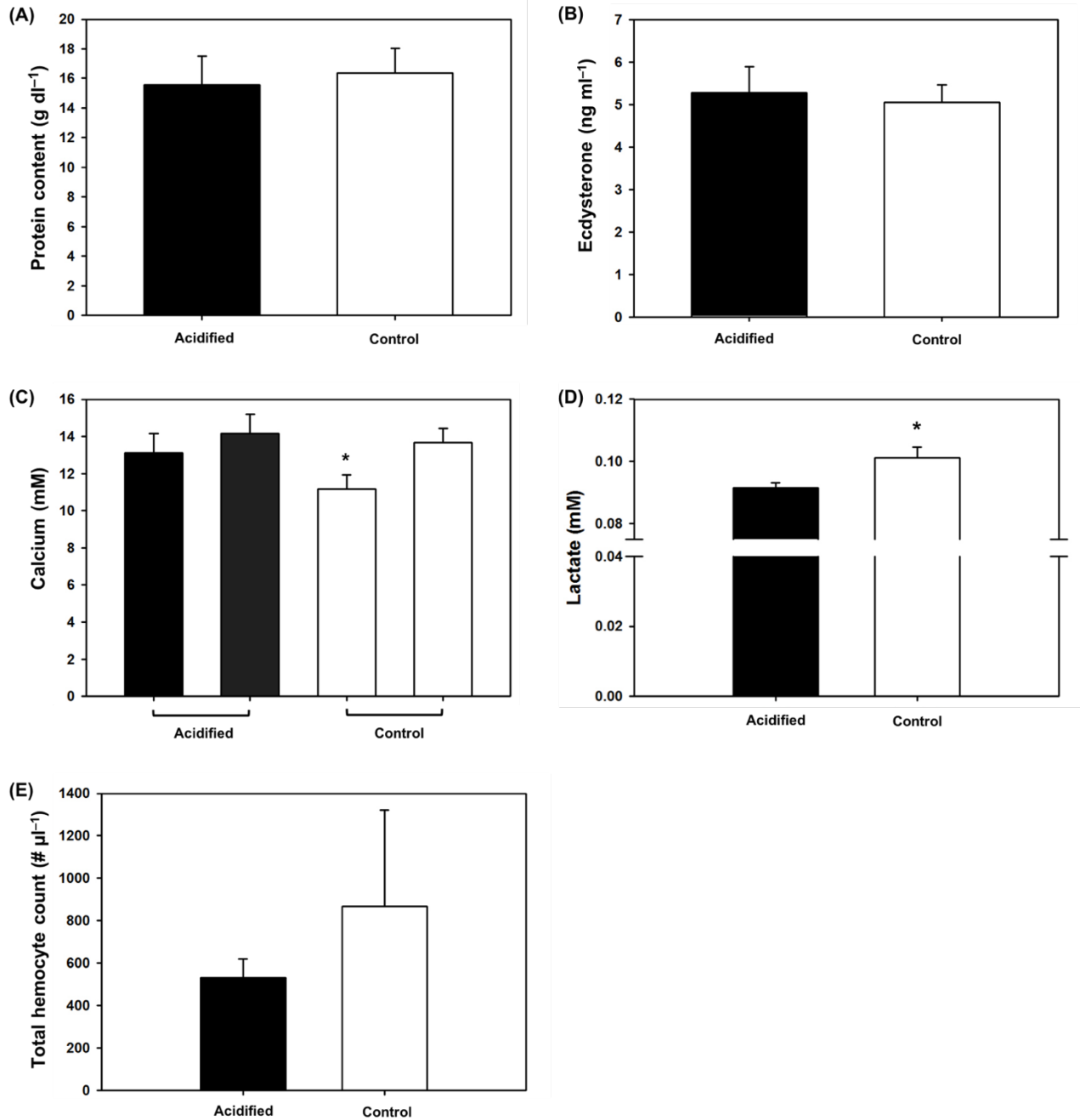
Figure 4.1. Biological assays of the hemolymph of subadult *Homarus americanus* following exposure to acidified (black) or control (white) pH conditions depicted as mean + SE. Total protein content ($N = 14$ lobsters per treatment) (**A**). Ecdysterone (20E) concentrations ($N = 12$ lobsters per treatment) (**B**). Calcium concentration ($N = 8$ lobsters per system), where the asterisk (*) indicates significance based on a GLM followed by post hoc LSD tests ($P < 0.01$) (**C**). L-lactate concentration ($N = 16$ lobsters per treatment) where the asterisk (*) indicates significance based on a Welch's t-test ($P = 0.01$) (**D**). Total hemocyte count ($N = 18$ lobsters per treatment) (**E**).
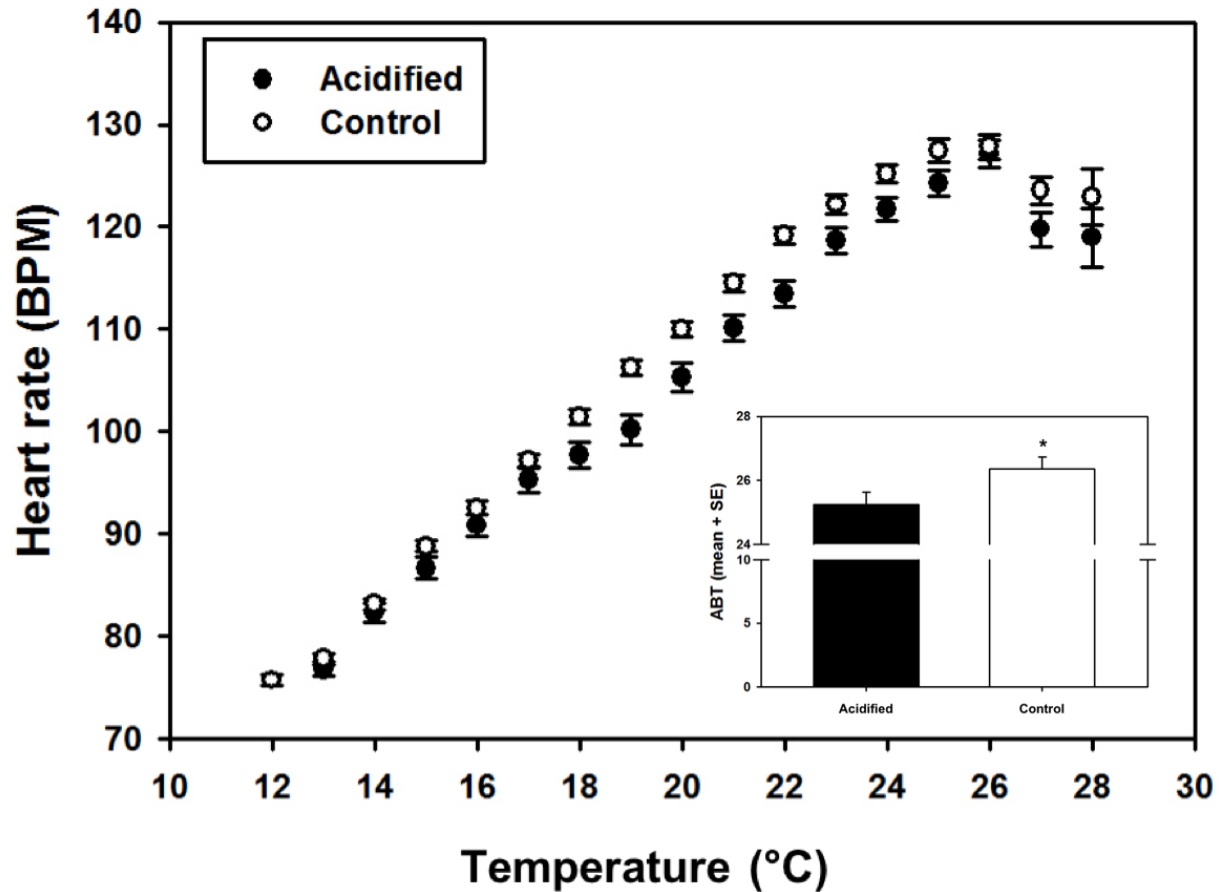
Figure 4.2. Mean heart rate (± SE) for *Homarus americanus* in the acidified (black circles) and control (white circles) treatments over the temperature ramp ($N = 18$ lobsters per treatment). The inset shows the mean ABT (+ SE) of acidified (black bar) vs. control (white bar) treatment lobsters. The asterisk (*) indicates significance at $P < 0.05$ in an independent samples t-test.

4.5. Discussion

To our knowledge, this is the first study to address how exposure to acidified conditions influences the physiological response of lobsters during an acute warming event. In line with the oxygen- and capacity-limited thermal tolerance (OCLTT) concept, we observed a steady and significant increase in heart rate as temperature increased during the acute thermal challenge (Figure 4.2), which we infer as an increase in metabolic rate to compensate for an increase in energy demand associated with moderate thermal stress (Pörtner and Farrell, 2008; Sokolova et al., 2012). Although there was no significant interactive effect of treatment pH and temperature on lobster heart rate, lobsters in the control group had

consistently higher heart rates compared to those in the acidified group, particularly between $17 - 25°C$.

Lobsters exposed to acidified conditions had significantly lower ABTs compared to lobsters in the control treatment, and this reduced cardiac performance as a consequence of low pH narrowed the thermal window of subadult lobsters by $1.1°C$. Similarly, spider crabs (*H. araneus* – Walther et al., 2009) and edible crabs (*C. pagurus* – Metzger et al., 2007) exposed to acidified conditions exhibited a narrowing of the upper thermal window for performance by $1.5 - 3.9°C$ and $5°C$, respectively, when compared to animals exposed to normocapnic conditions. Under the OCLTT framework, this suggests that chronic exposure to acidified conditions compresses the thermal performance curve, lowering the thermal limits of moderate and severe thermal stress in subadult *H. americanus* (Sokolova et al., 2012). As such, lobsters exposed to OA could be at risk for increases in oxidative cellular damage at lower temperatures compared to lobsters under normocapnic conditions, and they may incur greater short-term energetic costs in response to acute warming events to meet the energy demands associated with the stress response (e.g., antioxidant defense and the heat shock response; Sokolova et al., 2012; Pörtner et al., 2017). Although heart rate is often used as an indicator of a stress response and/or a proxy for metabolism, one must also consider stroke volume and contractility of the heart when assessing cardiac output (McGaw and Reiber, 2015), metrics that are often difficult to measure in late-stage crustacean hearts *in vivo*. One could also measure hemolymph oxygen partial pressure in conjunction with the ability to perform an energy-demanding behavior such as righting response (Zittier et al., 2013) to more fully explore if exposure to acidified conditions prevents organisms from meeting the increase in oxygen demand by tissues. While the results presented here offer compelling evidence that OA will impact the thermal physiology of subadult lobsters in the context of abrupt warming events, future research should benefit greatly from the inclusion of additional physiological and behavioral metrics.

Both calcium and L-lactate have been the focus of numerous studies examining the role of molecular modulators on the oxygen carrying capacity of hemocyanin in lobsters (Zeis et al., 1992; Nies et al., 1992; Olianas et al., 2009; Knapp et al., 2015, 2016). We found no significant effect of OA exposure on the concentration of Ca^{2+}, but concentrations of L-lactate were significantly reduced in

acidified vs. control lobsters (Figures 4.1C, D). Although concentrations of L-lactate in all lobsters here were slightly lower than those previously reported for un-manipulated European lobster *H. gammarus* (i.e., 0.26 ± 0.06 mM – Bouchet and Truchot, 1985; 0.5 ± 0.2 mM – Zeis et al., 1992), they are in line with measurements made on similarly sized rock lobster (*J. lalandii*) in the context of acute exposure to acidification (Knapp et al., 2016). Additional work on early-stage juvenile *J. lalandii*, however, found that exposure to hypercapnic conditions for 28 weeks significantly reduced Ca^{2+} concentrations by 38% relative to lobsters in normocapnic conditions, but did not significantly alter L-lactate concentrations (Knapp et al., 2015). Moderate exposure to low pH water also resulted in significant increases in the concentrations of Ca^{2+} and Mg^{2+} in the hemolymph of the velvet swimming crab (*Necora puber* – Small et al., 2010), and work on both the European lobster (Zeis et al., 1992; Nies et al., 1992) and the southern spiny lobster (*Palinurus gilchristi* – Olianas et al., 2009) indicated that urate was a more effective modulator than L-lactate, suggesting that alterations in molecular modulators in response to OA are likely species-specific. Future work with *H. americanus* would greatly benefit from an examination of changes in additional modulators in the context of acidification, particularly urate, as hemocyanin's affinity for urate was 40 times that of L-lactate in the conger *H. gammarus* (Nies et al., 1992). We also acknowledge that while both calcium and L-lactate are known molecular modulators of hemocyanin, changes in their concentrations in the context of environmental stress should be interpreted with caution as they cannot replace the direct measurement of hemocyanin oxygen affinity.

Showing a considerable trend toward significance (i.e., $P = 0.06$), lobsters exposed to acidified conditions had THCs that were 61% lower than THCs in control lobsters (Figure 4.1E), suggesting the potential for OA to be immunosuppressive. Norway lobsters (*N. norvegicus*) exposed to low pH for four months exhibited a similar 50% decline in THCs relative to control conditions, a difference that was accompanied by a 60% decline in phagocytotic activity (Hernroth et al., 2012). Importantly, hemocyte functionality may be compromised under OA without causing a significant change in THC, as was demonstrated in the blue mussel (*Mytilus edulis*) after 32 days of exposure (Bibby et al., 2008). Moreover, characterizing the status of hemocytes in circulation (i.e., dead or alive) in addition to activity level and

abundance may also elucidate sublethal effects of OA on hemocytes. For example, although THCs in Tanner crabs (*Chionoecetes bairdi*) exposed to acidified or control conditions for two years were not significantly different, the number of dead hemocytes in circulation, as well as rates of phagocytosis, were significantly higher under low pH conditions, suggesting that hemocytes were dying via apoptosis faster than could be removed phagocytotically by the remaining cells in circulation (Meseck et al., 2016). Taken together, these studies suggest that exposure to acidified conditions over moderate time scales has the potential to significantly affect several aspects of the primary cells of the immune response in calcifying invertebrates. To more fully understand the lobster immune response under acidification, however, future efforts should focus on describing additional characteristics, such as phagocytotic activity, ROS production, and levels of apoptosis (Bibby et al., 2008; Hernroth et al., 2012; Meseck et al., 2016; Wang et al., 2016). Most importantly, a follow-on pathogen challenge should be conducted to truly assess the impact of OA on immunity. Although we used only female lobsters to control for any potential sex-specific responses to environmental stress (e.g., *M. edulis* – Ellis et al., 2014), future work would benefit from including males as well.

Many of the parameters we measured can vary based on molting stage and nutritional condition of lobsters (i.e., calcium concentrations – Ahearn et al., 2004; total ecdysteroids – Snyder and Chang, 1991; and protein content – Mercaldo-Allen, 1991). Although there has been little research examining the effect of OA on hormones involved in the molt cycle, it is possible that ecdysteroid secretion is inhibited by acidification as suggested for the white shrimp (*Litopenaeus vannamei* – Mustafa et al., 2015). We found no significant effect of OA on the concentration of 20E, and values were extremely variable across both treatment groups. We also found no significant effect of OA on total protein content, a metric commonly used as an indicator of acute stress, such as handling, transport, and temperature, in *H. americanus* (Taylor et al., 1997; Lorenzon et al., 2007; Bernardi et al., 2015). While we did not explicitly assess molt condition, the majority the measured values of 20E (Shrivastava and Princy, 2015), total protein content (Barlow and Ridgway, 1969; Mercaldo-Allen, 1991; Wang and McGaw, 2014), and calcium concentrations (Ahearn et al., 2004) were in line with published values for crustaceans in

intermolt. None of the lobsters we studied molted, making it difficult to speculate on the potential downstream effects OA might have on subadults. Previous research on early benthic juvenile European lobster suggests that exposure to acidified conditions may cause morphological deformities (Agnalt et al., 2013) or lead to molt death syndrome (Small et al., 2016). Although our study attempted to explore the longer-term effects of OA on lobster, it would have benefited from sampling hemolymph throughout an extended exposure period that followed individuals throughout the molt cycle to determine both the pre- and post-molt health and survival of subadults. Moreover, as there are a number of other metrics of stress one could explore in addition to total protein content, such as CHH, glucose, glycogen, triglycerides, ammonia, and other ions (Taylor et al., 1997; Bernardi et al., 2015), as well as DNA damage (Yao and Somero, 2012), future work should benefit from exploring more explicit indicators of cellular stress.

We have focused primarily on interpreting our results in the context of exposure to acidification but acknowledge that this stressor will not impact lobsters in isolation. Carbonate chemistry co-varies with temperature and oxygen in water masses (Reum et al., 2016), and temperature, pH, and salinity may act synergistically to negatively affect both survival and sublethal responses in early life stages of marine organisms (Przeslawski et al., 2015). This is particularly important in *H. americanus* as it not only experiences a 25°C range in temperatures across its distribution, but it also inhabits an area that is warming significantly faster than the global ocean (Pershing et al., 2015; Thomas et al., 2017). Previous research demonstrated that *H. americanus* has the potential to acclimate to warming over short time scales (i.e., 3 – 14 d), increasing its upper thermal limit for cardiac function by 5°C compared to those acclimated to cooler temperatures (Camacho et al., 2006; Qadri et al., 2007). It is unclear, however, if this acclimatory ability will persist under both OA and warming, or if it will be compromised as has been suggested by recent work on polar fishes (e.g., *Trematomus bernacchii* – Davis et al., 2016, 2018; *Boreogadus saida* – Kunz et al., 2018). Resilience to thermal stress associated with warming among invertebrates is compromised by the additional exposure to OA (e.g., intertidal limpet *C. toremuma* – Wang et al., 2018), and warming and high pCO_2 act synergistically to shift thermal tolerance and reduce aerobic performance of the spider crab (*H. araneus* – Zittier et al., 2013). Research suggests that the

negative effects of OA on immunity are more evident in the presence of additional stressors such as temperature (Hernroth et al., 2012; Ellis et al., 2014) or hypoxia (Hernroth et al., 2015), further demonstrating the need to examine warming and OA in combination rather than in isolation. While we have addressed how exposure to OA influences the response of subadult lobsters to an acute warming event, future research should focus on the potential combined effects of OA and warming on the metrics measured in this study to truly address lobster acclimatory capacity in a changing environment.

In conclusion, we found that although total protein, calcium, and ecdysterone concentrations were not significantly altered by exposure to reduced pH, we observed some important changes in hemolymph chemistry and physiological performance as a result of acidification. Lobster heart rate significantly increased during an acute thermal challenge in both treatment groups; however, lobsters exposed to acidified conditions had significantly lower ABTs compared to lobsters in the control treatment. This important difference indicates that decreased pH reduces cardiac performance, potentially compressing the thermal performance window of lobsters under abrupt warming events. Lobsters exposed to pH levels expected by the end of the 21st century could be at risk of reduced oxygen affinity of hemocyanin as indicated by the lower levels of L-lactate in acidified vs. control-treatment lobsters. Compounding these issues, the decline in THCs of acidified lobsters may result in reduced immune function relative to control lobsters, which could potentially increase disease susceptibility. These data suggest that subadult *H. americanus* could be negatively impacted by exposure to reduced pH levels, particularly in the context of acute thermal stress. Future efforts should focus on understanding the combined effects of OA and warming on lobster physiology both in terms of multiple physiological traits and plasticity (Magozzi and Calosi, 2015), as well as how these physiological changes relate to downstream processes (e.g., behavior, reproductive output, or gene expression).

CHAPTER 5

CONCLUSION

5.1. Overarching Goals

The Gulf of Maine region is warming faster than almost anywhere in the world (Sherman et al., 2009; Taboada and Anadón, 2012; Pershing et al., 2015; Thomas et al., 2017), and it may be particularly vulnerable to acidification due to its many terrestrial geochemical influences (e.g., high freshwater input and nutrient loading; Gledhill et al., 2015). Numerous studies suggest that both ocean warming and acidification will have negative effects on marine calcifying invertebrates (Kroeker et al., 2013; Browman, 2016), but the sublethal or sub-cellular effects of these environmental factors have rarely been addressed. The primary goal of this dissertation was to examine biological endpoints to evaluate climate change impacts on the American lobster (*Homarus americanus*). Larval development is significantly accelerated under warming conditions (MacKenzie, 1988; Barret et al., 2017); however, the sublethal effects of faster growth under warming conditions are unclear, including the potential costs associated with inherent increases in metabolic rates as a consequence of Q_{10} effects (Somero et al., 2015, 2017). Moreover, although reduced pH conditions may not pose a threat to bulk calcification in *H. americanus* (Ries et al., 2009, 2011), the full impacts of acidification on the physiology of lobsters is unknown, particularly for the relatively understudied subadult lobster stage. What is clear, however, is that the impacts of climate change are species- and stage-specific (Kroeker et al., 2013; Przeslawski et al., 2015; Small et al., 2015, 2016; Davis et al., 2016, 2018). As such, this dissertation aimed to address ocean warming and acidification across multiple life history stages of *H. americanus* to provide a greater depth of understanding of how a changing environment will influence the physiology of this economically important species.

5.2. Statement of Major Findings

In Chapters 2 and 3, I exposed newly-hatched lobsters to four nominal temperature regimes (14, 16, 18, or 22°C) to examine the effects of ocean warming on the physiology, developmental stability, and

gene expression of larval lobsters. In Chapter 2, I determined that development proceeded significantly

faster as temperature increased, and that cumulative survival was significantly positively correlated with

temperature, in support of previous studies (e.g., MacKenzie, 1988; Barret et al., 2017). However,

postlarvae reared under the extreme temperatures (14°C and 22°C) exhibited higher levels of stress, as

indicated by elevated total hemocyte counts, a novel technique for work in larval lobster. Additionally,

postlarvae exposed to the temperature extremes also expressed significantly lower levels of variance in

midline asymmetry compared to those in intermediate temperature treatments. These findings indicate

that the potential benefits of warming may be outweighed by increased stress levels that could potentially

lead to increased disease susceptibility (Labaude et al., 2017). Moreover, reduced variation in midline

asymmetry may suggest a reduction in the ability of postlarval *H. americanus* to respond to additional

stressors (van Straalen and Timmermans, 2002; Venâncio et al., 2016), demonstrating that fluctuating

asymmetry could prove a useful bioindicator for population resilience in lobsters.

In Chapter 3, I continued to explore the potential downstream impacts of warming on developing

H. americanus by investigating changes in the postlarval lobster transcriptome. Transcriptomics has

proven a useful tool for exploring gene expression patterns in response to climate change in a variety of

marine species (Lockwood et al., 2010; Moya et al., 2012; Evans et al., 2017; Wong et al., 2018),

particularly in those that lack a fully annotated reference genome (Clark and Greenwood, 2016). Using a

de novo assembled transcriptome, I found that postlarval lobsters reared at 16°C over-expressed

transcripts annotated to proteins affiliated with cuticle formation and the innate immune system up to

14.4- and 8.5-fold, respectively, relative to lobsters exposed to warmer temperatures. In contrast,

postlarvae reared under increasingly warmer temperatures over-expressed transcripts associated with

metabolic turnover by up to 7.1-fold. This indicates a shift in the transcriptome that reflects a potential

trade-off between maintaining immune defenses and meeting the energetic demands associated with

increased physiological rates as a consequence of ocean warming. Together with the results of Chapter 2,

these findings suggest that warmer temperatures may facilitate faster growth at the expense of increased

physiological stress and disease susceptibility. Moreover, postlarvae may be unable to meet increasing

energetic demands associated with warming if prey availability declines (as suggested by Carloni et al., 2018), presenting additional challenges that could reduce post-settlement survival in a changing environment.

In Chapter 4, I used four recirculating seawater systems at the Aquaculture Research Center (ARC) to explore the sublethal effects of ocean acidification (OA) on the hemolymph chemistry and physiological response to acute thermal stress in subadult *H. americanus*. Lobsters were exposed to acidified (pH = 7.6) or control (pH = 8.0) conditions for 60 days at the ARC. Although calcium, total protein, and ecdysterone concentrations were not significantly altered by OA exposure, total hemocyte counts were 1.6 times higher in control vs. acidified lobsters, suggesting immunosuppression under chronic OA (Hernroth et al., 2012; Wang et al., 2016). Lobsters exposed to a reduced pH also had significantly lower levels of L-lactate in their hemolymph, suggesting reduced oxygen carrying capacity under OA that may have contributed to reduced cardiac performance under acute warming (as indicated by significantly lower Arrhenius Break Temperatures compared to control lobsters). These results suggest that although some physiological endpoints of American lobster are not impacted by OA, the stress of OA will likely be compounded by acute heat shock and may present additional physiological challenges for this species in the face of future change.

5.3. Future Directions

It is important to acknowledge that the experiments conducted in this dissertation focused on the effects of individual abiotic factors on *H. americanus*. Carbonate chemistry co-varies with temperature and oxygen in water masses (Reum et al., 2016), and temperature, pH, and salinity may act synergistically to negatively affect early life stages of marine organisms (Przeslawski et al., 2015). It is therefore critical to examine the potential interactive effects of temperature and OA, as well as other metrics of environmental change (e.g., dissolved oxygen content and salinity), on the biological endpoints measured here. This may be particularly important in the context of resilience to thermal stress, which can be compromised by additional exposure to OA, hypoxia, or pollutants (Sokolova et al., 2012). Moreover,

research suggests that the negative effects of OA on immunity are more evident in the presence of additional stressors, such as temperature (Hernroth et al., 2012; Ellis et al., 2014) or hypoxia (Hernroth et al., 2015), further demonstrating the importance of adopting a multi-factorial approach to ecophysiological studies.

In addition to focusing on multiple environmental factors, future efforts would greatly benefit by addressing the potential for carryover effects from larval to juvenile stages. Carryover effects may arise when the performance or experience of one life history stage has either positive or negative impacts on the performance of a subsequent life stage (Foo and Byrne, 2016; Ross et al., 2016), potentially conferring resilience under environmentally stressful conditions to a subsequent generation (Parker et al., 2015). It would be particularly interesting to explore the impacts of OA and warming on postlarvae following settlement to the benthos, especially in the context of behavioral metrics (e.g., finding adequate shelter from predators or intraspecific interactions) in addition to assessing biochemistry throughout subsequent molting events. Future efforts should also focus on exploring the potential for transgenerational effects (i.e., the influence of parental environment history on offspring performance – Foo and Byrne, 2016). Parental environmental history in molluscs and echinoderms influences the phenotypic response and/or performance of offspring through transgenerational carryover effects (Sunday et al., 2014; Ross et al., 2016; Foo and Byrne, 2016). Offspring of parents exposed to environments mimicking future conditions (i.e., high pCO_2 and elevated temperature) prior to fertilization events may exhibit greater performance under similar conditions. These benefits are conferred either through epigenetic effects or maternal provisioning (Ross et al., 2016), and they may result in pre-adapted offspring that exhibit increased fitness in environments similar to those experienced by their parents (Foo and Byrne, 2016).

Understanding the potential for transgenerational effects may prove particularly useful in the context of understanding the possibility for local adaptation to a changing climate in *H. americanus*. Across its distribution, the American lobster encounters a steep latitudinal gradient in environmental characteristics (Longhurst, 1988). Abrupt warming events in recent decades have caused mass mortality

and disease in lobster populations in southern New England while simultaneously promoting growth and reproduction in historically colder waters of the north, causing a net northward shift in the population (Pearce and Balcolm, 2005; Wahle et al., 2009; Chang et al., 2010). However, smaller-scale differences in environmental parameters may give rise to locally adapted populations that have different environmental tolerances (Kuo and Sanford, 2009; Kelly et al., 2013), which may present a more complicated response to climate change than just a simple poleward migration (Helmuth et al., 2002, 2006). Moreover, the action of one environmental stressor may mediate the predicted effects of another on species distributions, presenting additional complexity to the detection of regional adaptation (Calosi et al., 2017). Although difficult to assess, local adaptation may be the key to resilience of American lobster in the face of future change. Population genetic studies suggest a north-south differentiation between two sub-populations of *H. americanus* (i.e., Gulf of Maine and Gulf of St. Lawrence regions – Benestan et al., 2015) whereby geographic distance and ocean currents explain and shape neutral genetic structure and temperature serves as the main selective agent (Benestan et al., 2016). It is therefore prudent to incorporate regional sampling into the experimental design of future research, particularly in the context of understanding how exposure to environmental stressors influences developing *H. americanus*.

5.4. Concluding Remarks

The American lobster supports the most economically valuable fishery in the Gulf of Maine and Atlantic Canada and contributed more than $484 million to the total value of Maine's commercial fisheries landings in 2018 (ME DMR, 2019). Although the fishery has managed to persist in the face of intense harvesting pressure (Steneck and Wahle, 2013), the reliance on *H. americanus* as other fisheries have collapsed across the region has effectively created a monoculture (Steneck et al., 2011), the perturbation of which could lead to drastic socioeconomic impacts (e.g., the economic crisis that ensued following the 2012 ocean heat wave – Mills et al., 2013). Importantly, this dissertation suggests that climate change may impact two crucial life history stages of *H. americanus*: those transitioning to the benthos and recruiting to the population; and pre-reproductive individuals that have yet to contribute to

the brood stock. This research provides important steps toward understanding the sublethal effects of ocean warming and acidification on the American lobster and may also serve as a foundation upon which to further our understanding of how a changing environment will influence the physiology of marine calcifying invertebrates.

REFERENCES

Adamo, S.A., 2010. Why should an immune response activate the stress response? Insights from the insects (the cricket *Gryllus texensis*). Brain Behav. Immun. 24(2): 194-200.

Adamo, S.A., 2012. The effects of the stress response on immune function in invertebrates: An evolutionary perspective on an ancient connection. Horm. Behav. 62(3): 324-330.

Afgan, E., Baker, D., Batut, B., van den Beek, M., Bouvier, D., Cech, M., Chilton, J., Clements, D., Coraor, N., Grüning, B.A., Guerler, A., Hillman-Jackson, J., Hiltemann, S., Jalili, V., Rasche, H., Soranzo, N., Goecks, J., Taylor, J., Nekrutenko, A., Blankenberg, D., 2018. The Galaxy platform for accessible, reproducible and collaborative biomedical analyses: 2018 update. Nucleic Acids Res. 46(W1): W537-W544.

Agnalt, A., Grefsrud, E.S., Farestveit, E., Larsen, M., Keulder, F., 2013. Deformities in larvae and juvenile European lobster (*Homarus gammarus*) exposed to lower pH at two different temperatures. Biogeosciences 10(12): 7883-7895.

Ahearn, G.A., Mandal, P.K., Mandal, A., 2004. Calcium regulation in crustaceans during the molt cycle: a review and update. Comp. Biochem. Physiol. A Mol. Integr. Physiol. 137(2): 247-257.

Andersen, S.O., 1999. Exoskeletal proteins from the crab, *Cancer pagurus*. Comp. Biochem. Physiol. A Mol. Integr. Physiol. 123(2): 203-211.

Andrews, S., 2010. FastQC: a quality control tool for high throughput sequence data. Babraham Bioinformatics. http://www.bioinformatics.babraham.ac.uk/projects/fastqc/

Arnberg, M., Calosi, P., Spicer, J.I., Tandberg, A.H.S., Nilsen, M., Westerlund, S., Bechmann, R.K., 2013. Elevated temperature elicits greater effects than decreased pH on the development, feeding and metabolism of northern shrimp (*Pandalus borealis*) larvae. Mar. Biol. 160(8): 2037-2048.

Atema, J. and J.S. Cobb, 1980. Social behavior in the biology and management of lobsters. *In*: The Biology and Management of Lobsters (J.S. Cobb and B.F. Philips, eds.). pp. 409-450. Academic Press, New York, NY, USA.

Atema, J., Jacobson, S., Karnofsky, E., Oleszko-Szuts, S., Stein, L., 1979. Pair formation in the lobster, *Homarus americanus*: behavioral development pheromones and mating. Mar. Freshwater Behav. Physiol. 6(4): 277-296.

Babcock, D.T., Brock, A.R., Fish, G.S., Wang, Y., Perrin, L., Krasnow, M.A., Galko, M.J., 2008. Circulating blood cells function as a surveillance system for damaged tissue in *Drosophila* larvae. Proc. Natl. Acad. Sci. USA 105(29): 10017-10022.

Babraham Bioinformatics. Babraham Institute, Cambridge, England.

Barlow, J., Ridgway, G.J., 1969. Changes in serum protein during the molt and reproductive cycles of the American lobster (*Homarus americanus*). J. Fish. Res. Bd. Can. 26(8): 2101-2109.

Barret, L., Miron, G., Ouellet, P., Tremblay, R., 2017. Settlement behavior of American lobster (*Homarus americanus*): effect of female origin and developmental temperature. Fish. Oceanogr. 26(1): 69-82.

Barris, B.N., Shields, J.D., Small, H.J., Huchin-Mian, J.P., O'Leary, P., Shawver, J.V., Glenn, R.P., Pugh, T.L., 2018. Laboratory studies on the effect of temperature on epizootic shell disease in the American lobster, *Homarus americanus*. Bull. Mar. Sci. 94(4): 887-902.

Basti, D., Bricknell, I., Chang, E.S., Bouchard, D., 2010. Biochemical reference intervals for the resting state in the adult lobster *Homarus americanus*. J. Shellfish Res. 29(4): 1013-1019.

Battison, A., 2006. Tissue distribution and hemolymph activity of six enzymes in the American lobster (*Homarus americanus*): potential markers of tissue injury. J. Shellfish Res. 25(2): 553-560.

Battison, A., Cawthorn, R., Horney, B., 2003. Classification of *Homarus americanus* hemocytes and the use of differential hemocyte counts in lobsters infected with *Aerococcus viridans* var. *homari* (gaffkemia). J. Invertebr. Pathol. 84(3): 177-197.

Beasley, D.A.E., Bonisoli-Alquati, A., and Mousseau, T.A. 2013. The use of fluctuating asymmetry as a measure of environmentally induced developmental instability: A meta-analysis. Ecol. Ind. 30: 218-226.

Benestan, L., Gosselin, T., Perrier, C., Sainte-Marie, B., Rochette, R., Bernatchez, L. 2015. RAD genotyping reveals fine-scale genetic structuring and provides a powerful population assignment in a widely distributed marine species, the American lobster (*Homarus americanus*). Mol. Ecol. 24: 3299-3315.

Benestan, L., Quinn, B.K., Maaroufi, H., Laporte, M., Clark, F.K., Greenwood, S.J., Rochette, R., Bernatchez, L. 2016. Seascape genomics provides evidence for thermal adaptation and current-mediated population structure in American lobster (*Homarus americanus*). Mol. Ecol. 25: 5073-5092.

Bernardi, C., Baggiani, L., Tirloni, E., Stella, S., Colombo, F., Moretti, V.M., Cattaneo, P., 2015. Hemolymph parameters as physiological biomarkers in American lobster (*Homarus americanus*) for monitoring the effects of two commercial maintenance methods. Fish. Res. 161: 280-284.

Bibby, R., Widdicombe, S., Parry, H., Spicer, J., Pipe, R., 2008. Effects of ocean acidification on the immune response of the blue mussel *Mytilus edulis*. Aquat. Biol. 2(1): 67-74.

Bouchet, J.Y., Truchot, J.P., 1985. Effects of hypoxia and L-lactate on the haemocyanin-oxygen affinity of the lobster, *Homarus vulgaris*. Comp. Biochem. Physiol. A Physiol. 80(1): 69-73.

Bowden, T.J., 2017. The humoral immune systems of the American lobster (*Homarus americanus*) and the European lobster (*Homarus gammarus*). Fish. Res. 186: 367-371.

Braby, C.E., Somero, G.N., 2006. Following the heart: temperature and salinity effects on heart rate in native and invasive species of blue mussels (genus *Mytilus*). J. Exp. Biol. 209(13): 2554-2566.

Bridges, C.R., 2001. Modulation of haemocyanin oxygen affinity: properties and physiological implications in a changing world. J. Exp. Biol. 204(5): 1021-1032.

Browman, H.I., 2016. Applying organized scepticism to ocean acidification research. ICES J. Mar. Sci. 73(3): 529-536.

Calosi, P., Melatunan, S., Turner, L.M., Artioli, Y., Davidson, R.L., Byrne, J.J., Viant, M.R., Widdicombe, S., Rundle, S.D. 2017. Regional adaptation defines sensitivity to future ocean acidification. Nat. Commun. 8: 13994.

Camacho, J., Qadri, S.A., Wang, H., Worden, M.K., 2006. Temperature acclimation alters cardiac performance in the lobster *Homarus americanus*. J. Comp. Physiol. A 192(12): 1327-1334.

Campbell, A., 1986. Migratory movements of ovigerous lobsters, *Homarus americanus*, tagged off Grand Manan, eastern Canada. Can. J. Fish. Aquat. Sci. 43(11): 2197-2205.

Carloni, J.T., Wahle, R., Geoghegan, P., Bjorkstedt, E., 2018. Bridging the spawner-recruit disconnect: trends in American lobster recruitment linked to the pelagic food web. Bull. Mar. Sci. 94(3): 719-735.

Ceballos-Osuna, L., Carter, H.A., Miller, N.A., Stillman, J.H., 2013. Effects of ocean acidification on early life-history stages of the intertidal porcelain crab *Petrolisthes cinctipes*. J. Exp. Biol. 216(8): 1405-1411.

Cerenius, L., Soderhall, K., 2011. Coagulation in invertebrates. J. Innate Immun. 3(1): 3-8.

Chang, C., Hung, M., Cheng, W., 2011. Norepinephrine depresses the immunity and disease-resistance ability via α1-and β1-adrenergic receptors of *Macrobrachium rosenbergii*. Develop. Comp. Immunol. 35(6): 685-691.

Chang, C., Yeh, M., Cheng, W., 2009. Cold shock-induced norepinephrine triggers apoptosis of haemocytes via caspase-3 in the white shrimp, *Litopenaeus vannamei*. Fish. Shellfish Immunol. 27(6): 695-700.

Chang, E.S., Mykles, D.L., 2011. Regulation of crustacean molting: a review and our perspectives. Gen. Comp. Endocrinol. 172(3): 323-330.

Chang, J.-H., Chen, Y., Holland, D., Grabowski, J. 2010. Estimating spatial distribution of American lobster *Homarus americanus* using habitat variables. Mar. Ecol. Prog. Ser. 420: 145-156.

Cheng, L., Abraham, J., Hausfather, Z., Trenberth, K.E., 2019. How fast are the oceans warming? Science 363(6432): 128-129.

Cheng, W., Chieu, H., Ho, M., Chen, J., 2006. Noradrenaline modulates the immunity of white shrimp *Litopenaeus vannamei*. Fish Shellfish Immunol. 21(1): 11-19.

Clark, K.F., Greenwood, S.J., 2016. Next-generation sequencing and the crustacean immune system: the need for alternatives in immune gene annotation. Integ. Comp. Biol. 56(6): 1113-1130.

Clark, K.F., Acorn, A.R., Greenwood, S.J., 2013a. Differential expression of American lobster (*Homarus americanus*) immune related genes during infection of *Aerococcus viridans* var. *homari*, the causative agent of gaffkemia. J. Invertebr. Pathol. 112(2): 192-202.

Clark, K.F., Acorn, A.R., Greenwood, S.J., 2013b. A transcriptomic analysis of American lobster (*Homarus americanus*) immune response during infection with the bumper car parasite *Anophryoides haemophila*. Dev. Comp. Immunol. 40(2): 112-122.

Clark, K.F., Acorn, A.R., Wang, H., Greenwood, S.J., 2015. Comparative tissue expression of American lobster (*Homarus americanus*) immune genes during bacterial and scuticociliate challenge. Fish Shellfish Immunol. 47(2): 1054-1066.

Clark, K.F., Greenwood, S.J., Acorn, A.R., Byrne, P.J., 2013c. Molecular immune response of the American lobster (*Homarus americanus*) to the White Spot Syndrome Virus. J. Invertebr. Pathol. 114(3): 298-308.

Cobb, J.S., Wang, D., Campbell, D.B., Rooney, P., 1989. Speed and direction of swimming by postlarvae of the American lobster. Trans. Am. Fish. Soc. 118(1): 82-86.

Conesa, A., Madrigal, P., Tarazona, S., Gomez-Cabrero, D., Cervera, A., McPherson, A., Szcześniak, M.W., Gaffney, D.J., Elo, L.L., Zhang, X., 2016. A survey of best practices for RNA-seq data analysis. Genome Biol. 17(1): 13.

Conover, D.O., Schultz, E.T., 1995. Phenotypic similarity and the evolutionary significance of countergradient variation. Trends Ecol. Evolut. 10(6): 248-252.

Costa, R.N., Nomura, F., 2016. Measuring the impacts of Roundup Original® on fluctuating asymmetry and mortality in a Neotropical tadpole. Hydrobiologia 765(1): 85-96.

Crossin, G.T., Al-Ayoub, S.A., Jury, S.H., Howell, W.H., Watson, W.H., 1998. Behavioral thermoregulation in the American lobster *Homarus americanus*. J. Exp. Biol. 201(3): 365-374.

Cryonak, T., Schulz, K.G., Jokiel, P.L. 2016a. The omega myth: what really drives lower calcification rates in an acidifying ocean. ICES J. Mar. Sci. 73(3): 558-562.

Cryonak, T., Schulz, K.G., Jokiel, P.L. 2016b. Response to Waldbusser et al. (2016): "Calcium carbonate saturation state: on myths and this or that stories". ICES J. Mar. Sci. 73(3): 569-571.

Davis, B.E., Flynn, E.E., Miller, N.A., Nelson, F.A., Fangue, N.A., Todgham, A.E., 2018. Antarctic emerald rockcod have the capacity to compensate for warming when uncoupled from CO_2-acidification. Global Change Biol. 24(2): e655-e670.

Davis, B.E., Miller, N.A., Flynn, E.E., Todgham, A.E., 2016. Juvenile Antarctic rockcod, *Trematomus bernacchii*, are physiologically robust to CO_2–acidified seawater. J. Exp. Biol. 219(8): 1203-1213.

Dickson, A.G., Millero, F.J., 1987. A comparison of the equilibrium constants for the dissociation of carbonic acid in seawater media. Deep Sea Res. A. Oceanogr. Res. Pap. 34(10): 1733-1743.

Dickson, A.G., 1990. Standard potential of the reaction: AgCl (s) + $\frac{1}{2}H_2$ (g)= Ag (s) HCl (aq), and and the standard acidity constant of the ion HSO_4^- in synthetic sea water from 273.15 to 318.15 K. J. Chem. Thermodyn. 22(2): 113-127.

Dissanayake, A., Clough, R., Spicer, J.I., Jones, M.B., 2010. Effects of hypercapnia on acid–base balance and osmo-/iono-regulation in prawns (Decapoda: Palaemonidae). Aquat. Biol. 11(1): 27-36.

Dissanayake, A., Ishimatsu, A., 2011. Synergistic effects of elevated CO_2 and temperature on the metabolic scope and activity in a shallow-water coastal decapod (*Metapenaeus joyneri*; Crustacea: Penaeidae). ICES J. Mar. Sci.: Journal du Conseil 68(6): 1147-1154.

Dove, A.D., Allam, B., Powers, J.J., Sokolowski, M.S., 2005. A prolonged thermal stress experiment on the American lobster, *Homarus americanus*. J. Shellfish Res. 24(3): 761-765.

Ellis, R.P., Spicer, J.I., Byrne, J.J., Sommer, U., Viant, M.R., White, D.A., Widdicombe, S., 2014. 1H NMR metabolomics reveals contrasting response by male and female mussels exposed to reduced seawater pH, increased temperature, and a pathogen. Environ. Sci. Technol. 48(12): 7044-7052.

Ennis, G.P., 1975. Observations on hatching and larval release in the lobster *Homarus americanus*. J. Fish. Bd. Can. 32(11): 2210-2213.

Evans, T.G., 2015. Considerations for the use of transcriptomics in identifying the 'genes that matter' for environmental adaptation. J. Exp. Biol. 218(12): 1925-1935.

Evans, T.G., Pespeni, M.H., Hofmann, G.E., Palumbi, S.R., Sanford, E., 2017. Transcriptomic responses to seawater acidification among sea urchin populations inhabiting a natural pH mosaic. Mol. Ecol. 26(8): 2257-2275.

Factor, J., 1995. Biology of the Lobster*: Homarus americanus*. Academic Press, Boston, MA.

Fasola, E., Ribeiro, R., Lopes, I., 2015. Microevolution due to pollution in amphibians: a review on the genetic erosion hypothesis. Environ. Pollut. 204: 181-190.

Fisher, W.S., Rosemark, T.R., Nilson, E.H., 1976. The susceptibility of cultured American lobsters to a chitinolytic bacterium. Proc. Annl. Meet. World Maricul. Soc. 7(1-4): 511-520.

Fisher, W.S., Nilson, E.H., Steenbergen, J.F., Lightner, D.V., 1978. Microbial diseases of cultured lobsters: a review. Aquaculture 14(2): 115-140.

Foo, S.A., Byrne, M. 2016. Chapter 2: Acclimatization and adaptive capacity of marine species in a changing ocean. *In*: Advances in Marine Biology. Vol. 74, pp. 69-116.

Food and Agriculture Organization (FAO) of the United Nations, 2017. Fisheries and Aquaculture Department Statistics [online]. Available from http://www.fao.org/fishery/statistics/en [accessed 01 Jan 2018].

Fujitani, N., Hasegawa, H., Kakizaki, H., Ikeda, M., Matsumiya, M., 2014. Molecular cloning of multiple chitinase genes in swimming crab *Portunus trituberculatus*. J. Chitin and Chitosan Sci. 2(2): 149-156.

Ghosh, J., Lun, C.M., Majeske, A.J., Sacchi, S., Schrankel, C.S., Smith, L.C., 2011. Invertebrate immune diversity. Dev. Comp. Immunol. 35(9): 959-974.

Gledhill, D.K., White, M.M., Salisbury, J.E., Thomas, H., Mlsna, I., Liebman, M., Mook, B., Grear, J.S., Candelmo, A.C., Chambers, R.C., 2015. Ocean and coastal acidification off New England and Nova Scotia. Oceanogr. 28(2): 182-197.

Goncalves, P., Jones, D.B., Thompson, E.L., Parker, L.M., Ross, P.M., Raftos, D.A., 2017. Transcriptomic profiling of adaptive responses to ocean acidification. Mol. Ecol. 26(21): 5974-5988.

Götz, S., García-Gómez, J.M., Terol, J., Williams, T.D., Nagaraj, S.H., Nueda, M.J., Robles, M., Talón, M., Dopazo, J., Conesa, A., 2008. High-throughput functional annotation and data mining with the Blast2GO suite. Nucleic Acids Res. 36(10): 3420-3435.

Grabherr, M.G., Haas, B.J., Yassour, M., Levin, J.Z., Thompson, D.A., Amit, I., Adiconis, X., Fan, L., Raychowdhury, R., Zeng, Q., 2011. Full-length transcriptome assembly from RNA-Seq data without a reference genome. Nat. Biotechnol. 29(7): 644-652.

Groner, M.L., Shields, J.D., Landers Jr, D.F., Swenarton, J., Hoenig, J.M., 2018. Rising temperatures, molting phenology, and epizootic shell disease in the American lobster. Am. Nat. 192(5): E163-E177.

Guo, Z., Yang, Z., Cheng, Y., Ji, L., Que, Y., Liu, Z., Zeng, Q., 2013. Molecular characterization, tissue expression of acyl-CoAΔ 9-desaturase-like gene, and effects of dietary lipid levels on its expression in the hepatopancreas of the Chinese mitten crab (*Eriocheir sinensis*). Aquaculture 402: 58-65.

Haas, B.J., Papanicolaou, A., Yassour, M., Grabherr, M., Blood, P.D., Bowden, J., Couger, M.B., Eccles, D., Li, B., Lieber, M., 2013. *De novo* transcript sequence reconstruction from RNA-seq using the Trinity platform for reference generation and analysis. Nat. Protoc. 8(8): 1494-1512.

Hadley, P.B., 1906. Regarding the rate of growth of the American lobster. Biol. Bull. 10: 233-241.

Hansen, J., Sato, M., Ruedy, R., 2012. Perception of climate change. Proc. Natl. Acad. Sci. USA 109(37): E2415- E2423.

Harrington, A.M., Tudor, M.S., Reese, H.R., Bouchard, D.A., Hamlin, H.J., 2019. Effects of temperature on larval American lobster (*Homarus americanus*): is there a trade-off between growth rate and developmental stability? Ecol. Ind. 96: 404-411.

Helmuth, B., Harley, C.D., Halpin, P.M., O'Donnell, M., Hofmann, G.E., Blanchette, C.A. 2002. Climate change and latitudinal patterns of intertidal thermal stress. Science 298: 1015-1017.

Helmuth, B., Broitman, B.R., Blanchette, C.A., Gilman, S., Halpin, P., Harley, C.D., O'Donnell, M.J., Hofmann, G.E., Menge, B., Strickland, D. 2006. Mosaic patterns of thermal stress in the rocky intertidal zone: Implications for climate change. Ecol. Monog. 76: 461-479.

Hendriks, I.E., Duarte, C.M., Álvarez, M., 2010. Vulnerability of marine biodiversity to ocean acidification: a meta-analysis. Estuar. Coast. Shelf Sci. 86(2): 157-164.

Hernroth, B., Krang, A., Baden, S., 2015. Bacteriostatic suppression in Norway lobster (*Nephrops norvegicus*) exposed to manganese or hypoxia under pressure of ocean acidification. Aquat. Toxicol. 159: 217-224.

Hernroth, B., Skold, H.N., Wiklander, K., Jutfelt, F., Baden, S., 2012. Simulated climate change causes immune suppression and protein damage in the crustacean *Nephrops norvegicus*. Fish Shellfish Immunol. 33(5): 1095-1101.

Herrick, F.H., 1911. Natural History of the American Lobster. US Government Printing Office.

Herrick, F.H., 1895. The American Lobster: A Study of its Habits and Development. Govt. Print. Office.

Hines, D.J., Clark, K.F., Greenwood, S.J., 2014. Global gene expression profiling of *Homarus americanus* (Crustacea) larval stages during development and metamorphosis. Invertebr. Reprod. Dev. 58(2): 97-107.

Hoffmann, J.A., 2003. The immune response of *Drosophila*. Nature 426(6962): 33-38.

Holthuis, L.B., 1991. FAO species catalogue. v. 13: Marine lobsters of the world. An annotated and illustrated catalogue of species of interest to fisheries known to date.

Hovel, K.A., Wahle, R.A., 2010. Effects of habitat patchiness on American lobster movement across a gradient of predation risk and shelter competition. Ecology 91(7): 1993-2002.

Imasheva, A.G., Loeschcke, V., Zhivotovsky, L.A., Lazebny, O.E., 1997. Effects of extreme temperatures on phenotypic variation and developmental stability in *Drosophila melanogaster* and *Drosophila buzzatii*. Biol. J. Linn. Soc. 61(1): 117-126.

Inoue, H., Ohira, T., Ozaki, N., Nagasawa, H., 2003. Cloning and expression of a cDNA encoding a matrix peptide associated with calcification in the exoskeleton of the crayfish. Comp. Biochem. Physiol. B Biochem. Mol. Biol. 136(4): 755-765.

Inoue, H., Yuasa-Hashimoto, N., Suzuki, M., Nagasawa, H., 2008. Structural determination and functional analysis of a soluble matrix protein associated with calcification of the exoskeleton of the crayfish, *Procambarus clarkii*. Biosci. Biotechnol. Biochem. 72(10): 2697-2707.

IPCC. 2013. Climate Change 2013: The Physical Science Basis. Contribution of Working Group I to the Fifth Assessment Report of the Intergovernmental Panel on Climate Change. (T.F. Stocker, D. Qin, G.-K. Plattner, M. Tignor, S.K. Allen, J. Boschung, A. Nauels, Y. Xia, V. Bex and B.M. Midgley, eds.), 1535 pp. Cambridge University Press, Cambridge, UK, and New York, NY, USA.

Jussila, J., McBride, S., Jago, J., Evans, L.H., 2001. Hemolymph clotting time as an indicator of stress in western rock lobster (*Panulirus cygnus* George). Aquaculture 199(1): 185-193.

Karnofsky, E.B., Atema, J., Elgin,R.H., 1989. Field observations of social behavior, shelter use, and foraging in the lobster, *Homarus americanus*. Biol. Bull. 176(3): 239-246.

Kelly, M.W., Padilla-Gamiño, J.L., Hofmann, G.E. 2013. Natural variation and the capacity to adapt to ocean acidification in the keystone sea urchin *Strongylocentrotus purpuratus*. Global Change Biol. 19(8): 2536-2546.

Keppel, E.A., Scrosati, R.A., Courtenay, S.C., 2012. Ocean acidification decreases growth and development in American lobster (*Homarus americanus*) larvae. J. Northw. Atl. Fish. Sci 44: 61-66.

Khatri, P., Sirota, M., Butte, A.J., 2012. Ten years of pathway analysis: current approaches and outstanding challenges. PLoS computational biology 8(2): e1002375.

Kim, B., Kim, M., Kim, A.R., Yi, M., Choi, J., Park, H., Park, W., Kim, H., 2013. Differences in gene organization between type I and type II crustins in the morotoge shrimp, *Pandalopsis japonica*. Fish Shellfish Immunol. 35(4): 1176-1184.

Kim, D., Langmead, B., Salzberg, S.L., 2015. HISAT: a fast spliced aligner with low memory requirements. Nat. Methods 12(4): 357.

Kim, S., Lee, S., Park, M., Choi, H., Park, J., Min, G., 2011. The complete mitochondrial genome of the American lobster, *Homarus americanus* (Crustacea, Decapoda). Mitochondrial DNA 22(3): 47-49.

Kim, T.W., Taylor, J., Lovera, C., Barry, J.P., 2016. CO_2-driven decrease in pH disrupts olfactory behaviour and increases individual variation in deep-sea hermit crabs. ICES J. Mar. Sci. 73(3): 613-619.

Kleisner, K.M., Fogarty, M.J., McGee, S., Barnett, A., Fratantoni, P., Greene, J., Hare, J.A., Lucey, S.M., McGuire, C., Odell, J., 2016. The effects of sub-regional climate velocity on the distribution and spatial extent of marine species assemblages. PLoS One 11(2): e0149220.

Klisarić, N.B., Miljković, D., Avramov, S., Živković, U., Tarasjev, A., 2014. Fluctuating asymmetry in *Robinia pseudoacacia* leaves—possible in situ biomarker? Environ. Sci. Pollut. Res. 21(22): 12928-12940.

Knapp, J.L., Bridges, C.R., Krohn, J., Hoffman, L.C., Auerswald, L., 2016. The effects of hypercapnia on the West Coast rock lobster (*Jasus lalandii*) through acute exposure to decreased seawater pH. J. Exp. Mar. Biol. Ecol. 476: 58-64.

Knapp, J.L., Bridges, C.R., Krohn, J., Hoffman, L.C., Auerswald, L., 2015. Acid-base balance and changes in haemolymph properties of the South African rock lobsters, *Jasus lalandii*, a palinurid decapod, during chronic hypercapnia. Biochem. Biophys. Res. Commun. 461(3): 475-480.

Koopman, H.N., Westgate, A.J., Siders, Z.A., Cahoon, L.B., 2014. Rapid subsurface ocean warming in the Bay of Fundy as measured by free-swimming basking sharks. Oceanogr. 27(2): 14-17.

Kroeker, K.J., Kordas, R.L., Crim, R.N., Singh, G.G., 2010. Meta-analysis reveals negative yet variable effects of ocean acidification on marine organisms. Ecol. Lett. 13(11): 1419-1434.

Kroeker, K.J., Kordas, R.L., Crim, R., Hendriks, I.E., Ramajo, L., Singh, G.S., Duarte, C.M., Gattuso, J., 2013. Impacts of ocean acidification on marine organisms: quantifying sensitivities and interaction with warming. Global Change Biol. 19(6): 1884-1896.

Kuo, E.S., Sanford, E. 2009. Geographic variation in the upper thermal limits of an intertidal snail: Implications for climate envelope models. Mar. Ecol. Prog. Ser. 388: 137-146.

Kunz, K.L., Claireaux, G., Pörtner, H., Knust, R., Mark, F.C., 2018. Aerobic capacities and swimming performance of Polar cod (*Boreogadus saida*) under ocean acidification and warming conditions. J. Exp. Biol. 221(21): jeb184473.

Labaude, S., Moret, Y., Cézilly, F., Reuland, C., Rigaud, T., 2017. Variation in the immune state of *Gammarus pulex* (Crustacea, Amphipoda) according to temperature: are extreme temperatures a stress? Dev. Comp. Immunol. 76: 25-33.

Lavalli, K.L., Barshaw, D.E., 1986. Burrows protect postlarval lobsters Homarus americanus from predation by the non-burrowing cunner *Tautogolabrus adspersus*, but not from the burrowing mud crab *Neopanope texani*. Mar. Ecol. Prog. Ser. 32: 13-16.

Lavalli. K.L., Lawton, P. 1996. Historical review of lobster life history terminology and proposed modifications to current schemes. Crustaceana. 69(5): 594-609.

Lazić, M.M., Kaliontzopoulou, A., Carretero, M.A., Crnobrnja-Isailović, J., 2013. Lizards from urban areas are more asymmetric: using fluctuating asymmetry to evaluate environmental disturbance. PloS One 8(12): e84190.

Le Moullac, G., Haffner, P., 2000. Environmental factors affecting immune responses in Crustacea. Aquaculture 191(1-3): 121-131.

Lesk, A., 2013. Introduction to Bioinformatics. Oxford University Press, Oxford, UK.

Leung, B., Forbes, M.R., 1996. Fluctuating asymmetry in relation to stress and fitness: effects of trait type as revealed by meta-analysis. Ecoscience 3(4): 400-413.

Lezcano, A.H., Quiroga, M.L.R., Liberoff, A.L., Van der Molen, S., 2015. Marine pollution effects on the southern surf crab *Ovalipes trimaculatus* (Crustacea: Brachyura: Polybiidae) in Patagonia Argentina. Mar. Pollut. Bull. 91(2): 524-529.

Liao, Y., Smyth, G.K., Shi, W., 2013. featureCounts: an efficient general purpose program for assigning sequence reads to genomic features. Bioinformatics 30(7): 923-930.

Lin, Y., Vaseeharan, B., Chen, J., 2008. Molecular cloning and phylogenetic analysis on α2-macroglobulin (α2-M) of white shrimp *Litopenaeus vannamei*. Dev. Comp. Immunol. 32(4): 317-329.

Liu, R., Holik, A.Z., Su, S., Jansz, N., Chen, K., Leong, H.S., Blewitt, M.E., Asselin-Labat, M., Smyth, G.K., Ritchie, M.E., 2015. Why weight? Modelling sample and observational level variability improves power in RNA-seq analyses. Nucleic Acids Res. 43(15): e97.

Lockwood, B.L., Sanders, J.G., Somero, G.N., 2010. Transcriptomic responses to heat stress in invasive and native blue mussels (genus *Mytilus*): molecular correlates of invasive success. J. Exp. Biol. 213(20): 3548-3558.

Longhurst, A. 1998. Ecological Geography of the Sea. Academic Press, Burlington, MA.

Lorenzon, S., Giulianini, P.G., Martinis, M., Ferrero, E.A., 2007. Stress effect of different temperatures and air exposure during transport on physiological profiles in the American lobster *Homarus americanus*. Comp. Biochem. Physiol. A Mol. Integr. Physiol. 147(1): 94-102.

Love, M.I., Huber, W., Anders, S., 2014. Moderated estimation of fold change and dispersion for RNA-seq data with DESeq2. Genome Biol. 15(12): 550.

Lucey, S.M., Nye, J.A., 2010. Shifting species assemblages in the Northeast US Continental Shelf Large Marine Ecosystem. Mar. Ecol. Prog. Ser. 415: 23-33.

Ma, H., Wang, B., Zhang, J., Li, F., Xiang, J., 2010. Multiple forms of alpha-2 macroglobulin in shrimp *Fenneropenaeus chinesis* and their transcriptional response to WSSV or *Vibrio* pathogen infection. Dev. Comp. Immunol. 34(6): 677-684.

MacKenzie, B.R., 1988. Assessment of temperature effects on interrelationships between stage durations, mortality, and growth in laboratory-reared *Homarus americanus* Milne Edwards larvae. J. Exp. Mar. Biol. Ecol. 116: 87-98.

Madeira, D., Mendonça, V., Dias, M., Roma, J., Costa, P.M., Larguinho, M., Vinagre, C., Diniz, M.S., 2015. Physiological, cellular and biochemical thermal stress response of intertidal shrimps with different vertical distributions: *Palaemon elegans* and *Palaemon serratus*. Comp. Biochem. Physiol. A Mol. Integr. Physiol. 183: 107-115.

Magozzi, S., Calosi, P., 2015. Integrating metabolic performance, thermal tolerance, and plasticity enables for more accurate predictions on species vulnerability to acute and chronic effects of global warming. Global Change Biol. 21(1): 181-194.

Maine Department of Marine Resources (ME DMR). 2019. Most Recent Maine Commercial Landings – 2018 Landings Information. https://www.maine.gov/dmr/commercial-fishing/landings/index.html

Maine Department of Marine Resources (ME DMR). 2017. 2017 Lobster Monitory Update (K. Reardon, K. Thompson, and R. Russell, eds.). 2 pp. https://www.maine.gov/dmr/science-research/species/lobster/documents/2017monitoring.pdf

Martin, G.G., Hose, J.E. 1995. Circulation, the blood, and disease. *In*: Biology of the Lobster: *Homarus americanus* (J. Factor, ed). Elsevier, Academic Press, Inc., San Diego, CA. pp. 465-495.

Maxwell, S.E., Delaney, H.D. 2004. Designing experiments and analyzing data: a model comparison perspective, *2nd ed*. Psychology Press, New York, NY, USA.

McGrath, L.L., Vollmer, S.V., Kaluziak, S.T., Ayers, J., 2016. *De novo* transcriptome assembly for the lobster *Homarus americanus* and characterization of differential gene expression across nervous system tissues. BMC Genomics 17(1): 63.

McGaw, I.J., Reiber, C.L. 2015. Circulatory physiology. *In*: The Natural History of the Crustacea, Volume 4: Physiology (E. S. Chang and M. Thiel, eds.), pp. 199–248. Oxford University Press, Oxford, UK.

Mehrbach, C., Culberson, C.H., Hawley, J.E., Pytkowicx, R.M., 1973. Measurement of the apparent dissociation constants of carbonic acid in seawater at atmospheric pressure1. Limnol. Oceanogr. 18(6): 897-907.

Mercaldo-Allen, R., 1991. Changes in the blood chemistry of the American lobster, *Homarus americanus*, H. Milne Edwards, 1837, over the molt cycle. J. Shellfish Res. 10(1): 147-156.

Mercaldo-Allen, R., Thurberg, F.P., 1987. Heart and gill ventilatory activity in the lobster, *Homarus americanus,* at various temperatures. Fish. Bull. 85(3): 643-644.

Meseck, S.L., Alix, J.H., Swiney, K.M., Long, W.C., Wikfors, G.H., Foy, R.J., 2016. Ocean acidification affects hemocyte physiology in the Tanner crab (*Chionoecetes bairdi*). PloS One 11(2): e0148477.

Metzger, R., Sartoris, F.J., Langenbuch, M., Pörtner, H.O., 2007. Influence of elevated CO_2 concentrations on thermal tolerance of the edible crab *Cancer pagurus*. J. Therm. Biol. 32(3): 144-151.

Mills, K.E., Pershing, A.J., Brown, C.J., Chen, Y., Chiang, F.-S., Holland, D.S., Lehuta, S., Nye, J.A., Sun, J.C., Thomas, A.C., Wahle, R.A. 2013. Fisheries management in a changing climate: lessons from the 2012 ocean heat wave in the Northwest Atlantic. Oceanogr. 26(2): 191-195.

Milne Edwards, H. 1837. *Histoire naturelle des Crustacés, comprenant l'anatomie, la physiologie et la classi cation de ces animaux*. Vol. 2. Librairie Encyclopédique de Roret, Paris.

Møller, A.P. 2006. A review of developmental instability, parasitism and disease: infection, genetics and evolution. Infect. Genet. Evol. 6(2): 133-140.

Monna, F., Camizuli, E., Revelli, P., Biville, C., Thomas, C., Losno, R., Scheifler, R., Bruguier, O., Baron, S., Chateau, C., 2011. Wild brown trout affected by historical mining in the Cévennes National Park, France. Environ. Sci. Technol. 45(16): 6823-6830.

Mori, K., Stewart, J.E., 2006. Immunogen-dependent quantitative and qualitative differences in phagocytic responses of the circulating hemocytes of the lobster Homarus americanus. Dis. Aquat. Org. 69: 197-203.

Moriya, Y., Itoh, M., Okuda, S., Yoshizawa, A.C., Kanehisa, M., 2007. KAAS: an automatic genome annotation and pathway reconstruction server. Nucleic Acids Res. 35(Suppl_2): W182-W185.

Morris, M.R., Ludwar, B.C., Swingle, E., Mamo, M.N., Shubrook, J.H., 2016. A New Method to Assess Asymmetry in Fingerprints Could Be Used as an Early Indicator of Type 2 Diabetes Mellitus. Journal of diabetes science and technology 10(4): 864-871.

Moya, A., Huisman, L., Ball, E.E., Hayward, D.C., Grasso, L.C., Chua, C.M., Woo, H.N., Gattuso, J., Foret, S., Miller, D.J., 2012. Whole transcriptome analysis of the coral *Acropora millepora* reveals complex responses to CO_2-driven acidification during the initiation of calcification. Mol. Ecol. 21(10): 2440-2454.

Mustafa, S., Kharudin, S.N., Kian, A.Y.S., 2015. Effect of simulated ocean acidification on chitin content in the shell of white shrimp, *Litopenaeus vannamei*. J. FisheriesSciences.com 9(2): 6.

Nehemia, A., Huyghe, F., Kochzius, M., 2017. Genetic erosion in the snail *Littoraria subvittata* (Reid, 1986) due to mangrove deforestation. J. Molluscan Stud. 83(1): 1-10.

Nies, A., Zeis, B., Bridges, C.R., Grieshaber, M.K., 1992. Allosteric modulation of haemocyanin oxygen-affinity by L-lactate and urate in the lobster *Homarus vulgaris*: II. characterization of specific effector binding sites. J. Exp. Biol. 168(1): 111-124.

Nishizaki, M.T., Barron, S., Carew, E., 2015. Thermal stress increases fluctuating asymmetry in marine mussels: Environmental variation and developmental instability. Ecosphere 6(5): 1-15.

Nye, J.A., Link, J.S., Hare, J.A., Overholtz, W.J., 2009. Changing spatial distribution of fish stocks in relation to climate and population size on the Northeast United States continental shelf. Mar. Ecol. Prog. Ser. 393: 111-129.

Olianas, A., Manconi, B., Masia, D., Sanna, M.T., Castagnola, M., Salvadori, S., Messana, I., Giardina, B., Pellegrini, M., 2009. The oxygen-binding modulation of hemocyanin from the Southern spiny lobster *Palinurus gilchristi*. J. Comp. Physiol. B 179(2): 193.

Oppenheim, N.G., Wahle, R.A., Rochet, M.J., 2013. Cannibals by night? *In situ* video monitoring reveals diel shifts in inter-and intra-specific predation on the American lobster. Can. J. Fish. Aquat. Sci. 70(11): 1635-1640.

Orlando, F.E., Guillette, J.L., 2001. A re-examination of variation associated with environmentally stressed organisms. Apmis 109(S103): S178–S186.

Palma, A.T., Wahle, R., Steneck, R., 1998. Different early post-settlement strategies between American lobsters *Homarus americanus* and rock crabs *Cancer irroratus* in the Gulf of Maine. Mar. Ecol. Prog. Ser. 162: 215-225.

Palmer, A.R., Strobeck, C., 2003. CH 17. Fluctuating asymmetry analyses revisited. *In*: Developmental Instability: Causes and Consequences (M. Polak, ed). Oxford University Press, New York, NY, pp. 279-319.

Palmer, A.R., Strobeck, C., 1986. Fluctuating asymmetry: measurement, analysis, patterns. Annu. Rev. Ecol. Syst. 17(1): 391-421.

Pan, T.F., Applebaum, S.L., Manahan, D.T., 2015. Experimental ocean acidification alters the allocation of metabolic energy. Proc. Natl. Acad. Sci. USA 112(15): 4696-4701.

Parker, L.M., O'Connor, W.A., Raftos, D.A., Pörtner, H., Ross, P.M. 2015. Persistence of positive carryover effects in the oyster, *Saccostrea glomerata*, following transgenerational exposure to ocean acidification. PLoS One. 10(7): e0132276.

Pearce, J., Balcom, N., 2005. The 1999 Long Island Sound lobster mortality event: findings of the comprehensive research initiative. J. Shellfish Res. 24: 691-697.

Pershing, A.J., Alexander, M.A., Hernandez, C.M., Kerr, L.A., Le Bris, A., Mills, K.E., Nye, J.A., Record, N.R., Scannell, H.A., Scott, J.D., 2015. Slow adaptation in the face of rapid warming leads to collapse of the Gulf of Maine cod fishery. Science 350: 809-812.

Pertea, M., Kim, D., Pertea, G.M., Leek, J.T., Salzberg, S.L., 2016. Transcript-level expression analysis of RNA-seq experiments with HISAT, StringTie and Ballgown. Nat. Protoc. 11(9): 1650.

Pertea, M., Pertea, G.M., Antonescu, C.M., Chang, T., Mendell, J.T., Salzberg, S.L., 2015. StringTie enables improved reconstruction of a transcriptome from RNA-seq reads. Nat. Biotechnol. 33(3): 290.

Pespeni, M.H., Barney, B.T., Palumbi, S.R., 2013. Differences in the regulation of growth and biomineralization genes revealed through long-term common-garden acclimation and experimental genomics in the purple sea urchin. Evolution 67(7): 1901-1914.

Pierrot, D., Lewis, E., Wallace, D.W.R. 2006. MS Excel Program Developed for CO_2 System Calculations. ORNL/CDIAC-105a. Carbon Dioxide Information Analysis Center, Oak Ridge National Laboratory, U.S. Department of Energy, Oak Ridge, Tennessee.

Pisuttharachai, D., Fagutao, F.F., Yasuike, M., Aono, H., Yano, Y., Murakami, K., Kondo, H., Aoki, T., Hirono, I., 2009. Characterization of crustin antimicrobial proteins from Japanese spiny lobster *Panulirus japonicus*. Dev. Comp. Immunol. 33(10): 1049-1054.

Polak, M. 2003. Developmental instability: causes and consequences. Oxford University Press, New York, NY.

Pörtner, H., 2010. Oxygen-and capacity-limitation of thermal tolerance: a matrix for integrating climate-related stressor effects in marine ecosystems. J. Exp. Biol. 213(6): 881-893.

Pörtner, H., 2008. Ecosystem effects of ocean acidification in times of ocean warming: a physiologist's view. Mar. Ecol. Prog. Ser. 373: 203-217.

Pörtner, H., Bock, C., Mark, F.C., 2017. Oxygen-and capacity-limited thermal tolerance: bridging ecology and physiology. J. Exp. Biol. 220(15): 2685-2696.

Potvin, D.A., Parris, K.M., Smith Date, K.L., Keely, C.C., Bray, R.D., Hale, J., Hunjan, S., Austin, J.J., Melville, J., 2017. Genetic erosion and escalating extinction risk in frogs with increasing wildfire frequency. J. Appl. Ecol. 54(3): 945-954.

Preziosi, B.M., Runge, J.A., 2014. The effect of warm temperatures on hatching success of the marine planktonic copepod, *Calanus finmarchicus*. J. Plankton Res. 36(5): 1381-1384.

Przeslawski, R., Byrne, M., Mellin, C., 2015. A review and meta-analysis of the effects of multiple abiotic stressors on marine embryos and larvae. Global Change Biol. 21(6): 2122-2140.

Qadri, S.A., Camacho, J., Wang, H., Taylor, J.R., Grosell, M., Worden, M.K., 2007. Temperature and acid–base balance in the American lobster *Homarus americanus*. J. Exp. Biol. 210(7): 1245-1254.

Quinn, B.K., 2017. Threshold temperatures for performance and survival of American lobster larvae: A review of current knowledge and implications to modeling impacts of climate change. Fish. Res. 186: 383-396.

Quinn, B.K., Rochette, R., 2015. Potential effect of variation in water temperature on development time of American lobster larvae. ICES J. Mar. Sci. 72(Suppl_1): i90.

Quinn, B.K., Chassé, J., Rochette, R., 2017. Potential connectivity among American lobster fisheries as a result of larval drift across the species' range in eastern North America. Can. J. Fish. Aquat. Sci.74: 1-15.

Quinn, B.K., Rochette, R., Ouellet, P., Sainte-Marie, B., 2013. Effect of temperature on development rate of larvae from cold-water American lobster (*Homarus americanus*). J. Crust. Biol. 33(4): 527-536.

Rantala, M.J., Ahtiainen, J.J., Suhonen, J., 2004. Fluctuating asymmetry and immune function in a field cricket. Oikos 107(3): 479-484.

Reid, P.C., Beaugrand, G., 2012. Global synchrony of an accelerating rise in sea surface temperature. J. Mar. Biol. Assoc. UK 92: 1435-1450.

Reum, J.C., Alin, S.R., Harvey, C.J., Bednaršek, N., Evans, W., Feely, R.A., Hales, B., Lucey, N., Mathis, J.T., McElhany, P., 2015. Interpretation and design of ocean acidification experiments in upwelling systems in the context of carbonate chemistry co-variation with temperature and oxygen. ICES J. Mar. Sci. 73(3): 582-595.

Ribeiro, R., Lopes, I., 2013. Contaminant driven genetic erosion and associated hypotheses on alleles loss, reduced population growth rate and increased susceptibility to future stressors: an essay. Ecotoxicology 22(5): 889-899.

Richards, R.A., Fogarty, M.J., Mountain, D.G., Taylor, M.H., 2012. Climate change and northern shrimp recruitment variability in the Gulf of Maine. Mar. Ecol. Prog. Ser. 464: 167-178.

Riebesell, U., Fabry, V.J., Hansson, L., Gattuso, J. 2011. Guide to best practices for ocean acidification research and data reporting. Office for Official Publications of the European Communities.

Ries, J.B., 2011. A physicochemical framework for interpreting the biological calcification response to CO_2-induced ocean acidification. Geochim. Cosmochim. Acta 75(14): 4053-4064.

Ries, J.B., Cohen, A.L., McCorkle, D.C., 2009. Marine calcifiers exhibit mixed responses to CO_2-induced ocean acidification. Geology 37(12): 1131-1134.

Robinson, M.D., McCarthy, D.J., Smyth, G.K., 2010. edgeR: a Bioconductor package for differential expression analysis of digital gene expression data. Bioinformatics 26(1): 139-140.

Rosa, R.D., Bandeira, P.T., Barracco, M.A., 2007. Molecular cloning of crustins from the hemocytes of Brazilian penaeid shrimps. FEMS Microbiol. Lett. 274(2): 287-290.

Ross, P.M., Parker, L., Byrne, M. 2016. Transgenerational responses of molluscs and echinoderms to changing ocean conditions. ICES J. Mar. Sci. 73(3): 537-549.

Royet, J., 2004. Infectious non-self recognition in invertebrates: lessons from Drosophila and other insect models. Mol. Immunol. 41(11): 1063-1075.

Rubidge, E.M., Patton, J.L., Lim, M., Burton, A.C., Brashares, J.S., Moritz, C., 2012. Climate-induced range contraction drives genetic erosion in an alpine mammal. Nat. Clim. Change 2(4): 285-288.

Rueden, C.T., Schindelin, J., Hiner, M.C., DeZonia, B.E., Walter, A.E., Arena, E.T., Eliceiri, K.W., 2017. ImageJ2: ImageJ for the next generation of scientific image data. BMC Bioinformatics 18(1): 529.

Rumisha, C., Leermakers, M., Elskens, M., Mdegela, R.H., Gwakisa, P., Kochzius, M., 2017. Genetic diversity of the giant tiger prawn Penaeus monodon in relation to trace metal pollution at the Tanzanian coast. Mar. Pollut. Bull. 114(2): 759-767.

Sanford, E., Holzman, S.B., Haney, R.A., Rand, D.M., Bertness, M.D., 2006. Larval tolerance, gene flow, and the northern geographic range limit of fiddler crabs. Ecology 87(11): 2882-2894.

Savage, A., Hogarth, P.J., 1999. An analysis of temperature-induced fluctuating asymmetry in *Asellus aquaticus* (Linn.). Hydrobiologia 411: 139-143.

Scannell, H.A., Pershing, A.J., Alexander, M.A., Thomas, A.C., Mills, K.E., 2016. Frequency of marine heatwaves in the North Atlantic and North Pacific since 1950. Geophys. Res. Lett. 43(5): 1-8.

Shafer, T.H., Knapp, W.E., Golus, J.M., 2009. A new family of crustacean cuticle proteins possibly related to mineralization of pre-exuvial cuticle. Integr. Comp. Biol. 49: E305.

Sherman, K., Belkin, I.M., Friedland, K.D., O'Reilly, J., Hyde, K., 2009. Accelerated warming and emergent trends in fisheries biomass yields of the world's large marine ecosystems. Ambio 38(4): 215-224.

Shrivastava, S., Princy, S.A., 2015. Effect of a novel compound as dietary supplement on growth of decapod crustaceans. RSC Advances 5(80): 65546-65553.

Sigurdsson, G.M., Rochette, R., 2013. Predation by green crab and sand shrimp on settling and recently settled American lobster postlarvae. J. Crustac. Biol. 33(1): 10-14.

Smale, D.A., Wernberg, T., Oliver, E.C., Thomsen, M., Harvey, B.P., Straub, S.C., Burrows, M.T., Alexander, L.V., Benthuysen, J.A., Donat, M.G., 2019. Marine heatwaves threaten global biodiversity and the provision of ecosystem services. Nat. Clim. Change 1.

Small, D.P., Calosi, P., Boothroyd, D., Widdicombe, S., Spicer, J.I., 2016. The sensitivity of the early benthic juvenile stage of the European lobster *Homarus gammarus* (L.) to elevated pCO_2 and temperature. Mar. Biol. 163(3): 1-12.

Small, D.P., Calosi, P., Boothroyd, D., Widdicombe, S., Spicer, J.I., 2015. Stage-specific changes in physiological and life-history responses to elevated temperature and pCO_2 during the larval development of the European lobster *Homarus gammarus* (L.). Physiol. Biochem. Zool. 88(5): 494-507.

Small, D., Calosi, P., White, D., Spicer, J.I., Widdicombe, S., 2010. Impact of medium-term exposure to CO_2 enriched seawater on the physiological functions of the velvet swimming crab *Necora puber*. Aquat. Biol. 10(1): 11-21.

Snyder, M.J., Chang, E.S., 1991. Ecdysteroids in relation to the molt cycle of the American lobster, *Homarus americanus*: I. Hemolymph titers and metabolites. Gen. Comp. Endocrinol. 81(1): 133-145.

Sokolova, I.M., Frederich, M., Bagwe, R., Lannig, G., Sukhotin, A.A., 2012. Energy homeostasis as an integrative tool for assessing limits of environmental stress tolerance in aquatic invertebrates. Mar. Environ. Res. 79: 1-15.

Somero, G.N., Beers, J.M., Chan, F., Hill, T.M., Klinger, T., Litvin, S.Y., 2015. What changes in the carbonate system, oxygen, and temperature portend for the Northeastern Pacific Ocean: A physiological perspective. BioScience 66(1): 14-26.

Somero, G.N., Lockwood, B.L., Tomanek, L., 2017. Biochemical Adaptation: Response to Environmental Challenges, from Life's Origins to the Anthropocene. Sinauer Associates, Incorporated Publishers.

Spicer, J.I., Raffo, A., Widdicombe, S., 2007. Influence of CO_2-related seawater acidification on extracellular acid–base balance in the velvet swimming crab *Necora puber*. Mar. Biol. 151(3): 1117-1125.

Steneck, R.S., Hughes, T.P., Cinner, J.E., Adger, W.N., Arnold, S.N., Berkes, F., Boudreau, S.A., Brown, K., Folke, C., Gunderson, L., Olsson, P., Scheffer, M., Stephenson, E., Walker, B., Wilson, J., Worm, B., 2011. Creation of a gilded trap by the high economic value of the Maine lobster fishery. Conserv. Biol. 25(5): 904-912.

Steneck, R.S., Wahle, R.A., 2013. American lobster dynamics in a brave new ocean. Can. J. Fish. Aquat. Sci. 70(11): 1612-1624.

Stenseng, E., Braby, C.E., Somero, G.N., 2005. Evolutionary and acclimation-induced variation in the thermal limits of heart function in congeneric marine snails (genus *Tegula*): implications for vertical zonation. Biol. Bull. 208(2): 138-144.

Stillman, J.H., Somero, G.N., 2000. A comparative analysis of the upper thermal tolerance limits of eastern Pacific porcelain crabs, genus *Petrolisthes*: influences of latitude, vertical zonation, acclimation, and phylogeny. Physiol. Biochem. Zool. 73(2): 200-208.

Sunday, J.M., Calosi, P., Dupont, S., Munday, P.L., Stillman, J.H., Reusch, T.B. 2014. Evolution in an acidifying ocean. Trends in Ecology & Evolution. 29(2): 117-125.

Taboada, F.G., Anadón, R., 2012. Patterns of change in sea surface temperature in the North Atlantic during the last three decades: beyond mean trends. Clim. Change 115(2): 419-431.

Taylor, H.H., Paterson, B.D., Wong, R.J., Wells, R., 1997. Physiology and live transport of lobsters: report from a workshop. Mar. Freshwater Res. 48(8): 817-822.

Templeman, W., 1936. The influence of temperature, salinity, light and food conditions on the survival and growth of the larvae of the lobster (*Homarus americanus*). J. Biol. Bd. Can. 2(5): 485-497.

Tepolt, C.K., Somero, G.N., 2014. Master of all trades: thermal acclimation and adaptation of cardiac function in a broadly distributed marine invasive species, the European green crab, *Carcinus maenas*. J. Exp. Biol. 217(7): 1129-1138.

Thomas, A.C., Pershing, A.J., Friedland, K.D., Nye, J.A., Mills, K.E., Alexander, M.A., Record, N.R., Weatherbee, R., Henderson, M.E., 2017. Seasonal trends and phenology shifts in sea surface temperature on the North American northeastern continental shelf. Elem. Sci. Anth. 5: 1-17.

Thornhill, R., Gangestad, S.W., 2006. Facial sexual dimorphism, developmental stability, and susceptibility to disease in men and women. Evol. Hum. Behav. 27(2): 131-144.

Tomanek, L., 2002. The heat-shock response: its variation, regulation and ecological importance in intertidal gastropods (genus *Tegula*). Integr. Comp. Biol. 42(4): 797-807.

Tomanek, L., Somero, G.N., 1999. Evolutionary and acclimation-induced variation in the heat-shock responses of congeneric marine snails (genus *Tegula*) from different thermal habitats: implications for limits of thermotolerance and biogeography. J. Exp. Biol. 202(21): 2925-2936.

Truchot, J.P., 1975. Factors controlling the in vitro and in vivo oxygen affinity of the hemocyanin in the crab *Carcinus maenas* (L.). Respir. Physiol. 24(2): 173-189.

Uppström, L.R., 1974. The boron/chlorinity ratio of deep-sea water from the Pacific Ocean. Deep Sea Res. Oceanogr. Abs. 21: 161-162.

van Straalen, N.M., Timmermans, M.J., 2002. Genetic variation in toxicant-stressed populations: an evaluation of the "genetic erosion" hypothesis. Hum. Ecol. Risk Assess. 8(5): 983-1002.

Venâncio, C., Ribeiro, R., Soares, A., and Lopes, I. 2016. Multiple stressor differential tolerances: possible implications at the population level. PloS One. 11(3): e0151847.

Wahle, R.A., 1992. Body-size dependent anti-predator mechanisms of the American lobster. Oikos 65(1): 52-60.

Wahle, R.A., Steneck, R.S., 1992. Habitat restrictions in early benthic life: experiments on habitat selection and in situ predation with the American lobster. 157(1): 91-114.

Wahle, R.A., Brown, C., Hovel, K., 2013. The geography and body-size dependence of top-down forcing in New England's lobster-groundfish interaction. Bull. Mar. Sci. 89(1): 189-212.

Wahle, R.A., Gibson, M., Fogarty, M., 2009. Distinguishing disease impacts from larval supply effects in a lobster fishery collapse. Mar. Ecol. Prog. Ser. 376: 185-192.

Waldbusser, G.G., Hales, B., Haley, B.A., 2016. Calcium carbonate saturation state: on myths and this or that stories. ICES J. Mar. Sci. 73(3): 563-568.

Waller, J.D., Wahle, R.A., McVeigh, H., Fields, D.M., 2017. Linking rising pCO_2 and temperature to the larval development and physiology of the American lobster (*Homarus americanus*). ICES J. Mar. Sci.: Journal du Conseil 74(4): 1210-1219.

Walther, K., Sartoris, F.J., Bock, C., Pörtner, H., 2009. Impact of anthropogenic ocean acidification on thermal tolerance of the spider crab *Hyas araneus*. Biogeosciences 6(10): 2207-2215.

Wang, G., Mcgaw, I.J., 2014. Use of serum protein concentration as an indicator of quality and physiological condition in the lobster *Homarus americanus* (Milne-Edwards, 1837). J. Shellfish Res. 33(3): 805-813.

Wang, J., Russell, B.D., Ding, M., Dong, Y., 2018. Ocean acidification increases the sensitivity of and variability in physiological responses of an intertidal limpet to thermal stress. Biogeosciences 15(9): 2803-2817.

Wang, P., Liang, J., Gu, Z., Wan, D., Weng, S., Yu, X., He, J., 2012. Molecular cloning, characterization and expression analysis of two novel Tolls (LvToll2 and LvToll3) and three putative Spätzle-like Toll ligands (LvSpz1–3) from *Litopenaeus vannamei*. Dev. Comp. Immunol. 36(2): 359-371.

Wang, Q., Cao, R., Ning, X., You, L., Mu, C., Wang, C., Wei, L., Cong, M., Wu, H., Zhao, J., 2016. Effects of ocean acidification on immune responses of the Pacific oyster *Crassostrea gigas*. Fish Shellfish Immunol. 49: 24-33.

Whiteley, N.M., 2011. Physiological and ecological responses of crustaceans to ocean acidification. Mar. Ecol. Prog. Ser. 430: 257-271.

Whiteley, N.M., Taylor, E. W. 2015. Responses to environmental stresses: oxygen, temperature, and pH. *In*: The Natural History of the Crustacea, Volume 4: Physiology (E.S. Chang and M. Thiel, eds.), pp. 320–358. Oxford University Press, Oxford, UK.

Wittmann, A.C., Pörtner, H., 2013. Sensitivities of extant animal taxa to ocean acidification. Nat. Clim. Change 3(11): 995-1001.

Wong, J.M., Johnson, K.M., Kelly, M.W., Hofmann, G.E., 2018. Transcriptomics reveal transgenerational effects in purple sea urchin embryos: adult acclimation to upwelling conditions alters the response of their progeny to differential pCO_2 levels. Mol. Ecol. 27(5): 1120-1137.

Yao, C., Somero, G.N., 2012. The impact of acute temperature stress on hemocytes of invasive and native mussels (*Mytilus galloprovincialis* and *Mytilus californianus*): DNA damage, membrane integrity, apoptosis and signaling pathways. J. Exp. Biol. 215(24): 4267-4277.

Zasloff, M., 2002. Antimicrobial peptides of multicellular organisms. Nature 415(6870): 389-395.

Zeis, B., Nies, A., Bridges, C.R., Grieshaber, M.K., 1992. Allosteric modulation of haemocyanin oxygen-affinity by L-lactate and urate in the lobster *Homarus vulgaris*: I. specific and additive effects on haemocyanin oxygen-affinity. J. Exp. Biol. 168(1): 93-110.

Zhou, Y., Gu, W., Tu, D., Zhu, Q., Zhou, Z., Chen, Y., Shu, M., 2018. Hemocytes of the mud crab *Scylla paramamosain*: cytometric, morphological characterization and involvement in immune responses. Fish. Shellfish Immunol. 72: 459-469.

Zittier, Z.M., Hirse, T., Pörtner, H., 2013. The synergistic effects of increasing temperature and CO2 levels on activity capacity and acid–base balance in the spider crab, Hyas araneus. Mar. Biol. 160, 2049-2062.

APPENDIX: CHAPTER 3 SUPPLEMENTARY DATA

Table A.1. Supplemental information for the top 100 differentially expressed (DE) transcripts for each temperature comparison. Log$_2$ fold change (FC) values are expressed as the first temperature relative to the second temperature listed (e.g., in the 16°C vs. 22°C comparison, transcripts are over- or under-expressed in postlarvae reared at 16°C relative to those reared at 22°C), and adjusted *p*-values reflect correction via the Benjamini-Hochberg procedure to account for multiple testing. Annotations were retrieved using NCBI non-redundant (nr) protein databases (E-value ≤ 1e − 10; downloaded in July 2018), and gene ontology (GO) IDs and names were obtained using Blast2GO (the letters "C", "P", and "F" refer to GO terms attributed to cellular functions, biological processes, and molecular functions, respectively). Data were uploaded to the Kyoto Encyclopedia of Genes and Genomes (KEGG) Automatic Annotation Server (KAAS) to determine KEGG Orthology (KO) assignments, and to explore KAAS pathways and BRITE hierarchies. We include information on the additional 14 DE transcripts identified by edgeR for the 16°C vs. 22°C comparison.

16°C vs. 22°C: over-expressed, DESeq2

Transcript ID	Log$_2$FC	Adjusted p-value	Annotation	KO	KAAS Pathways	BRITE Hierarchies	GO IDs	GO Names
DN44323_c21_g1_i1	4.572	1.16E-10	ACR78689.1 hypothetical cuticle protein, partial [Rimicaris exoculata]	0			no GO terms	no GO terms
DN14111_c0_g1_i1	3.942	3.52E-08	XP_013189132.1 PREDICTED: uncharacterized protein LOC106133808, partial [Amyelois transitella]	0			no GO terms	no GO terms
DN44500_c22_g2_i1	3.852	5.43E-08	XP_018022127.1 PREDICTED: cuticle protein 8-like isoform X2 [Hyalella azteca]	0			no GO terms	no GO terms
DN43598_c16_g1_i1	3.851	1.46E-07	AFZ78450.1 chitinase 2, partial [Procambarus clarkii]	0			P:GO:0005975	P:carbohydrate metabolic process

Table A.1. continued

DN43598_c15_g1_i1	3.805	1.69E-07	BAP28983.1 chitinase [Portunus trituberculatus]	K01183	Carbohydrate metabolism- amino sugar and nucleotide sugar metabolism			P:GO:0005975	P:carbohydrate metabolic process
DN20237_c0_g1_i1	3.770	1.64E-07	ASK05861.1 chitin-binding protein [Macrobrachium nipponense]	0				no GO terms	no GO terms
DN6694_c0_g1_i1	3.765	3.61E-07	BAM99303.1 strongly chitin-binding protein-1 [Procambarus clarkii]	0				F:GO:0042302	F:structural constituent of cuticle
DN44540_c24_g1_i1	3.664	2.56E-08	BAM99303.1 strongly chitin-binding protein-1 [Procambarus clarkii]	0				F:GO:0042302	F:structural constituent of cuticle
DN45561_c0_g1_i1	3.635	4.23E-07	XP_018009280.1 PREDICTED: probable pathogenesis-related protein ARB_02861 [Hyalella azteca]	0				no GO terms	no GO terms
DN41099_c3_g1_i1	3.627	1.67E-08	XP_023323118.1 cuticle protein 7-like [Eurytemora affinis]	0				F:GO:0042302	F:structural constituent of cuticle
DN41988_c2_g3_i1	3.623	1.62E-07	XP_018013858.1 PREDICTED: alkylglycerol monooxygenase-like [Hyalella azteca]	K15537		Unclassified: metabolism - enzymes with EC numbers		no GO terms	no GO terms
DN37657_c0_g1_i1	3.596	2.19E-07	XP_022243886.1 apolipophorins-like, partial [Limulus polyphemus]	0				F:GO:0005319; P:GO:0006869	F:lipid transporter activity; P:lipid transport

106

Table A.1. continued

DN40720_c5_g1_i1	3.589	1.40E-07	BAF73806.1 calcification associated soluble matrix protein 2 [Procambarus clarkii]	0			F:GO:0042302	F:structural constituent of cuticle
DN44540_c17_g1_i1	3.566	5.07E-07	ADI59750.1 early cuticle protein 2 [Callinectes sapidus]	0			no GO terms	no GO terms
DN44500_c28_g1_i1	3.562	5.20E-07	ACO12877.1 Cuticle protein 19.8 [Lepeophtheirus salmonis]	0			no GO terms	no GO terms
DN41976_c2_g1_i1	3.560	5.75E-08	XP_002024924.1 GL17853 [Drosophila persimilis] EDW30397.1 GL17853 [Drosophila persimilis]	0			no GO terms	no GO terms
DN41939_c1_g1_i2	3.525	1.86E-06	ASK05861.1 chitin-binding protein [Macrobrachium nipponense]	0			F:GO:0042302	F:structural constituent of cuticle
DN41939_c1_g1_i1	3.445	1.40E-07	ASK05861.1 chitin-binding protein [Macrobrachium nipponense]	0			F:GO:0042302	F:structural constituent of cuticle
DN44540_c11_g2_i1	3.419	2.21E-06	ADI59753.1 early cuticle protein 5 [Callinectes sapidus]	0			F:GO:0042302	F:structural constituent of cuticle
DN44293_c2_g1_i1	3.419	1.67E-08	XP_018025308.1 PREDICTED: sodium/glucose cotransporter 4-like [Hyalella azteca]	K14158	Digestive system-bile secretion, carbohydrate digestion and absorption, mineral absorption	Protein families: signaling and cellular processes - transporters, exosome	no GO terms	no GO terms

107

Table A.1. continued

DN43869_c5_g1_i1	3.411	1.52E-05	SOX55400.1 hypothetical protein MAAFP003_4092, partial [Mycobacterium ahvazicum]	0				no GO terms	no GO terms
DN42192_c1_g2_i1	3.408	4.87E-06	EEW08769.1 hypothetical protein VMD_37440 [Vibrio mimicus VM573]	0				no GO terms	no GO terms
DN40937_c0_g1_i1	3.400	1.76E-06	XP_022918567.1 uncharacterized protein LOC111427588 [Onthophagus taurus]	0				F:GO:0042302	F:structural constituent of cuticle
DN6535_c0_g1_i1	3.396	1.50E-05	XP_018017512.1 PREDICTED: pro-resilin-like isoform X1 [Hyalella azteca] XP_018017514.1 PREDICTED: pro-resilin-like isoform X2 [Hyalella azteca]	0				no GO terms	no GO terms
DN44540_c4_g1_i1	3.382	4.14E-06	BAM99303.1 strongly chitin-binding protein-1 [Procambarus clarkii]	0				F:GO:0042302	F:structural constituent of cuticle
DN44540_c20_g1_i1	3.381	2.15E-06	ADI59754.1 early cuticle protein 6 [Callinectes sapidus]	0				F:GO:0042302	F:structural constituent of cuticle
DN44500_c1_g1_i1	3.376	2.57E-06	ASK05861.1 chitin-binding protein [Macrobrachium nipponense]	0				F:GO:0042302	F:structural constituent of cuticle
DN43869_c9_g1_i1	3.363	2.44E-05	GAN74957.1 hypothetical protein Apmu_0247_01 [Acidiphilium multivorum AIU301]	0				no GO terms	no GO terms

Table A.1. continued

DN42837_c0_g1_i1	3.263	2.23E-05	ASK05861.1 chitin-binding protein [Macrobrachium nipponense]	0				no GO terms	no GO terms
DN7224_c0_g1_i1	3.260	8.06E-06	XP_018013996.1 PREDICTED: translation initiation factor IF-2-like [Hyalella azteca]	0				F:GO:0042302	F:structural constituent of cuticle
DN42837_c1_g1_i1	3.250	1.99E-05	ASK05861.1 chitin-binding protein [Macrobrachium nipponense]	0				no GO terms	no GO terms
DN43128_c24_g1_i1	3.242	2.15E-06	XP_018015907.1 PREDICTED: protein zntD-like [Hyalella azteca] XP_018015915.1 PREDICTED: protein zntD-like [Hyalella azteca]	K14709	Protein Families: signaling and cellular processes-transporters			C:GO:0016020; P:GO:0030001; F:GO:0046873; P:GO:0055085	C:membrane; P:metal ion transport; F:metal ion transmembrane transporter activity; P:transmembrane transport
DN42594_c10_g1_i1	3.240	3.54E-06	P81576.1 RecName: Full=Cuticle protein AM1159; Short=CPAM1159	0				F:GO:0042302	F:structural constituent of cuticle
DN44108_c7_g1_i2	3.238	1.52E-05	XP_018024394.1 PREDICTED: protein FAM98A-like [Hyalella azteca]	0				no GO terms	no GO terms
DN44323_c11_g1_i3	3.229	1.90E-07	ACR78689.1 hypothetical cuticle protein, partial [Rimicaris exoculata]	0				F:GO:0042302	F:structural constituent of cuticle

DN34949_c0_g1_i1	3.220	1.65E-05	ALC79580.1 gastrolith protein 18.2 [Cherax quadricarinatus]	0				no GO terms	no GO terms
DN43104_c5_g1_i1	3.185	1.76E-05	ASK05861.1 chitin-binding protein [Macrobrachium nipponense]	0				F:GO:0042302	F:structural constituent of cuticle
DN22920_c0_g1_i1	3.184	2.62E-07	XP_018027517.1 PREDICTED: uncharacterized protein LOC108682788 [Hyalella azteca]	0				no GO terms	no GO terms
DN44500_c18_g1_i1	3.175	1.49E-05	ASK05861.1 chitin-binding protein [Macrobrachium nipponense]	0				F:GO:0042302	F:structural constituent of cuticle
DN43640_c5_g1_i1	3.165	7.74E-06	XP_018027294.1 PREDICTED: glucose dehydrogenase [FAD, quinone]-like [Hyalella azteca]	0				F:GO:0016614; F:GO:0050660; P:GO:0055114	F:oxidoreductase activity, acting on CH-OH group of donors; F:flavin adenine dinucleotide binding; P:oxidation-reduction process
DN43201_c18_g1_i1	3.160	1.25E-05	XP_018024750.1 PREDICTED: glycine-rich cell wall structural protein 1-like [Hyalella azteca]	0				C:GO:0005576; P:GO:0006030; F:GO:0008061	C:extracellular region; P:chitin metabolic process; F:chitin binding

Table A.1. continued

DN14715_c0_g1_i1	3.125	1.79E-05	XP_023327997.1 cuticle protein 7-like [Eurytemora affinis]	0			F:GO:0042302	F:structural constituent of cuticle
DN42837_c11_g1_i1	3.124	1.06E-05	ASK05861.1 chitin-binding protein [Macrobrachium nipponense]	0			F:GO:0042302	F:structural constituent of cuticle
DN40709_c1_g2_i1	3.117	6.81E-06	ATN38697.1 cuticle-like protein [Macrobrachium nipponense]	0			F:GO:0042302	F:structural constituent of cuticle
DN44500_c17_g1_i1	3.108	5.93E-06	ASK05861.1 chitin-binding protein [Macrobrachium nipponense]	0			F:GO:0042302	F:structural constituent of cuticle
DN42867_c0_g1_i1	3.089	3.91E-06	AEK86524.1 Spz3 [Litopenaeus vannamei]	0			no GO terms	no GO terms
DN44108_c6_g1_i2	3.071	4.76E-06	XP_018024394.1 PREDICTED: protein FAM98A-like [Hyalella azteca]	0			no GO terms	no GO terms
DN34772_c1_g1_i1	3.056	2.14E-05	XP_001868236.1 cuticle protein [Culex quinquefasciatus] EDS26362.1 cuticle protein [Culex quinquefasciatus]	0			F:GO:0042302	F:structural constituent of cuticle
DN42867_c3_g1_i1	3.021	5.16E-06	AEK86524.1 Spz3 [Litopenaeus vannamei]	0			no GO terms	no GO terms
DN40296_c1_g1_i1	3.016	1.23E-05	XP_023323118.1 cuticle protein 7-like [Eurytemora affinis]	0			F:GO:0042302	F:structural constituent of cuticle

Table A.1. continued

DN43665_c12_g1_i1	2.980	4.75E-06	XP_018026344.1 PREDICTED: venom phosphodiesterase 2-like [Hyalella azteca]	K01513	Carbohydrate metabolism- starch and sucrose metabolism; Nucleotide metabolism- purine metabolism, pyrimidine metabolism; Metabolism of cofactors and vitamins- riboflavin metabolism, nicotinate and nicotinamide metabolism, pantothenate and CoA biosynthesis	Protein families: signaling and cellular processes- CD molecules, GPI-anchored proteins	F:GO:0003676 ; F:GO:0003824 ; F:GO:0016787 ; F:GO:0046872	F:nucleic acid binding; F:catalytic activity; F:hydrolase activity; F:metal ion binding
DN36156_c3_g1_i1	2.946	2.98E-06	AGU01545.1 antimicrobial peptide type 2 precursor IIc [Pandalopsis japonica]	0			no GO terms	no GO terms
DN39435_c0_g1_i1	2.935	1.67E-05	ASK05861.1 chitin-binding protein [Macrobrachium nipponense]	0			F:GO:0042302	F:structural constituent of cuticle
DN37162_c4_g1_i1	2.866	4.68E-06	AEK86522.1 Spz1 [Litopenaeus vannamei]	0			no GO terms	no GO terms
DN41318_c0_g1_i2	2.828	4.13E-06	XP_003240981.1 PREDICTED: skin secretory protein xP2-like [Acyrthosiphon pisum]	0			F:GO:0042302	F:structural constituent of cuticle

Table A.1. continued

DN44465_c7_g1_i1	2.758	2.98E-06	ALG65274.1 glucose transporter 2 [Litopenaeus vannamei]	0			C:GO:0016021; F:GO:0022857; P:GO:0055085	C:integral component of membrane; F:transmembrane transporter activity; P:transmembrane transport
DN39340_c1_g1_i1	2.755	4.80E-06	AIM45534.1 peritrophin-44-like protein [Eriocheir sinensis]	0			C:GO:0005576; P:GO:0006030; F:GO:0008061	C:extracellular region; P:chitin metabolic process; F:chitin binding
DN43765_c7_g1_i1	2.747	2.13E-06	XP_018021695.1 PREDICTED: uncharacterized protein LOC108677901 [Hyalella azteca]	0			no GO terms	no GO terms
DN30852_c0_g1_i1	2.747	6.02E-06	XP_003436050.1 AGAP002186-PB [Anopheles gambiae str. PEST] EGK96211.1 AGAP002186-PB [Anopheles gambiae str. PEST]	K20053		Protein families: genetic information processing - membrane trafficking	F:GO:0005509; F:GO:0005515	F:calcium ion binding; F:protein binding
DN44637_c17_g1_i1	2.729	1.16E-07	ABQ96197.1 crustin [Farfantepenaeus brasiliensis]	0			C:GO:0005576; F:GO:0030414	C:extracellular region; F:peptidase inhibitor activity
DN44323_c11_g1_i1	2.724	1.42E-05	ACR78689.1 hypothetical cuticle protein, partial [Rimicaris exoculata]	0			no GO terms	no GO terms

Table A.1. continued

DN41976_c4_g1_i1	2.693	2.14E-05	XP_013172611.1 PREDICTED: uncharacterized protein LOC106121472 [Papilio xuthus]	K09614			F:GO:0004252; P:GO:0006508	F:serine-type endopeptidase activity; P:proteolysis
DN36690_c0_g2_i1	2.691	1.67E-05	EFX66629.1 hypothetical protein DAPPUDRAFT_331880 [Daphnia pulex]	0			no GO terms	no GO terms
DN40121_c11_g1_i1	2.674	9.87E-07	XP_018008896.1 PREDICTED: uncharacterized protein LOC108666520 isoform X1 [Hyalella azteca]	0			no GO terms	no GO terms
DN44517_c5_g1_i1	2.670	2.91E-07	ABI79454.2 alpha 2 macroglobulin [Litopenaeus vannamei]	K03910	Immune system-complement and coagulation cascades	Protein families: genetic information processing - membrane trafficking	C:GO:0005576; C:GO:0005615	C:extracellular region; C:extracellular space
DN41318_c0_g1_i1	2.622	1. 69E-07	XP_025406143.1 cuticle protein 16.5-like [Sipha flava]	0			F:GO:0042302	F:structural constituent of cuticle
DN44136_c18_g1_i1	2.617	1.52E-05	XP_021968560.1 sodium-coupled monocarboxylate transporter 1-like [Folsomia candida]	K14388		Protein families: signaling and cellular processes - transporters	C:GO:0016020; F:GO:0022857; P:GO:0055085	C:membrane; F:transmembrane transporter activity; P:transmembrane transport
DN43999_c14_g1_i1	2.614	4.75E-06	XP_023320995.1 metalloreductase STEAP4-like [Eurytemora affinis]	K19876		Membrane trafficking	no GO terms	no GO terms

Table A.1. continued

DN44664_c13_g1_i1	2.602	4.70E-06	XP_015764650.1 PREDICTED: uncharacterized protein LOC107343577 [Acropora digitifera]	0				no GO terms	no GO terms
DN41717_c1_g1_i1	2.588	1.37E-07	XP_002033137.1 GM21151 [Drosophila sechellia] EDW47150.1 GM21151 [Drosophila sechellia]	K05038	Nervous system - synaptic vesicle cycle	Protein families: signaling and cellular processes - transporters	F:GO:0005328; P:GO:0006836; C:GO:0016021	F:neurotransmitter:sodium symporter activity; P:neurotransmitter transport; C:integral component of membrane
DN39479_c0_g4_i1	2.588	2.54E-06	ALC79580.1 gastrolith protein 18.2 [Cherax quadricarinatus]	0				no GO terms	no GO terms
DN44508_c8_g1_i1	2.576	1.79E-05	AGG20312.1 peritrophin [Palaemon carinicauda]	0				C:GO:0005576; P:GO:0006030; F:GO:0008061	C:extracellular region; P:chitin metabolic process; F:chitin binding
DN43034_c4_g3_i2	2.511	1.11E-05	XP_018016956.1 PREDICTED: L-asparaginase 1-like [Hyalella azteca]	K13278		Unclassified: metabolism - enzymes with EC numbers	F:GO:0005515	F:protein binding
DN42594_c10_g2_i1	2.480	2.33E-05	P81577.1 RecName: Full=Cuticle protein AM1199; Short=CPAM1199	0			F:GO:0042302	F:structural constituent of cuticle

Table A.1. continued

DN44080_c4_g1_i1	2.461	5.39E-06	XP_019870689.1 PREDICTED: uncharacterized protein LOC109599183 [Aethina tumida]	K09443		Protein families: genetic information processing - transcription factors	F:GO:0003700; C:GO:0005634; P:GO:0006355; F:GO:0043565	F:DNA-binding transcription factor activity; C:nucleus; P:regulation of transcription, DNA-templated; F:sequence-specific DNA binding
DN44664_c5_g1_i1	2.389	3.54E-09	KFD47056.1 hypothetical protein M513_12044 [Trichuris suis]	0			no GO terms	no GO terms
DN40121_c5_g1_i1	2.381	1.84E-05	XP_018008897.1 PREDICTED: uncharacterized protein LOC108666520 isoform X2 [Hyalella azteca]	0			no GO terms	no GO terms
DN40877_c0_g1_i1	2.360	4.14E-06	XP_018010073.1 PREDICTED: alkaline phosphatase, tissue-nonspecific isozyme-like [Hyalella azteca]	K01077	Metabolism of cofactors and vitamins- thiamine metabolism, folate biosynthesis; Signal transduction- two-component system	Protein families: signaling and cellular processes-exosome, glycosylphosphatidy lino-stol (GPI)-anchored proteins	F:GO:0003824; F:GO:0016791	F:catalytic activity; F:phosphatase activity
DN44471_c12_g1_i1	2.355	1.22E-06	XP_021177623.1 uncharacterized protein LOC110369190 [Fundulus heteroclitus]	0			F:GO:0003676	F:nucleic acid binding
DN43856_c18_g1_i1	2.339	5.07E-07	XP_018398794.1 PREDICTED: proclotting enzyme-like [Cyphomyrmex costatus]	0			F:GO:0004252; P:GO:0006508	F:serine-type endopeptidase activity; P:proteolysis

116

Table A.1. continued

DN44664_c0_g2_i1	2.332	8.85E-06	XP_003725052.1 PREDICTED: uncharacterized protein LOC100888496 [Strongylocentrotus purpuratus]	0			no GO terms	no GO terms
DN41674_c2_g1_i1	2.330	7.63E-06	XP_018024821.1 PREDICTED: cell wall protein PRY3-like [Hyalella azteca]	K19919		Protein families: genetic information processing - membrane trafficking	no GO terms	no GO terms
DN43829_c4_g1_i1	2.328	1.06E-05	XP_015437411.1 PREDICTED: Niemann-Pick C1 protein isoform X1 [Dufourea novaeangliae]	K12385	Cellular processes-transport and catabolism - lysosome; Digestive system-cholesterol metabolism	Protein families: signaling and cellular processes - transporters	F:GO:0005319 ; C:GO:0016021	F:lipid transporter activity; C:integral component of membrane
DN33886_c2_g1_i1	2.326	9.44E-06	EFX70562.1 hypothetical protein DAPPUDRAFT_61224, partial [Daphnia pulex]	0			F:GO:0042302	F:structural constituent of cuticle
DN43888_c2_g1_i1	2.293	3.54E-12	XP_018009694.1 PREDICTED: uncharacterized protein LOC108667210 [Hyalella azteca]	K04599	Protein families: signaling and cellular processes		F:GO:0004888 ; F:GO:0004930 ; P:GO:0007166 ; P:GO:0007186 ; C:GO:0016021	F:transmembrane signaling receptor activity; F:G protein-coupled receptor activity; P:cell surface receptor signaling pathway; P:G protein-coupled receptor signaling pathway;

Table A.1. continued

								C:integral component of membrane
DN44540_c3_g1_i1	2.231	1.01E-06	XP_018006524.1 PREDICTED: sialin-like [Hyalella azteca]	K12301	Cellular processes-transport and catabolism - lysosome	Protein Families: signaling and cellular processes-transporters	C:GO:0016021; P:GO:0055085	C:integral component of membrane; P:transmembrane transport
DN44393_c16_g1_i1	2.201	4.38E-06	XP_023964737.1 tigger transposable element-derived protein 1-like [Chrysemys picta bellii] XP_008170509.2 tigger transposable element-derived protein 1-like [Chrysemys picta bellii]	0			no GO terms	no GO terms
DN43171_c0_g1_i1	2.076	8.74E-06	XP_019879486.1 PREDICTED: putative carbonic anhydrase 3 [Aethina tumida]	K01672	Energy metabolism-nitrogen metabolism		F:GO:0004089; F:GO:0008270	F:carbonate dehydratase activity; F:zinc ion binding
DN44598_c10_g3_i1	2.017	8.14E-07	XP_018013832.1 PREDICTED: uncharacterized protein LOC108670853 [Hyalella azteca]	0			no GO terms	no GO terms
DN43978_c6_g1_i1	1.991	3.04E-06	XP_012536395.1 PREDICTED: uncharacterized protein LOC105836713 [Monomorium pharaonis] XP_012522927.1	0			no GO terms	no GO terms

Table A.1. continued

			PREDICTED: uncharacterized protein LOC105828907 [Monomorium pharaonis]					
DN43953_c6_g1_i1	1.973	1.69E-07	XP_018027293.1 PREDICTED: glucose dehydrogenase [FAD, quinone]-like [Hyalella azteca]	K00108	Amino acid metabolism (glycine, serine and threonine)		F:GO:0016614; F:GO:0050660; P:GO:0055114	F:oxidoreductase activity, acting on CH-OH group of donors; F:flavin adenine dinucleotide binding; P:oxidation-reduction process
DN41548_c0_g1_i1	1.912	1.90E-05	XP_018022073.1 PREDICTED: uncharacterized protein LOC108678215 [Hyalella azteca]	K08145		Protein families: signaling and cellular processes - transporters	C:GO:0016021; F:GO:0022857; P:GO:0055085	C:integral component of membrane; F:transmembrane transporter activity; P:transmembrane transport
DN43739_c7_g1_i2	1.894	2.45E-05	XP_018016458.1 PREDICTED: protein eyes shut-like [Hyalella azteca]	0			P:GO:0007154; C:GO:0016020	P:cell communication; C:membrane
DN42803_c8_g1_i1	1.779	1.92E-05	AAV63540.1 fed tick salivary protein 6 [Ixodes scapularis]	0			no GO terms	no GO terms
DN42553_c10_g1_i1	1.706	6.53E-06	XP_023706362.1 beta,beta-carotene 9',10'-oxygenase-like [Cryptotermes secundus] PNF43184.1 Beta,beta-	K18048		Unclassified: metabolism - enzymes with EC numbers	no GO terms	no GO terms

Table A.1. continued

			carotene 9',10'-oxygenase [Cryptotermes secundus]						
DN43301_c8_g1_i1	1.700	2.74E-06	XP_018026690.1 PREDICTED: histone-lysine N-methyltransferase, H3 lysine-79 specific-like isoform X1 [Hyalella azteca]	0				no GO terms	no GO terms
DN42680_c0_g1_i1	1.649	6.18E-06	XP_018016120.1 PREDICTED: probable cytochrome P450 49a1 [Hyalella azteca]	K17960		Protein families: metabolism-cytochrome P450	F:GO:0005506; F:GO:0016705; F:GO:0020037; P:GO:0055114	F:iron ion binding; F:oxidoreductase activity, acting on paired donors, with incorporation or reduction of molecular oxygen; F:heme binding; P:oxidation-reduction process
DN41396_c0_g1_i1	1.266	2.14E-06	XP_018012189.1 PREDICTED: uncharacterized protein LOC108669385 [Hyalella azteca]	0				no GO terms	no GO terms
DN43088_c10_g2_i1	1.262	3.04E-06	XP_023237634.1 arylsulfatase I-like [Centruroides sculpturatus]	K01135	Glycan biosynthesis and metabolism-glycosaminoglycan degradation; Cellular processes-			F:GO:0003824; F:GO:0008484	F:catalytic activity; F:sulfuric ester hydrolase activity

Table A.1. continued

					transport and catabolism-lysosome			
DN42659_c3_g2_i1	1.241	3.58E-10	XP_008476053.1 PREDICTED: transcription cofactor vestigial-like protein 4 [Diaphorina citri]	0			P:GO:0006355	P:regulation of transcription, DNA-templated

16°C vs. 22°C: over-expressed, edgeR

Transcript ID	Log$_2$FC	Adjusted p-value	Annotation	KO	KAAS Pathways	BRITE Hierarchies	GO IDs	GO Names
DN44517_c5_g1_i1	3.049	1.49E-02	ACU31810.1 alpha2 macroglobulin isoform 2 [Fenneropenaeus chinensis]	K03910	Immune system-Complement and coagulation cascades	Protein families: genetic information processing-Membrane trafficking; Protein families: signaling and cellular processes- Exosome	C:GO:0005615	C:extracellular space
DN7804_c0_g1_i1	2.180	2.55E-02	ODN03525.1 Cuticle protein 7 [Orchesella cincta]	0			F:GO:0042302	F:structural constituent of cuticle
DN42226_c0_g3_i1	1.583	2.29E-02	AOG12994.1 octopamine receptor beta-2R [Homarus americanus]	K22790		Protein families: signaling and cellular processes-G protein-coupled receptors	F:GO:0004935 ; P:GO:0007186 ; C:GO:0016021	F:adrenergic receptor activity; P:G protein-coupled receptor signaling pathway; C:integral component of membrane

121

Table A.1. continued

DN40848_c2_g2_i1	1.278	2.44E-02	ATW66457.1 hormone receptor, partial [Marsupenaeus japonicus]	K14033		Protein families: genetic information processing- Transcription factors; Protein families: signaling and cellular processes- Nuclear receptors	F:GO:0003677 ; F:GO:0003707 ; F:GO:0004879 ; C:GO:0005634 ; P:GO:0006355	F:DNA binding; F:steroid hormone receptor activity; F:nuclear receptor activity; C:nucleus; P:regulation of transcription, DNA-templated
DN42633_c6_g2_i1	1.103	2.67E-02	ANJ04742.1 spaetzle 4 [Litopenaeus vannamei]	0			0	0

16°C vs. 22°C: under-expressed, DESeq2

Transcript ID	Log$_2$FC	Adjusted p-value	Annotation	KO	KAAS Pathways	BRITE Hierarchies	GO IDs	GO Names
DN36928_c0_g2_i1	-4.500	1.41E-10	XP_015349413.1 PREDICTED: methylmalonate-semialdehyde dehydrogenase [acylating], mitochondrial isoform X1 [Marmota marmota marmota]	K00140	Metabolism- propanoate metabolism, inositol phosphate metabolism; Amino acid metabolism- valine, leucine and isoleucine degradation		F:GO:0004491 ; F:GO:0016491 ; F:GO:0016620 ; P:GO:0055114	F:methylmalona te-semialdehyde dehydrogenase (acylating) activity; F:oxidoreductas e activity; F:oxidoreductas e activity, acting on the aldehyde or oxo group of donors, NAD or NADP as acceptor; P:oxidation-

Table A.1. continued

								reduction process
DN44253_c4_g1_i2	-3.132	9.82E-05	P84293.1 RecName: Full=Hemocyanin subunit 2; AltName: Full=CaeSS2	K00505	Amino acid metabolism-Tyrosine metabolism; Biosynthesis of other secondary metabolites-Isoquinolie alkaloid biosynthesis, Betalain biosynthesis; Endocrine system-Melangenesis		no GO terms	no GO terms
DN41202_c4_g2_i1	-2.897	2.40E-06	XP_018015969.1 PREDICTED: UNC93-like protein MFSD11 isoform X2 [Hyalella azteca]	0			no GO terms	no GO terms
DN44136_c16_g4_i1	-2.836	1.03E-05	YP_004563983.1 NADH dehydrogenase subunit 2 (mitochondrion) [Homarus americanus] ADP08205.1 NADH dehydrogenase subunit 2 (mitochondrion) [Homarus americanus]	K03879	Energy metabolism-Oxidative phosphorylation; Nervous system-Retrograde endocannabinoid signaling; Environmental adaptation-Thermogenesis	Protein families: genetic information processing-Mitochondrial biogenesis	no GO terms	no GO terms

Table A.1. continued

DN41202_c4_g1_i1	-2.714	1.41E-10	XP_018015969.1 PREDICTED: UNC93-like protein MFSD11 isoform X2 [Hyalella azteca]	0			no GO terms	no GO terms
DN43737_c13_g14_i1	-2.614	2.17E-08	XP_015439268.1 PREDICTED: aconitate hydratase, mitochondrial-like [Dufourea novaeangliae]	K01681	Metabolism- carbohydrate metabolism- citrate cycle (TCA cycle), glyoxylate and dicarboxylate metabolism; Energy metabolism- carbon fixation pathways in prokaryotes		F:GO:0003994; P:GO:0006099; F:GO:0051539	F:aconitate hydratase activity; P:tricarboxylic acid cycle; F:4 iron, 4 sulfur cluster binding
DN44476_c7_g1_i1	-2.413	1.16E-04	XP_018010355.1 PREDICTED: pyroglutamyl-peptidase 1-like [Hyalella azteca]	K01304		Protein families: metabolism- peptidases	C:GO:0005829; P:GO:0006508; F:GO:0016920	C:cytosol; P:proteolysis; F:pyroglutamyl-peptidase activity
DN44146_c12_g3_i1	-2.371	1.08E-05	XP_018027696.1 PREDICTED: uncharacterized protein LOC108682943 isoform X1 [Hyalella azteca]	0			no GO terms	no GO terms
DN44614_c6_g1_i2	-2.232	1.26E-05	XP_015437916.1 PREDICTED: myosin heavy chain, muscle isoform X4 [Dufourea novaeangliae]	K17751	Circulatory system- cardiac muscle contraction, adrenergic signaling in cardiomyocytes	Protein families: signaling and cellular processes- cytoskeleton proteins	F:GO:0003774; F:GO:0005515; F:GO:0005524; C:GO:0016459	F:motor activity; F:protein binding; F:ATP binding; C:myosin complex

Table A.1. continued

DN44614_c6_g1_i3	-2.073	1.36E-04	XP_015437916.1 PREDICTED: myosin heavy chain, muscle isoform X4 [Dufourea novaeangliae]	K17751	Circulatory system-cardiac muscle contraction, adrenergic signaling in cardiomyocytes	Protein families: signaling and cellular processes-cytoskeleton proteins	F:GO:0003774; F:GO:0005515; F:GO:0005524; C:GO:0016459	F:motor activity; F:protein binding; F:ATP binding; C:myosin complex
DN44386_c0_g1_i1	-2.061	7.94E-05	XP_023215727.1 uncharacterized protein LOC111618422 [Centruroides sculpturatus]	0			P:GO:0000723	P:telomere maintenance
DN43729_c17_g1_i1	-2.002	8.07E-05	XP_018017174.1 PREDICTED: alpha-(1,3)-fucosyltransferase C-like [Hyalella azteca]	K14464	Glycan biosynthesis and metabolism-Various types of N-glycan biosynthesis		P:GO:0006486; F:GO:0008417; C:GO:0016020	P:protein glycosylation; F:fucosyltransferase activity; C:membrane
DN40922_c0_g1_i1	-1.909	2.03E-09	XP_018015412.1 PREDICTED: organic cation transporter protein-like [Hyalella azteca]	K08202		Protein families: signaling and cellular processes-transporters	C:GO:0016021; F:GO:0022857; P:GO:0055085	C:integral component of membrane; F:transmembrane transporter activity; P:transmembrane transport
DN42480_c3_g1_i1	-1.892	1.86E-05	AKL71620.1 juvenile hormone epoxide hydrolase [Macrobrachium rosenbergii]	K10719	Metabolism of terpenoids and polyketides- Insect hormone biosynthesis		F:GO:0003824; F:GO:0033961	F:catalytic activity; F:cis-stilbene-oxide hydrolase activity
DN33800_c0_g1_i1	-1.878	1.09E-05	AQW41379.1 selenium independent glutathione	K00432	Metabolism of other amino acids-Glutathione metabolism;		F:GO:0004602; P:GO:0006979	F:glutathione peroxidase activity; P:response to

125

			peroxidase [Penaeus monodon]		Endocrine system-Thyroid hormone synthesis		; P:GO:0055114	oxidative stress; P:oxidation-reduction process
DN44597_c21_g1_i1	-1.803	1.17E-05	EMP29728.1 L-fucose kinase [Chelonia mydas]	K05305	Carbohydrate metabolism-Fructose and mannose metabolism, amino sugar and nucleotide sugar metabolism		F:GO:0005524	F:ATP binding
DN42052_c0_g1_i1	-1.785	7.21E-05	WP_069134491.1 SDR family NAD(P)-dependent oxidoreductase, partial [Gammaproteobacteria bacterium 2W06] PYZ99277.1 SDR family NAD(P)-dependent oxidoreductase, partial [Gammaproteobacteria bacterium 2W06]	0			no GO terms	no GO terms
DN44498_c12_g1_i1	-1.774	5.73E-05	EFX89894.1 DNA primase-like protein [Daphnia pulex]	K02685	Replication and Repair- DNA replication	Protein families: genetic information processing- DNA replication proteins	F:GO:0003896 ; P:GO:0006269 ; F:GO:0016779	F:DNA primase activity; P:DNA replication, synthesis of RNA primer; F:nucleotidyltra nsferase activity
DN44364_c6_g1_i1	-1.709	4.77E-05	XP_021941234.1 NAD-dependent protein deacetylase sirtuin-2 [Zootermopsis nevadensis] KDR06661.1 NAD-dependent deacetylase sirtuin-2	K11412		Protein families: genetic information processing-Chromosome and associated proteins	F:GO:0008270 ; F:GO:0017136 ; F:GO:0070403	F:zinc ion binding; F:NAD-dependent histone deacetylase activity;

Table A.1. continued

			[Zootermopsis nevadensis]					F:NAD+ binding
DN42675_c3_g1_i1	-1.705	5.88E-05	XP_018023994.1 PREDICTED: uncharacterized protein LOC108679781 [Hyalella azteca]	0			no GO terms	no GO terms
DN44146_c12_g2_i1	-1.681	1.24E-04	XP_018027698.1 PREDICTED: uncharacterized protein LOC108682944 [Hyalella azteca] XP_018027699.1 PREDICTED: uncharacterized protein LOC108682944 [Hyalella azteca]	0			no GO terms	no GO terms
DN42561_c9_g1_i1	-1.680	4.11E-05	XP_018018519.1 PREDICTED: uncharacterized protein LOC108675046 [Hyalella azteca]	0			no GO terms	no GO terms
DN41730_c0_g2_i1	-1.662	1.61E-04	XP_022234972.1 kinetochore-associated protein 1-like, partial [Limulus polyphemus]	K11577		Protein families: genetic information processing-Chromosome and associated proteins	no GO terms	no GO terms
DN30473_c1_g1_i1	-1.660	1.16E-04	EFX80265.1 hypothetical protein DAPPUDRAFT_243907 [Daphnia pulex]	0			no GO terms	no GO terms

DN41730_c0_g1_i1	-1.630	1.01E-04	PNF21937.1 hypothetical protein B7P43_G01785 [Cryptotermes secundus]	K11577		Protein families: genetic information processing- Chromosome and associated proteins	no GO terms	no GO terms
DN40754_c0_g1_i1	-1.626	9.71E-05	XP_015413423.1 PREDICTED: DNA mismatch repair protein Msh2 [Myotis davidii]	K08735	Replication and Repair- Mismatch repair	Protein families: genetic information processing- DNA repair and recombination proteins	F:GO:0003677; F:GO:0005524; P:GO:0006298; F:GO:0030983; C:GO:0032300	F:DNA binding; F:ATP binding; P:mismatch repair; F:mismatched DNA binding; C:mismatch repair complex
DN44135_c11_g1_i1	-1.620	9.35E-06	XP_015375566.1 PREDICTED: 1,4-alpha-glucan-branching enzyme [Diuraphis noxia]	K00700	Carbohydrate metabolism- Starch and sucrose metabolism	Protein families: signaling and cellular processes-exosome	F:GO:0003824; F:GO:0003844; F:GO:0004553; P:GO:0005975; P:GO:0005978; F:GO:0043169	F:catalytic activity; F:1,4-alpha-glucan branching enzyme activity; F:hydrolase activity, hydrolyzing O-glycosyl compounds; P:carbohydrate metabolic process; P:glycogen biosynthetic process; F:cation binding
DN40634_c1_g2_i1	-1.619	5.58E-06	XP_018015947.1 PREDICTED: ubiA prenyltransferase domain-	K00810		Unclassified metabolism-enzymes with EC numbers	F:GO:0004659; C:GO:0016021	F:prenyltransferase activity; C:integral component of membrane;

Table A.1. continued

							; F:GO:0016765	F:transferase activity, transferring alkyl or aryl (other than methyl) groups
DN43656_c6_g1_i1	-1.575	2.04E-06	XP_018026809.1 PREDICTED: DNA ligase 1-like [Hyalella azteca]	K10747	Replication and Repair- DNA replication, base excision repair, nucleotide excision repair, mismatch repair	Protein families: genetic information processing- DNA replication proteins, DNA repair and recombination proteins	F:GO:0003910 ; P:GO:0006281 ; P:GO:0006310	F:DNA ligase (ATP) activity; P:DNA repair; P:DNA recombination
DN34002_c1_g1_i1	-1.557	2.48E-05	AFV15454.1 acyl-CoA delta-9 desaturase [Eriocheir sinensis]	K00507	Lipid metabolism- biosynthesis of unsaturated fatty acids; Environmental Information Processing- Signal transduction- AMPK signaling pathway; Endocrine system- PPAR signaling pathway; Aging- Longevity regulating pathway (worm)	Protein families: metabolism- Lipid biosynthesis proteins	P:GO:0006629 ; F:GO:0016717 ; P:GO:0055114	P:lipid metabolic process; F:oxidoreductase activity, acting on paired donors, with oxidation of a pair of donors resulting in the reduction of molecular oxygen to two molecules of water; P:oxidation-reduction process
DN39759_c0_g1_i1	-1.544	2.16E-06	XP_013387891.1 ankyrin repeat domain-containing protein 10 isoform X3 [Lingula anatina]	0			F:GO:0005515	F:protein binding

Table A.1. continued

DN42896_c2_g1_i1	-1.540	3.04E-05	XP_021371502.1 tetratricopeptide repeat protein 32-like [Mizuhopecten yessoensis]	0			F:GO:0005515	F:protein binding
DN43585_c9_g1_i1	-1.524	3.20E-05	XP_018026869.1 PREDICTED: uncharacterized protein LOC108682249 [Hyalella azteca]	0			no GO terms	no GO terms
DN42510_c4_g1_i1	-1.517	2.05E-05	XP_018020927.1 PREDICTED: uncharacterized protein LOC108677241 [Hyalella azteca]	K10735	DNA	Protein families: genetic information processing- DNA replication proteins	F:GO:0004252 ; F:GO:0005515 ; P:GO:0006508	F:serine-type endopeptidase activity; F:protein binding; P:proteolysis
DN44303_c10_g1_i1	-1.514	5.20E-06	XP_018007934.1 PREDICTED: uncharacterized protein LOC108665670 [Hyalella azteca]	K00586		Protein families: genetic information processing- translation factors	F:GO:0004164 ; F:GO:0008168 ; P:GO:0017183	F:diphthine synthase activity; F:methyltransfer ase activity; P:peptidyl-diphthamide biosynthetic process from peptidyl-histidine

Table A.1. continued

| DN43640_c10_g1_i1 | -1.511 | 2.36E-08 | XP_015435958.1 PREDICTED: aldehyde dehydrogenase, mitochondrial [Dufourea novaeangliae] | K00128 | Metabolism-carbohydrate metabolism-glycolysis/gluconeogenesis, ascorbate and aldarate metabolism, pyruvate metabolism; Lipid metabolism- fatty acid degradation, glycolipid metabolism; Amino acid metabolism- valine, leucine and isoleucine degradation, lysine degradation, arginine and proline metabolism, histidine metabolism, tryptophan metabolism; Metabolism of other amino acids- beta-alanine metabolism; Metabolism of terpenoids and polyketides- insect hormone biosynthesis, limonene and pinene degradation; Xenobiotics biodegradation and metabolism-chloroalkane and | | F:GO:0016491; F:GO:0016620; P:GO:0055114 | F:oxidoreductase activity; F:oxidoreductase activity, acting on the aldehyde or oxo group of donors, NAD or NADP as acceptor; P:oxidation-reduction process |

Table A.1. continued

				chloroalkene degradation					
DN43671_c15_g1_i1	-1.510	4.92E-05	AOE48155.1 hypothetical protein [Eumigus monticolus]	0				no GO terms	no GO terms
DN44650_c4_g1_i1	-1.508	5.71E-05	XP_014349861.1 PREDICTED: uncharacterized protein LOC102358259 [Latimeria chalumnae]	0				no GO terms	no GO terms
DN42292_c12_g1_i1	-1.507	2.20E-05	XP_022098867.1 protein Spindly-like [Acanthaster planci] XP_022098868.1 protein Spindly-like [Acanthaster planci] XP_022098869.1 protein Spindly-like [Acanthaster planci]	0				no GO terms	no GO terms
DN42250_c5_g1_i1	-1.502	1.29E-04	XP_018014480.1 PREDICTED: uncharacterized protein LOC108671443 [Hyalella azteca]	0				no GO terms	no GO terms

Table A.1. continued

DN44386_c9_g2_i1	-1.477	1.28E-04	XP_002596777.1 hypothetical protein BRAFLDRAFT_73707 [Branchiostoma floridae] EEN52789.1 hypothetical protein BRAFLDRAFT_73707 [Branchiostoma floridae]	K19531		Protein families: genetic information processing- Chromosome and associated proteins	no GO terms	no GO terms
DN39939_c1_g2_i1	-1.459	3.60E-07	XP_015334841.1 PREDICTED: exportin-2 [Marmota marmota marmota]	K18423		Protein families: genetic information processing- chromosome and associate proteins	F:GO:0005515 ; P:GO:0006886 ; F:GO:0008536	F:protein binding; P:intracellular protein transport; F:Ran GTPase binding
DN43735_c1_g1_i1	-1.428	1.06E-04	XP_018018295.1 PREDICTED: GTP-binding nuclear protein GSP1/Ran-like [Hyalella azteca]	K07936	Genetic Information Processing-Translation- RNA transport, Ribosome biogenesis in eukaryotes	Protein families: genetic information processing- Messenger RNA biogenesis, Ribosome biogenesis, Transfer RNA biogenesis, Chromosome and associated proteins; Protein families: signaling and cellular processes: Exosome, GTP-binding proteins	F:GO:0003924 ; F:GO:0005525 ; P:GO:0006913	F:GTPase activity; F:GTP binding; P:nucleocytoplasmic transport
DN44638_c0_g1_i1	-1.411	2.40E-05	XP_015433294.1 PREDICTED: DNA replication licensing factor Mcm5 [Dufourea novaeangliae] KZC11207.1 DNA replication licensing factor	K02209	Genetic Information Processing-Replication and repair- DNA replication; Cell growth and death-Cell cycle, Cell	Protein families: genetic information processing- DNA replication proteins, Chromosome and associated proteins	F:GO:0003677 ; F:GO:0003688 ; F:GO:0005524 ; C:GO:0005634	F:DNA binding; F:DNA replication origin binding; F:ATP binding; C:nucleus; P:DNA

Table A.1. continued

			Mcm5 [Dufourea novaeangliae]		cycle (yeast), Meiosis (yeast)		; P:GO:0006270 ; C:GO:0042555	replication initiation; C:MCM complex
DN38788_c0_g1_i1	-1.384	1.14E-04	XP_018018565.1 PREDICTED: disks large-associated protein 5-like [Hyalella azteca] XP_018018573.1 PREDICTED: disks large-associated protein 5-like [Hyalella azteca]	K16804		Protein families: genetic information processing-Chromosome and associated proteins	P:GO:0023052	P:signaling
DN42270_c14_g3_i1	-1.381	2.82E-05	XP_023713986.1 2',5'-phosphodiesterase 12 isoform X2 [Cryptotermes secundus] PNF27206.1 2',5'-phosphodiesterase 12 [Cryptotermes secundus]	K19612		Protein families: genetic information processing-Messenger RNA biogenesis, Mitochondrial biogenesis	no GO terms	no GO terms
DN46511_c0_g1_i1	-1.376	1.03E-04	XP_015432603.1 PREDICTED: glucose-6-phosphate isomerase [Dufourea novaeangliae] KZC10609.1 Glucose-6-phosphate isomerase [Dufourea novaeangliae]	K01810	Carbohydrate metabolism-Glycolysis/Glucone ogenesis, Pentose phosphate pathway, Starch and sucrose metabolism, Amino sugar and nucleotide sugar metabolism	Protein families: signaling and cellular processes-exosome	F:GO:0004347 ; P:GO:0006094 ; P:GO:0006096	F:glucose-6-phosphate isomerase activity; P:gluconeogenes is; P:glycolytic process
DN43557_c0_g2_i1	-1.371	9.91E-05	XP_023716377.1 N-acetyltransferase 9-like protein isoform X2 [Cryptotermes secundus] PNF24691.1 N-acetyltransferase 9-like	0			F:GO:0016747	F:transferase activity, transferring acyl groups other than amino-acyl groups

Table A.1. continued

			protein [Cryptotermes secundus]						
DN43449_c6_g2_i1	-1.360	9.53E-06	XP_003427163.1 PREDICTED: KDEL motif-containing protein 1-like [Nasonia vitripennis]	0			F:GO:0005515	F:protein binding
DN44010_c7_g1_i1	-1.330	3.11E-05	XP_015435418.1 PREDICTED: LOW QUALITY PROTEIN: uncharacterized protein LOC107191011 [Dufourea novaeangliae]	K02649	Environmental Information Processing- Signal transduction- all categories; Cellular Processes- Transport and catabolism- Autophagy, Apoptosis, Cellular senescence; Immune system (most categories within); Endocrine system	Protein families: genetic information processing- membrane trafficking	F:GO:0005515; C:GO:0005942; P:GO:0007165; F:GO:0035014; P:GO:0035556	F:protein binding; C:phosphatidylinositol 3-kinase complex; P:signal transduction; F:phosphatidylinositol 3-kinase regulator activity; P:intracellular signal transduction
DN44611_c14_g1_i1	-1.323	1.46E-07	ATP62320.1 L-type lectin [Litopenaeus vannamei]	K10082	Translation- folding, sorting and degradation- protein processing in endoplasmic reticulum	Protein families: genetic information processing- membrane trafficking; Protein families: signaling and cellular processes- lectins	C:GO:0016020	C:membrane

Table A.1. continued

DN44546_c7_g1_i1	-1.302	6.66E-05	XP_013419657.1 beta-1,4-mannosyl-glycoprotein 4-beta-N-acetylglucosaminyltransferase isoform X5 [Lingula anatina]	K00737	Glycan biosynthesis and metabolism- N-Glycan biosynthesis	Protein families: metabolism-Glycosyltransferases	F:GO:0003830; P:GO:0006487; C:GO:0016020	F:beta-1,4-mannosylglycoprotein 4-beta-N-acetylglucosaminyltransferase activity; P:protein N-linked glycosylation; C:membrane
DN35633_c0_g1_i1	-1.297	9.77E-05	XP_015343329.1 PREDICTED: DNA replication licensing factor MCM3 [Marmota marmota marmota]	K02541	Replication and repair- DNA replication; Cell growth and death- cell cycle, cell cycle (yeast), meiosis (yeast)	Protein families: genetic information processing- DNA replication proteins, Chromosome and associated proteins	F:GO:0003677; F:GO:0005524; P:GO:0006270; C:GO:0042555	F:DNA binding; F:ATP binding; P:DNA replication initiation; C:MCM complex
DN42366_c5_g1_i1	-1.287	1.39E-06	XP_018014164.1 PREDICTED: bestrophin-3-like [Hyalella azteca]	K22204		Protein families: signaling and cellular processes-transporters	no GO terms	no GO terms
DN43235_c9_g1_i1	-1.281	8.47E-06	AAH06165.3 Minichromosome maintenance complex component 2 [Homo sapiens]	MCM2; DNA replication licensing factor MCM2 [EC:3.6.4.12]	Replication and Repair- DNA replication; Cell growth and death- cell cycle, cell cycle (yeast), meiosis (yeast)	Protein families: genetic information processing- DNA replication proteins, Chromosome and associated proteins	F:GO:0003677; F:GO:0005524; C:GO:0005634; P:GO:0006270; C:GO:0042555; P:GO:1905775	F:DNA binding; F:ATP binding; C:nucleus; P:DNA replication initiation; C:MCM complex; P:negative regulation of DNA helicase activity

136

Table A.1. continued

DN43609_c11_g2_i2	-1.267	5.57E-06	XP_018024815.1 PREDICTED: uridine 5'-monophosphate synthase-like [Hyalella azteca]	K13421	Nucleotide metabolism-pyrimidine metabolism; Xenobiotics biodegradation and metabolism- drug metabolism (other enzymes)		F:GO:0003824 ; F:GO:0004588 ; F:GO:0004590 ; P:GO:0006207 ; P:GO:0006221 ; P:GO:0009116 ; P:GO:0044205	F:catalytic activity; F:orotate phosphoribosyltransferase activity; F:orotidine-5'-phosphate decarboxylase activity; P:'de novo' pyrimidine nucleobase biosynthetic process; P:pyrimidine nucleotide biosynthetic process; P:nucleoside metabolic process; P:'de novo' UMP biosynthetic process
DN38198_c0_g1_i1	-1.263	4.61E-06	XP_018025206.1 PREDICTED: tubulin-specific chaperone A-like [Hyalella azteca]	K17292		Protein families: signaling and cellular processes-cytoskeleton proteins, exosome	no GO terms	no GO terms
DN42525_c5_g1_i1	-1.258	2.58E-06	XP_015352751.1 PREDICTED: importin-11 isoform X1 [Marmota marmota marmota] XP_015352752.1 PREDICTED: importin-	0			P:GO:0006886 ; F:GO:0008536	P:intracellular protein transport; F:Ran GTPase binding

Table A.1. continued

			11 isoform X1 [Marmota marmota marmota]					
DN34542_c2_g1_i1	-1.256	2.09E-05	XP_018023096.1 PREDICTED: PQ-loop repeat-containing protein 1-like [Hyalella azteca]	0			no GO terms	no GO terms
DN41433_c0_g1_i1	-1.253	1.90E-05	XP_009062349.1 hypothetical protein LOTGIDRAFT_220203 [Lottia gigantea] ESO86952.1 hypothetical protein LOTGIDRAFT_220203 [Lottia gigantea]	K14801		Protein families: genetic information processing- Ribosome biogenesis	C:GO:0005737	C:cytoplasm
DN43282_c8_g2_i1	-1.251	1.28E-06	ACD13595.1 mitotic checkpoint protein [Penaeus monodon]	K02180	Cellular Processes- Cell growth and death- Cell cycle, cell cycle yeast	Protein families: genetic information processing- spliceosome; chromosome and associated proteins	F:GO:0005515	F:protein binding
DN43736_c0_g2_i1	-1.248	1.23E-05	AAW22143.1 SERCA [Panulirus argus] CAH10336.1 SERCA Ca(2+)-ATPase pump [Panulirus argus]	K05853	Environmental Information Processing- Signal transduction- Calcium signaling pathway; Digestive system- pancreatic secretion		F:GO:0005388; F:GO:0005524; C:GO:0005783; C:GO:0016021; C:GO:0033017; P:GO:0070588	F:calcium-transporting ATPase activity; F:ATP binding; C:endoplasmic reticulum; C:integral component of membrane; C:sarcoplasmic reticulum membrane; P:calcium ion

Table A.1. continued

							transmembrane transport
DN43749_c1_g1_i1	-1.230	8.56E-05	XP_015429704.1 PREDICTED: probable ATP-dependent RNA helicase DHX35 [Dufourea novaeangliae] KZC08160.1 putative ATP-dependent RNA helicase DHX35 [Dufourea novaeangliae]	K13117		Protein families: genetic information processing-Spliceosome	F:GO:0004386	F:helicase activity
DN36475_c0_g1_i1	-1.211	2.14E-05	XP_015339114.1 PREDICTED: isoleucine--tRNA ligase, mitochondrial [Marmota marmota marmota]	K01870	Genetic Information Processing-Translation-Aminoacyl-tRNA biosynthesis	Protein families: metabolism- Amino acid related enzymes; Protein families: genetic information processing- Transfer RNA biogenesis	F:GO:0000049; F:GO:0000166; F:GO:0002161; F:GO:0004812; F:GO:0004822; F:GO:0005524; P:GO:0006418; P:GO:0006428	F:tRNA binding; F:nucleotide binding; F:aminoacyl-tRNA editing activity; F:aminoacyl-tRNA ligase activity; F:isoleucine-tRNA ligase activity; F:ATP binding; P:tRNA aminoacylation for protein translation; P:isoleucyl-tRNA aminoacylation

Table A.1. continued

DN19145_c0_g1_i1	-1.201	8.49E-05	XP_018009815.1 PREDICTED: tudor domain-containing protein 7-like isoform X3 [Hyalella azteca]	K18405		Protein families: genetic information processing- Chromosome and associated proteins	no GO terms	no GO terms
DN42595_c3_g1_i1	-1.178	3.92E-05	XP_023241425.1 heterogeneous nuclear ribonucleoprotein Q-like [Centruroides sculpturatus]	0			no GO terms	no GO terms
DN43411_c19_g1_i1	-1.151	3.63E-05	XP_023705243.1 RNA pseudouridylate synthase domain-containing protein 1-like isoform X1 [Cryptotermes secundus] XP_023705244.1 RNA pseudouridylate synthase domain-containing protein 1-like isoform X1 [Cryptotermes secundus] XP_023705246.1 RNA pseudouridylate synthase domain-containing protein 1-like isoform X1 [Cryptotermes secundus] PNF36000.1 hypothetical protein B7P43_G00576 [Cryptotermes secundus]	0			P:GO:0001522; F:GO:0003723; P:GO:0009451; F:GO:0009982	P:pseudouridine synthesis; F:RNA binding; P:RNA modification; F:pseudouridine synthase activity
DN43449_c19_g1_i1	-1.130	6.97E-05	KZS18554.1 Phosphoethanolamine/pho sphocholine phosphatase [Daphnia magna]	K13248	Metabolism of cofactors and vitamins- Vitamin B6 metabolism	Protein families: metabolism- Protein phosphatases and associated proteins	F:GO:0016791	F:phosphatase activity
DN43566_c7_g2_i1	-1.128	8.77E-05	XP_023332964.1 tRNA:m(4)X modification	K15446		Protein families: genetic information	P:GO:0008033; F:GO:0008168	P:tRNA processing; F:methyltransfer

Table A.1. continued

			enzyme TRM13 homolog [Eurytemora affinis]			processing- Transfer RNA biogenesis	; P:GO:0030488 ; F:GO:0106050	ase activity; P:tRNA methylation; F:tRNA 2'-O-methyltransferas e activity
DN44494_c0_g1_i1	-1.119	1.84E-05	AKB96201.1 heat shock protein [Cherax destructor]	0			no GO terms	no GO terms
DN44174_c6_g1_i1	-1.117	8.98E-05	XP_021935995.1 uncharacterized protein LOC110837781 [Zootermopsis nevadensis]	0			C:GO:0005634 ; P:GO:0031144 ; P:GO:0071630	C:nucleus; P:proteasome localization; P:nuclear protein quality control by the ubiquitin-proteasome system
DN42606_c5_g1_i1	-1.109	9.35E-06	XP_013399368.1 transmembrane protein 214-B [Lingula anatina]	0			no GO terms	no GO terms
DN42943_c5_g1_i1	-1.101	4.33E-05	XP_015436951.1 PREDICTED: FACT complex subunit spt16 isoform X1 [Dufourea novaeangliae]	0			C:GO:0035101	C:FACT complex
DN42292_c19_g1_i1	-1.081	6.40E-07	XP_018023028.1 PREDICTED: TBCC domain-containing protein 1-like [Hyalella azteca]	K16810		Protein families: genetic information processing-chromosome and associate proteins	P:GO:0000902	P:cell morphogenesis

Table A.1. continued

DN43509_c9_g1_i1	-1.077	1.25E-06	XP_018026731.1 PREDICTED: X-ray repair cross-complementing protein 5-like [Hyalella azteca]	K10885	Genetic Information Processing- Replication and repair- non-homologous end-joining	Protein families: genetic information processing- DNA repair and recombination proteins	P:GO:0000723 ; F:GO:0003677 ; F:GO:0003684 ; F:GO:0004003 ; C:GO:0005634 ; P:GO:0006303 ; P:GO:0006310 ; F:GO:0016817 ; F:GO:0042162 ; C:GO:0043564	P:telomere maintenance; F:DNA binding; F:damaged DNA binding; F:ATP-dependent DNA helicase activity; C:nucleus; P:double-strand break repair via nonhomologous end joining; P:DNA recombination; F:hydrolase activity, acting on acid anhydrides; F:telomeric DNA binding; C:Ku70:Ku80 complex
DN43905_c16_g1_i1	-1.076	1.02E-04	PZC85548.1 hypothetical protein B5X24_HaOG216656 [Helicoverpa armigera]	0			C:GO:0016021	C:integral component of membrane
DN43195_c5_g1_i1	-1.073	1.18E-04	XP_015432515.1 PREDICTED: LOW QUALITY PROTEIN: signal transducer and activator of transcription 5B [Dufourea novaeangliae]	K11224	Environmental Information Processing- Signal transduction- ErbB signaling pathway, Jak-STAT signaling pathway; Cell growth and death- Necroptosis; Immune system-	Protein families: genetic information processing- transcription factors	F:GO:0003677 ; F:GO:0003700 ; C:GO:0005634 ; P:GO:0006355 ; P:GO:0007165	F:DNA binding; F:DNA-binding transcription factor activity; C:nucleus; P:regulation of transcription, DNA-templated; P:signal transduction;

142

					Th1 and Th2 cell differentiation, Th17 cell differentiation, Chemokine signaling pathway; Endocrine system-Prolactin signaling pathway		; P:GO:0060397	P:growth hormone receptor signaling pathway via JAK-STAT
DN43949_c5_g1_i1	-1.066	1.27E-04	XP_015433387.1 PREDICTED: FACT complex subunit Ssrp1 [Dufourea novaeangliae]	K09272		Protein families: genetic information processing-transcription factors	F:GO:0003677 ; C:GO:0005634	F:DNA binding; C:nucleus
DN43340_c9_g1_i1	-1.064	2.36E-05	XP_015604384.1 ADP-ribosylation factor-binding protein GGA1 isoform X2 [Cephus cinctus]	K12404	Cellular Processes-Transport and catabolism-Lysosome	Protein families: genetic information processing-membrane trafficking	C:GO:0005622 ; P:GO:0006886 ; P:GO:0016192	C:intracellular; P:intracellular protein transport; P:vesicle-mediated transport
DN43879_c7_g1_i1	-1.036	5.01E-06	XP_971567.1 PREDICTED: rhythmically expressed gene 2 protein [Tribolium castaneum] EFA00363.1 Rhythmically expressed gene 2 protein-like Protein [Tribolium castaneum]	0			F:GO:0005515	F:protein binding
DN39729_c0_g1_i1	-1.034	5.02E-05	XP_019621706.1 PREDICTED: LOW QUALITY PROTEIN: iduronate 2-sulfatase-like [Branchiostoma belcheri]	K01136	Glycan biosynthesis and metabolism-Glycosaminoglycan degradation; Cell Processes-Lysosome		F:GO:0003824 ; F:GO:0004423 ; F:GO:0008484	F:catalytic activity; F:iduronate-2-sulfatase activity; F:sulfuric ester

Table A.1. continued

								hydrolase activity
DN24171_c0_g2_i1	-1.030	7.53E-05	AAI34813.1 LOC733291 protein, partial [Xenopus laevis]	K08776		Protein families: metabolism-Peptidases	P:GO:0006508; F:GO:0008237; F:GO:0008270	P:proteolysis; F:metallopeptidase activity; F:zinc ion binding
DN43142_c9_g1_i1	-1.026	2.51E-08	XP_022249137.1 sphingomyelin phosphodiesterase 4-like isoform X2 [Limulus polyphemus]	K12353	Lipid metabolism-sphingolipid metabolism		F:GO:0050290	F:sphingomyelin phosphodiesterase D activity
DN43014_c0_g1_i1	-1.019	1.11E-04	XP_015436514.1 PREDICTED: exportin-5 [Dufourea novaeangliae]	K14289	Genetic Information Processing-Translation- RNA transport	Protein families: genetic information processing- Transfer RNA biogenesis, Chromosome and associated proteins	P:GO:0006886; F:GO:0008536; P:GO:0051168	P:intracellular protein transport; F:Ran GTPase binding; P:nuclear export
DN38577_c0_g1_i1	-1.019	8.92E-05	XP_014282477.1 phosphatidylinositol 5-phosphate 4-kinase type-2 alpha [Halyomorpha halys]	K00920	Carbohydrate metabolism-Inositol phosphate metabolism; Environmental Information Processing- Signal transduction-Phosphatidylinosital signaling pathway; Cell motility-Regulation of actin cytoskeleton		F:GO:0016307; P:GO:0046488	F:phosphatidylinositol phosphate kinase activity; P:phosphatidylinositol metabolic process
DN44072_c2_g1_i1	-1.013	5.21E-05	XP_018018193.1 PREDICTED: altered inheritance of	0			no GO terms	no GO terms

Table A.1. continued

			mitochondria protein 3-1-like [Hyalella azteca]					
DN43033_c9_g1_i1	-1.009	1.55E-04	XP_018009874.1 PREDICTED: transient receptor potential cation channel subfamily A member 1 homolog [Hyalella azteca]	K04984	Sensory system- Inflammatory mediator regulation of TRP channels	Protein families: signaling and cellular processes- exosome	F:GO:0005216; F:GO:0005515; C:GO:0016021; P:GO:0034220	F:ion channel activity; F:protein binding; C:integral component of membrane; P:ion transmembrane transport
DN38811_c0_g3_i1	-1.004	1.06E-05	EDL39578.1 mCG9152, isoform CRA_a, partial [Mus musculus]	K20224		Protein families: genetic information processing- Ribosome biogenesis	no GO terms	no GO terms
DN43258_c10_g1_i1	-0.969	1.41E-05	XP_013380878.1 TELO2-interacting protein 1 homolog [Lingula anatina]	K20403	Environmental Information Processing- Signal transduction- mTOR signaling pathway		no GO terms	no GO terms
DN43859_c2_g1_i1	-0.950	1.39E-04	XP_015430721.1 PREDICTED: LOW QUALITY PROTEIN: ATP-dependent RNA helicase Ddx1-like [Dufourea novaeangliae]	K13177		Protein families: genetic information processing- Spliceosome, Transfer RNA biogenesis	F:GO:0003676; F:GO:0005515; F:GO:0005524	F:nucleic acid binding; F:protein binding; F:ATP binding
DN42869_c7_g1_i2	-0.940	1.48E-04	XP_018009973.1 PREDICTED: BRCA1-associated RING domain protein 1-like [Hyalella azteca]	K10683	Replication and repair- Homologous recombination	Protein families: genetic information processing- Messenger RNA biogenesis,	F:GO:0005515; P:GO:0016567; C:GO:0031436	F:protein binding; P:protein ubiquitination; C:BRCA1-

Table A.1. continued

							; P:GO:0043065	BARD1 complex; P:positive regulation of apoptotic process
DN44111_c9_g1_i1	-0.893	7.67E-05	XP_968070.1 PREDICTED: glutathione synthetase isoform X2 [Tribolium castaneum]	K21456	Amino acid metabolism-Cysteine and methionine metabolism; Metabolism of other amino acids-Glutathione metabolism; Cell growth and death-Ferroptosis	Protein families: signaling and cellular processes-exosome	F:GO:0004363 ; F:GO:0005524 ; P:GO:0006750 ; F:GO:0016874	F:glutathione synthase activity; F:ATP binding; P:glutathione biosynthetic process; F:ligase activity
DN41962_c3_g1_i1	-0.880	8.10E-05	XP_019621847.1 PREDICTED: nuclear pore complex protein Nup88-like isoform X1 [Branchiostoma belcheri]	K14318	Genetic Information Processing-Translation- RNA transport	Protein families: genetic information processing-Messenger RNA biogenesis	P:GO:0000055 ; P:GO:0000056 ; F:GO:0005515 ; P:GO:0006913 ; F:GO:0017056	P:ribosomal large subunit export from nucleus; P:ribosomal small subunit export from nucleus; F:protein binding; P:nucleocytoplasmic transport; F:structural constituent of nuclear pore

Table A.1. continued

DN44635_c1_g1_i1	-0.871	1.46E-04	AGG55292.1 p53 protein [Litopenaeus vannamei] AGG55293.1 p53 protein [Litopenaeus vannamei]	K10149	Environmental Information Processing- Signal transduction- Hippo signaling pathway; Cell growth and death- Apoptosis (fly)	Protein families: genetic information processing- transcription factors	F:GO:0003677 ; F:GO:0003700 ; C:GO:0005634 ; P:GO:0006355 ; P:GO:0006915 ; F:GO:0044212	F:DNA binding; F:DNA-binding transcription factor activity; C:nucleus; P:regulation of transcription, DNA-templated; P:apoptotic process; F:transcription regulatory region DNA binding
DN44043_c8_g1_i1	-0.827	1.38E-04	XP_015438047.1 PREDICTED: vacuolar protein sorting-associated protein 26B-like [Dufourea novaeangliae] KZC04920.1 Vacuolar protein sorting-associated protein 26 [Dufourea novaeangliae]	K18466	Cellular Processes- Transport and catabolism- Endocytosis	Protein families: genetic information processing- membrane trafficking	no GO terms	no GO terms
DN39935_c1_g1_i1	-0.793	7.21E-05	XP_015434585.1 PREDICTED: probable glutamine--tRNA ligase [Dufourea novaeangliae]	K01886	Genetic Information Processing- Translation- Aminoacyl-tRNA biosynthesis	Protein families: metabolism- Amino acid related enzymes; Protein families: genetic information processing- Transfer RNA biogenesis	F:GO:0000166 ; F:GO:0004812 ; F:GO:0004819 ; F:GO:0005524 ; C:GO:0005737 ; P:GO:0006412 ; P:GO:0006418 ;	F:nucleotide binding; F:aminoacyl-tRNA ligase activity; F:glutamine-tRNA ligase activity; F:ATP binding; C:cytoplasm; P:translation; P:tRNA aminoacylation for protein

Table A.1. continued

							P:GO:0006425; P:GO:0043039	translation; P:glutaminyl-tRNA aminoacylation; P:tRNA aminoacylation
DN43438_c13_g1_i1	-0.788	6.76E-05	XP_017778796.1 PREDICTED: PITH domain-containing protein GA19395 [Nicrophorus vespilloides]	0			no GO terms	no GO terms
DN43586_c8_g1_i1	-0.786	6.89E-06	XP_017889657.1 PREDICTED: U1 small nuclear ribonucleoprotein A [Ceratina calcarata]	0			F:GO:0003676	F:nucleic acid binding
DN43975_c14_g1_i1	-0.785	1.11E-04	XP_002597643.1 hypothetical protein BRAFLDRAFT_77443 [Branchiostoma floridae] EEN53655.1 hypothetical protein BRAFLDRAFT_77443 [Branchiostoma floridae]	K10308		Protein families: genetic information processing Ubiquitin system	P:GO:0006974; C:GO:0019005; F:GO:0030332; P:GO:0031146; P:GO:0031571	P:cellular response to DNA damage stimulus; C:SCF ubiquitin ligase complex; F:cyclin binding; P:SCF-dependent proteasomal ubiquitin-dependent protein catabolic process; P:mitotic G1 DNA damage checkpoint

Table A.1. continued

Transcript ID	Log₂FC	Adjusted p-value	Annotation	KO	KAAS Pathways	BRITE Hierarchies	GO IDs	GO Names
DN44386_c20_g1_i1	-0.698	1.08E-04	XP_013191358.1 PREDICTED: vacuolar-sorting protein SNF8 [Amyelois transitella]	K12188	Cellular Processes-Transport and catabolism-Endocytosis	Protein families: genetic information processing-membrane trafficking; Protein families: signaling and cellular processes: Exosome	C:GO:0000814 ; P:GO:0071985	C:ESCRT II complex; P:multivesicular body sorting pathway

16°C vs. 22°C: under-expressed, edgeR

Transcript ID	Log₂FC	Adjusted p-value	Annotation	KO	KAAS Pathways	BRITE Hierarchies	GO IDs	GO Names
DN36928_c0_g2_i1	-6.720	1.49E-02	XP_011439505.1 PREDICTED: probable methylmalonate-semialdehyde dehydrogenase [acylating], mitochondrial [Crassostrea gigas] EKC35210.1 Putative methylmalonate-semialdehyde dehydrogenase [acylating], mitochondrial [Crassostrea gigas]	K00140	Carbohydrate metabolism-Propanoate metabolism, Inositol phosphate metabolism; Amino acid metabolism-Valine, leucine and isoleucine degradation; Metabolism of other amino acids- beta-Alanine metabolism		F:GO:0004491 ; P:GO:0055114	F:methylmalonate-semialdehyde dehydrogenase (acylating) activity; P:oxidation-reduction process
DN44614_c6_g1_i2	-2.519	1.90E-02	BAM65720.1 myosin heavy chain type 2 [Penaeus monodon]	K17751	Circulatory system-Cardiac muscle contraction, Adrenergic signaling in cardiomyocytes	Protein families: signaling and cellular processes-Cytoskeleton proteins, Exosome	F:GO:0003774 ; F:GO:0005515 ; F:GO:0005524 ; C:GO:0016459	F:motor activity; F:protein binding; F:ATP binding; C:myosin complex

Table A.1. continued

DN44135_c11_g1_i1	-1.708	2.19E-02	XP_011434285.1 PREDICTED: 1,4-alpha-glucan-branching enzyme [Crassostrea gigas] EKC42072.1 1,4-alpha-glucan-branching enzyme [Crassostrea gigas]	K00700	Carbohydrate metabolism- Starch and sucrose metabolism	Protein families: signaling and cellular processes- Exosome	F:GO:0003844; F:GO:0004553; P:GO:0005978; F:GO:0043169	F:1,4-alpha-glucan branching enzyme activity; F:hydrolase activity, hydrolyzing O-glycosyl compounds; P:glycogen biosynthetic process; F:cation binding
DN34002_c1_g1_i1	-1.636	2.21E-02	AMQ48727.1 delta-9 desaturase [Macrobrachium nipponense]	K00507	Lipid metabolism- Biosynthesis of unsaturated fatty acids; Signal transduction- AMPK signaling pathway; Endocrine system- PPAR signaling pathway; Aging- Longevity regulating pathway	Protein families: metabolism- Lipid biosynthesis proteins	P:GO:0006629; F:GO:0016717; P:GO:0055114	P:lipid metabolic process; F:oxidoreductase activity, acting on paired donors, with oxidation of a pair of donors resulting in the reduction of molecular oxygen to two molecules of water; P:oxidation-reduction process
DN42550_c8_g5_i1	-1.626	2.55E-02	XP_023320668.1 mitotic spindle assembly checkpoint protein MAD2A-like [Eurytemora affinis]	K02537	Cell growth and death- Cell cycle, Cell cycle (yeast), Meiosis (yeast), Oocyte meiosis; Endocrine system-	Protein families: genetic information processing- Chromosome and associated proteins	P:GO:0007094	P:mitotic spindle assembly checkpoint

						Progesterone-mediated oocyte maturation		
DN39939_c1_g2_i1	-1.510	1.90E-02	XP_011445200.1 PREDICTED: exportin-2 [Crassostrea gigas] EKC30336.1 Exportin-2 [Crassostrea gigas]	K18423		Protein families: genetic information processing- Chromosome and associated proteins	P:GO:0006886; F:GO:0008536	P:intracellular protein transport; F:Ran GTPase binding
DN44638_c0_g1_i1	-1.471	2.23E-02	XP_011451587.1 PREDICTED: DNA replication licensing factor mcm5 [Crassostrea gigas] EKC32126.1 DNA replication licensing factor mcm5 [Crassostrea gigas]	K02209	Replication and repair- DNA replication; Cell growth and death- Cell cycle, Cell cycle (yeast), Meiosis (yeast)	Protein families: genetic information processing- DNA replication proteins, Chromosome and associated proteins	F:GO:0003688; F:GO:0005524; C:GO:0005634; P:GO:0006270; C:GO:0042555	F:DNA replication origin binding; F:ATP binding; C:nucleus; P:DNA replication initiation; C:MCM complex
DN49657_c0_g1_i1	-1.440	2.86E-02	KMQ96290.1 protein disulfide-isomerase a3 [Lasius niger]	K08056	Genetic Information Processing- Folding, sorting and degradation- Protein processing in the endoplasmic reticulum; Immune system- Antigen processing and presentation	Protein families: genetic information processing- Chaperones and folding catalysts; Membrane trafficking; Protein families: signaling and cellular processes- Exosome	F:GO:0003756; P:GO:0045454	F:protein disulfide isomerase activity; P:cell redox homeostasis
DN22339_c0_g1_i2	-1.411	2.86E-02	XP_011443137.1 PREDICTED: DNA replication licensing factor mcm7 [Crassostrea gigas] EKC32434.1 DNA	K02210	Replication and repair- DNA replication; Cell growth and death- Cell cycle, Cell	Protein families: metabolism- Protein phosphatases and associated proteins; Protein families: genetic information	F:GO:0003677; F:GO:0003678; F:GO:0005524; P:GO:0006270	F:DNA binding; F:DNA helicase activity; F:ATP binding; P:DNA replication initiation;

Table A.1. continued

			replication licensing factor mcm7 [Crassostrea gigas]		cycle (yeast), Meiosis (yeast)	processing- DNA replication proteins	; C:GO:0042555	C:MCM complex
DN32480_c0_g2_i1	-1.392	2.59E-02	PSN38759.1 CDP-diacylglycerol--inositol 3-phosphatidyltransferase [Blattella germanica]	K00999	Carbohydrate metabolism- Inositol phosphate metabolism; Lipid metabolism- Glycerophospholipid metabolism; Signal transduction- Phosphatidylinositol signaling system		P:GO:0008654 ; C:GO:0016020 ; F:GO:0016780	P:phospholipid biosynthetic process; C:membrane; F:phosphotransferase activity, for other substituted phosphate groups
DN35633_c0_g1_i1	-1.352	2.55E-02	EKC33730.1 DNA replication licensing factor MCM3 [Crassostrea gigas]	K02541	Replication and repair- DNA replication; Cell growth and death- Cell cycle, Cell cycle (yeast), Meiosis (yeast)	Protein families: genetic information processing- DNA replication proteins, Chromosome and associated proteins	F:GO:0003677 ; F:GO:0005524 ; P:GO:0006270 ; C:GO:0042555	F:DNA binding; F:ATP binding; P:DNA replication initiation; C:MCM complex
DN43235_c9_g1_i1	-1.331	2.31E-02	EKC27055.1 DNA replication licensing factor mcm2 [Crassostrea gigas]	K02540	Replication and repair- DNA replication; Cell growth and death- Cell cycle, Cell cycle (yeast), Meiosis (yeast)	Protein families: genetic information processing- DNA replication proteins, Chromosome and associated proteins	F:GO:0003677 ; F:GO:0005524 ; C:GO:0005634 ; P:GO:0006270 ; C:GO:0042555 ; P:GO:1905775	F:DNA binding; F:ATP binding; C:nucleus; P:DNA replication initiation; C:MCM complex; P:negative regulation of DNA helicase activity

Table A.1. continued

DN37277_c0_g1_i1	-1.298	2.80E-02	ACY66399.1 RuvB-like 2, partial [Scylla paramamosain]	K11338		Protein families: genetic information processing-Chromosome and associated proteins	F:GO:0005524; C:GO:0031011; C:GO:0035267; F:GO:0043141; C:GO:0097255	F:ATP binding; C:Ino80 complex; C:NuA4 histone acetyltransferase complex; F:ATP-dependent 5'-3' DNA helicase activity; C:R2TP complex
DN43282_c8_g2_i1	-1.282	1.90E-02	XP_025094156.1 mitotic checkpoint protein BUB3-like [Pomacea canaliculata] XP_025094157.1 mitotic checkpoint protein BUB3-like [Pomacea canaliculata] XP_025094158.1 mitotic checkpoint protein BUB3-like [Pomacea canaliculata] XP_025094160.1 mitotic checkpoint protein BUB3-like [Pomacea canaliculata] XP_025094161.1 mitotic checkpoint protein BUB3-like [Pomacea canaliculata] PVD29616.1 hypothetical protein C0Q70_08871 [Pomacea canaliculata]	K02180	Cell growth and death- Cell cycle, Cell cycle (yeast)	Protein families: genetic information processing-Spliceosome	F:GO:0005515	F:protein binding

Table A.1. continued

DN26575_c0_g1_i1	-1.215	2.76E-02	XP_023291662.1 protein kish [Lucilia cuprina]	0			0	0
DN42943_c5_g1_i1	-1.127	2.55E-02	XP_011445672.1 PREDICTED: FACT complex subunit SPT16 [Crassostrea gigas] EKC29643.1 FACT complex subunit spt16 [Crassostrea gigas]	0			C:GO:0035101	C:FACT complex

16°C vs. 18°C: over-expressed, DESeq2

Transcript ID	Log₂FC	Adjusted p-value	Annotation	KO	KAAS Pathways	BRITE Hierarchies	GO IDs	GO Names
DN43047_c4_g2_i1	3.710	2.97E-07	XP_018011013.1 PREDICTED: uncharacterized protein LOC108668336 [Hyalella azteca]	0			C:GO:0005576; P:GO:0006030; F:GO:0008061	C:extracellular region; P:chitin metabolic process; F:chitin binding
DN43869_c5_g1_i1	3.546	6.67E-05	SOX55400.1 hypothetical protein MAAFP003_4092, partial [Mycobacterium ahvazicum]	0			0	0
DN44293_c2_g1_i1	3.440	8.57E-08	XP_018025308.1 PREDICTED: sodium/glucose cotransporter 4-like [Hyalella azteca]	K14158	Digestive system-Bile secretion, Carbohydrate digestion and absorption, Mineral absorption	Protein families: signaling and cellular processes-Transporters, Exosome	0	0
DN43869_c9_g1_i1	3.283	4.30E-04	GAN74957.1 hypothetical protein Apmu_0247_01	0			0	0

Table A.1. continued

			[Acidiphilium multivorum AIU301]					
DN43421_c5_g3_i1	3.136	4.30E-04	PRD19514.1 Dipeptidyl peptidase 1 [Nephila clavipes]	K01275	Cellular Processes-Transport and catabolism-Lysosome; Cell growth and death-Apoptosis	Protein families: metabolism-Peptidases; Protein families: genetic information processing-Chaperones and folding catalysts; Protein families: signaling and cellular processes-Exosome	0	0
DN43869_c23_g1_i1	3.084	1.12E-03	CBY13234.1 unnamed protein product, partial [Oikopleura dioica]	0			0	0
DN6535_c0_g1_i1	3.044	1.14E-03	XP_018017512.1 PREDICTED: pro-resilin-like isoform X1 [Hyalella azteca] XP_018017514.1 PREDICTED: pro-resilin-like isoform X2 [Hyalella azteca]	0			0	0
DN41988_c2_g3_i1	3.018	1.99E-04	XP_018013858.1 PREDICTED: alkylglycerol monooxygenase-like [Hyalella azteca]	K15537		Not Included in Pathway or Brite-Unclassified: metabolism-Enzymes with EC numbers	0	0
DN44500_c22_g2_i1	3.006	3.88E-04	XP_018022127.1 PREDICTED: cuticle protein 8-like isoform X2 [Hyalella azteca]	0			0	0

155

Table A.1. continued

DN44323_c21_g1_i1	2.999	3.88E-04	ACR78689.1 hypothetical cuticle protein, partial [Rimicaris exoculata]	0				0	0
DN7224_c0_g1_i1	2.959	5.93E-04	XP_018013996.1 PREDICTED: translation initiation factor IF-2-like [Hyalella azteca]	0				F:GO:0042302	F:structural constituent of cuticle
DN37657_c0_g1_i1	2.932	3.99E-04	XP_022243886.1 apolipophorins-like, partial [Limulus polyphemus]	0				F:GO:0005319 ; P:GO:0006869	F:lipid transporter activity; P:lipid transport
DN41976_c2_g1_i1	2.889	1.79E-04	XP_002024924.1 GL17853 [Drosophila persimilis] EDW30397.1 GL17853 [Drosophila persimilis]	0				0	0
DN44500_c28_g1_i1	2.801	1.12E-03	ACO12877.1 Cuticle protein 19.8 [Lepeophtheirus salmonis]	0				0	0
DN42837_c0_g1_i1	2.786	2.78E-03	ASK05861.1 chitin-binding protein [Macrobrachium nipponense]	0				0	0
DN20237_c0_g1_i1	2.776	1.67E-03	ASK05861.1 chitin-binding protein [Macrobrachium nipponense]	0				0	0
DN46935_c0_g1_i1	2.755	5.00E-03	CIN51991.1 Uncharacterised protein [Salmonella enterica subsp. enterica serovar Typhi]	0				0	0

Table A.1. continued

DN44500_c1_g1_i1	2.716	2.00E-03	ASK05861.1 chitin-binding protein [Macrobrachium nipponense]	0			F:GO:0042302	F:structural constituent of cuticle
DN44096_c10_g1_i1	2.702	5.13E-03	ACV95456.1 reverse transcriptase/endonuclease [Adineta vaga] ACV95458.1 reverse transcriptase/endonuclease [Adineta vaga]	0			F:GO:0003676	F:nucleic acid binding
DN41939_c1_g1_i2	2.700	3.02E-03	ASK05861.1 chitin-binding protein [Macrobrachium nipponense]	0			F:GO:0042302	F:structural constituent of cuticle
DN41099_c3_g1_i1	2.692	5.09E-04	XP_023323118.1 cuticle protein 7-like [Eurytemora affinis]	0			F:GO:0042302	F:structural constituent of cuticle
DN44562_c3_g3_i1	2.691	3.67E-03	XP_014460030.1 PREDICTED: general transcription factor II-I repeat domain-containing protein 2-like [Alligator mississippiensis] XP_019337941.1 PREDICTED: general transcription factor II-I repeat domain-containing protein 2-like [Alligator mississippiensis] XP_019337943.1 PREDICTED: general transcription factor II-I repeat domain-containing protein 2-like [Alligator mississippiensis]	0			0	0

Table A.1. continued

			XP_019337944.1 PREDICTED: general transcription factor II-I repeat domain-containing protein 2-like [Alligator mississippiensis]							
DN41939_c1_g1_i1	2.689	5.93E-04	ASK05861.1 chitin-binding protein [Macrobrachium nipponense]	0				F:GO:0042302	F:structural constituent of cuticle
DN42192_c2_g1_i1	2.663	6.78E-03	OKL50402.1 hypothetical protein BSZ40_11135 [Actinomyces hordeovulneris]	0				0	0
DN46582_c0_g1_i1	2.650	6.19E-03	BAM99303.1 strongly chitin-binding protein-1 [Procambarus clarkii]	0				F:GO:0042302	F:structural constituent of cuticle
DN39757_c2_g1_i1	2.642	1.36E-03	ABF69938.1 DNA/RNA non-specific endonuclease [Penaeus monodon]	0				F:GO:0003676; F:GO:0016787; F:GO:0046872	F:nucleic acid binding; F:hydrolase activity; F:metal ion binding
DN42248_c6_g1_i2	2.637	7.21E-03	AQT26399.1 chitin-binding protein, partial [Macrobrachium nipponense]	0				F:GO:0042302	F:structural constituent of cuticle

Table A.1. continued

DN42192_c11_g1_i1	2.631	2.71E-03	ADI18109.1 hypothetical protein [uncultured Acidobacteriales bacterium HF0200_23L05]	0			0	0
DN43463_c15_g1_i1	2.589	5.17E-03	ASK05861.1 chitin-binding protein [Macrobrachium nipponense]	0			0	0
DN42430_c4_g1_i1	2.586	7.24E-03	KMS65245.1 hypothetical protein BVRB_037930, partial [Beta vulgaris subsp. vulgaris]	0			0	0
DN41998_c3_g1_i1	2.544	1.05E-02	XP_008469099.1 PREDICTED: forkhead box protein P2-like [Diaphorina citri]	K09409		Protein families: genetic information processing-Transcription factors	0	0
DN43463_c13_g1_i2	2.543	7.17E-03	XP_018022125.1 PREDICTED: cuticle protein 19-like [Hyalella azteca]	0			0	0
DN44079_c3_g1_i1	2.505	6.29E-03	XP_018017721.1 PREDICTED: uncharacterized protein LOC108674296 [Hyalella azteca]	0			F:GO:0005515	F:protein binding
DN34635_c0_g1_i1	2.502	1.05E-02	CEH44546.1 conserved hypothetical protein [Xanthomonas citri pv. citri] CEH53230.1 conserved hypothetical protein	0			0	0

Table A.1. continued

DN44500_c18_g1_i1	2.498	5.91E-03	ASK05861.1 chitin-binding protein [Macrobrachium nipponense]	0			F:GO:0042302	F:structural constituent of cuticle
DN39217_c0_g1_i1	2.496	4.16E-03	KFM64065.1 Glutamate-gated chloride channel, partial [Stegodyphus mimosarum]	0			F:GO:0004888 ; F:GO:0005230 ; C:GO:0016021 ; P:GO:0034220	F:transmembrane signaling receptor activity; F:extracellular ligand-gated ion channel activity; C:integral component of membrane; P:ion transmembrane transport
DN28561_c0_g1_i1	2.490	7.40E-03	ASC55678.1 putative trypsin serine protease, partial [Procambarus clarkii]	0			F:GO:0004252 ; P:GO:0006508	F:serine-type endopeptidase activity; P:proteolysis
DN42430_c6_g2_i1	2.482	8.99E-03	ABM53544.1 conserved hypothetical protein [uncultured beta proteobacterium CBNPD1 BAC clone 578]	0			0	0
DN45561_c0_g1_i1	2.470	6.43E-03	XP_018009280.1 PREDICTED: probable pathogenesis-related protein ARB_02861 [Hyalella azteca]	0			0	0

Table A.1. continued

DN35871_c0_g1_i1	2.470	6.94E-03	EDQ97287.1 hypothetical protein CLOBAR_00774 [Intestinibacter bartlettii DSM 16795] EDQ97485.1 hypothetical protein CLOBAR_00537 [Intestinibacter bartlettii DSM 16795]	0				0	0
DN6694_c0_g1_i1	2.466	8.14E-03	BAM99303.1 strongly chitin-binding protein-1 [Procambarus clarkii]	0				F:GO:0042302	F:structural constituent of cuticle
DN40709_c1_g2_i1	2.460	3.96E-03	ATN38697.1 cuticle-like protein [Macrobrachium nipponense]	0				F:GO:0042302	F:structural constituent of cuticle
DN43511_c6_g4_i1	2.452	7.21E-03	AUM60049.1 cuticle protein AMP13.4 [Litopenaeus vannamei]	0				0	0
DN37162_c4_g1_i1	2.410	1.41E-03	AEK86522.1 Spz1 [Litopenaeus vannamei]	0				0	0
DN41317_c0_g1_i1	2.402	8.00E-03	XP_022244298.1 T-box transcription factor TBX15-like, partial [Limulus polyphemus]	K10176	Environmental Information Processing- Signal transduction- MAPK signaling pathway	Protein families: genetic information processing- Transcription factors	F:GO:0003700; C:GO:0005634; P:GO:0006355	F:DNA-binding transcription factor activity; C:nucleus; P:regulation of transcription, DNA-templated	
DN42867_c3_g1_i1	2.395	3.37E-03	AEK86524.1 Spz3 [Litopenaeus vannamei]	0				0	0

Table A.1. continued

DN41631_c0_g2_i1	2.393	7.88E-03	AAC28351.1 cytochrome P450 [Homarus americanus]	K14999		Protein families: metabolism-Cytochrome P450	F:GO:0005506 ; F:GO:0016705 ; F:GO:0020037 ; P:GO:0055114	F:iron ion binding; F:oxidoreductase activity, acting on paired donors, with incorporation or reduction of molecular oxygen; F:heme binding; P:oxidation-reduction process
DN40709_c1_g1_i1	2.389	2.71E-03	ATN38697.1 cuticle-like protein [Macrobrachium nipponense]	0			F:GO:0042302	F:structural constituent of cuticle
DN40992_c5_g1_i1	2.367	6.88E-03	ACU25383.1 crustin 2 [Panulirus japonicus]	0			0	0
DN43626_c3_g2_i1	2.355	5.69E-03	AHH29324.1 cytokine receptor [Scylla paramamosain]	0			F:GO:0005515	F:protein binding
DN42837_c11_g1_i1	2.330	8.44E-03	ASK05861.1 chitin-binding protein [Macrobrachium nipponense]	0			F:GO:0042302	F:structural constituent of cuticle
DN44031_c7_g1_i3	2.315	4.70E-03	AWK57548.1 vasotocin-neurophysin [Cherax quadricarinatus]	K05242	Environmental Information Processing- Signal transduction-Phospholipase D signaling pathway; Circulatory system-Vascular smooth		0	0

Table A.1. continued

					muscle contraction; Excretory system-Vasopressin-regulated water reabsorption			
DN44508_c8_g1_i1	2.310	1.28E-03	AGG20312.1 peritrophin [Palaemon carinicauda]	0			C:GO:0005576; P:GO:0006030; F:GO:0008061	C:extracellular region; P:chitin metabolic process; F:chitin binding
DN42594_c10_g1_i1	2.273	1.02E-02	P81576.1 RecName: Full=Cuticle protein AM1159; Short=CPAM1159	0			F:GO:0042302	F:structural constituent of cuticle
DN43053_c3_g2_i1	2.262	1.28E-03	XP_018011799.1 PREDICTED: S phase cyclin A-associated protein in the endoplasmic reticulum-like [Hyalella azteca]	0			0	0
DN42132_c14_g3_i1	2.226	5.00E-03	KMQ83546.1 transposase-like protein [Lasius niger]	0			0	0
DN39280_c1_g1_i1	2.217	8.05E-03	XP_019771601.1 PREDICTED: enhancer of split mbeta protein-like [Dendroctonus ponderosae] ENN70558.1 hypothetical protein YQE_12733, partial [Dendroctonus ponderosae] ERL84430.1 hypothetical protein D910_01862	K09090		Protein families: genetic information processing-Transcription factors, Messenger RNA biogenesis	0	0

Table A.1. continued

			[Dendroctonus ponderosae]					
DN44080_c4_g1_i1	2.209	5.53E-04	XP_019870689.1 PREDICTED: uncharacterized protein LOC109599183 [Aethina tumida]	K09443		Protein families: genetic information processing- Transcription factors	F:GO:0003700; C:GO:0005634; P:GO:0006355; F:GO:0043565	F:DNA-binding transcription factor activity; C:nucleus; P:regulation of transcription, DNA-templated; F:sequence-specific DNA binding
DN43247_c10_g1_i1	2.201	6.67E-03	ODN01117.1 Arrestin [Orchesella cincta]	K04439	Environmental Information Processing- Signal transduction- MAPK signaling pathway, Hedgehog signaling pathway; Cellular Processes- Transport and catabolism- Endocytosis; Immune system- Chemokine signaling pathway; Endocrine system- Relaxin signaling pathway, Parathyroid hormone synthesis, secretion and action; Sensory system-	Protein families: genetic information processing- Membrane trafficking	P:GO:0007165	P:signal transduction

					Olfactory transduction			
DN39757_c1_g1_i1	2.188	5.13E-03	CBG22733.1 northern shrimp nuclease [Pandalus borealis]	0			F:GO:0003676; F:GO:0016787; F:GO:0046872	F:nucleic acid binding; F:hydrolase activity; F:metal ion binding
DN41976_c4_g1_i1	2.182	5.13E-03	XP_013172611.1 PREDICTED: uncharacterized protein LOC106121472 [Papilio xuthus]	0			F:GO:0004252; P:GO:0006508	F:serine-type endopeptidase activity; P:proteolysis
DN41289_c0_g1_i1	2.170	6.67E-03	XP_018026139.1 PREDICTED: extensin-like isoform X1 [Hyalella azteca] XP_018026140.1 PREDICTED: extensin-like isoform X2 [Hyalella azteca]	0			F:GO:0042302	F:structural constituent of cuticle
DN40460_c0_g1_i1	2.163	8.66E-03	AIZ03421.1 spatzle [Penaeus monodon]	0			0	0
DN37162_c6_g1_i1	2.131	7.21E-03	AEK86522.1 Spz1 [Litopenaeus vannamei]	0			0	0
DN44517_c5_g1_i1	2.061	9.96E-04	ABI79454.2 alpha 2 macroglobulin [Litopenaeus vannamei]	K03910	Immune system-Complement and coagulation cascades	Protein families: genetic information processing-Membrane trafficking; Protein	C:GO:0005615	C:extracellular space

Table A.1. continued

						families: signaling and cellular processes- Exosome		
DN40686_c1_g1_i1	2.053	6.67E-03	XP_018019513.1 PREDICTED: uncharacterized protein LOC108675968 [Hyalella azteca]	0			0	0
DN41381_c1_g1_i1	2.044	7.17E-03	APO14259.1 juvenile hormone esterase-like carboxylesterase 1 [Eriocheir sinensis]	0			0	0
DN45424_c0_g1_i1	2.041	3.34E-03	XP_018025942.1 PREDICTED: la-related protein 6-like [Hyalella azteca]	K18733		Protein families: genetic information processing- Messenger RNA biogenesis	F:GO:0003723; C:GO:0005634; P:GO:0006396; C:GO:1990904	F:RNA binding; C:nucleus; P:RNA processing; C:ribonucleoprotein complex
DN43765_c7_g1_i1	2.015	5.16E-03	XP_018021695.1 PREDICTED: uncharacterized protein LOC108677901 [Hyalella azteca]	0			0	0
DN41959_c0_g2_i1	2.002	6.78E-03	XP_018011342.1 PREDICTED: ankyrin repeat domain-containing protein 50-like [Hyalella azteca]	K21440		Protein families: genetic information processing- Membrane trafficking	F:GO:0005515	F:protein binding
DN41318_c0_g1_i2	1.994	1.01E-02	XP_003240981.1 PREDICTED: skin	0			F:GO:0042302	F:structural constituent of cuticle

Table A.1. continued

			secretory protein xP2-like [Acyrthosiphon pisum]				
DN40522_c1_g1_i2	1.974	7.71E-03	XP_018011510.1 PREDICTED: regulator of G-protein signaling 2-like [Hyalella azteca]	K16449		Not Included in Pathway or Brite-Unclassified: signaling and cellular processes-Signaling proteins	0	0
DN43212_c11_g1_i1	1.969	7.72E-03	AJO70029.1 cytoglobin 2 isoform Ci1 [Cherax cainii] AJO70030.1 cytoglobin 2 isoform Ci2 [Cherax cainii]	K21894		Protein families: signaling and cellular processes-Transporters	C:GO:0005576; C:GO:0005833; P:GO:0015671; F:GO:0019825; F:GO:0020037	C:extracellular region; C:hemoglobin complex; P:oxygen transport; F:oxygen binding; F:heme binding
DN44662_c10_g1_i1	1.852	6.94E-03	XP_018024465.1 PREDICTED: uncharacterized protein LOC108680202 [Hyalella azteca]	0			0	0
DN43555_c13_g2_i1	1.839	1.12E-03	XP_018419419.1 PREDICTED: hsc70-interacting protein isoform X2 [Nanorana parkeri]	K09560		Protein families: genetic information processing-Chaperones and foldng catalysts, Membran trafficking	F:GO:0046983	F:protein dimerization activity
DN44591_c15_g1_i1	1.822	1.09E-02	EAT46621.1 AAEL002236-PA [Aedes aegypti]	K05038	Nervous system-Synaptic vesicle cycle	Protein families: signaling and cellular processes-Transporters	F:GO:0005328; P:GO:0006836	F:neurotransmitter:sodium symporter activity; P:neurotransmitt

Table A.1. continued

								; C:GO:0016021	er transport; C:integral component of membrane
DN41318_c0_g1_i1	1.821	3.65E-03	XP_025406143.1 cuticle protein 16.5-like [Sipha flava]	0			F:GO:0042302	F:structural constituent of cuticle
DN41717_c1_g1_i1	1.764	4.01E-03	XP_002033137.1 GM21151 [Drosophila sechellia] EDW47150.1 GM21151 [Drosophila sechellia]	K05038	Nervous system-Synaptic vesicle cycle	Protein families: signaling and cellular processes-Transporters	F:GO:0005328 ; P:GO:0006836 ; C:GO:0016021	F:neurotransmitt er:sodium symporter activity; P:neurotransmitt er transport; C:integral component of membrane
DN33886_c2_g1_i1	1.735	8.05E-03	EFX70562.1 hypothetical protein DAPPUDRAFT_61224, partial [Daphnia pulex]	0			F:GO:0042302	F:structural constituent of cuticle
DN43373_c15_g1_i1	1.712	5.63E-03	AUI80373.1 vrille [Euphausia superba]	K12114	Environmental adaptation-Circadian rhythm (fly)	Protein families: genetic information processing-Transcription factors	F:GO:0003700 ; P:GO:0006355	F:DNA-binding transcription factor activity; P:regulation of transcription, DNA-templated
DN42855_c5_g1_i1	1.685	5.04E-03	XP_018016854.1 PREDICTED: mucin-17-like [Hyalella azteca]	K14971		Protein families: genetic information processing-Membrane trafficking, Chromosome and associated proteins	0	0

Table A.1. continued

DN44393_c16_g1_i1	1.648	5.25E-03	XP_023964737.1 tigger transposable element-derived protein 1-like [Chrysemys picta bellii] XP_008170509.2 tigger transposable element-derived protein 1-like [Chrysemys picta bellii]	0			0	0
DN40829_c4_g1_i1	1.589	3.03E-03	XP_018008217.1 PREDICTED: uncharacterized protein LOC108665925 isoform X1 [Hyalella azteca]	K09173		Protein families: genetic information processing-Transcription factors	F:GO:0003677; F:GO:0003700; P:GO:0006355	F:DNA binding; F:DNA-binding transcription factor activity; P:regulation of transcription, DNA-templated
DN43428_c8_g3_i1	1.558	2.23E-03	XP_018018774.1 PREDICTED: uncharacterized protein LOC108675285 [Hyalella azteca]	0			F:GO:0005515	F:protein binding
DN41785_c0_g2_i1	1.464	3.50E-04	XP_018013552.1 PREDICTED: uncharacterized protein LOC108670596 isoform X1 [Hyalella azteca]	K17495		Protein families: metabolism- Protein phosphatases and associated proteins	0	0
DN44664_c5_g1_i1	1.455	3.40E-03	KFD47056.1 hypothetical protein M513_12044 [Trichuris suis]	0			0	0
DN43888_c2_g1_i1	1.444	2.28E-04	XP_018009694.1 PREDICTED: uncharacterized protein LOC108667210 [Hyalella azteca]	K04599		Protein families: signaling and cellular processes-G protein-coupled receptors	F:GO:0004930; P:GO:0007166; P:GO:0007186	F:G protein-coupled receptor activity; P:cell surface receptor signaling pathway; P:G

Table A.1. continued

								; C:GO:0016021	protein-coupled receptor signaling pathway; C:integral component of membrane
DN43953_c6_g1_i1	1.375	3.48E-03	XP_018027293.1 PREDICTED: glucose dehydrogenase [FAD, quinone]-like [Hyalella azteca]	K00108	Amino acid metabolism- Glycine, serine and threonine metabolism			F:GO:0016614 ; F:GO:0050660 ; P:GO:0055114	F:oxidoreductase activity, acting on CH-OH group of donors; F:flavin adenine dinucleotide binding; P:oxidation-reduction process
DN44571_c7_g2_i1	1.324	8.66E-03	XP_023239670.1 uncharacterized protein LOC111638243 [Centruroides sculpturatus]	0				F:GO:0046983	F:protein dimerization activity
DN42181_c6_g1_i1	1.300	6.78E-03	XP_018018604.1 PREDICTED: hemicentin-2-like [Hyalella azteca]	0				F:GO:0005515	F:protein binding
DN43088_c10_g2_i1	1.254	4.09E-05	XP_023237634.1 arylsulfatase I-like [Centruroides sculpturatus]	K01135	Metabolism- Glycan biosynhesis and metabolism- Glycosaminoglycan degradation; Cellular Processes- Transport and			F:GO:0008484	F:sulfuric ester hydrolase activity

Table A.1. continued

						catabolism-Lysosome		
DN40848_c2_g2_i1	1.130	2.71E-03	ATW66457.1 hormone receptor, partial [Marsupenaeus japonicus]	K14033		Protein families: genetic information processing-Transcription factors; Protein families: signaling and cellular processes- Nuclear receptors	F:GO:0003677 ; F:GO:0003707 ; F:GO:0004879 ; C:GO:0005634 ; P:GO:0006355	F:DNA binding; F:steroid hormone receptor activity; F:nuclear receptor activity; C:nucleus; P:regulation of transcription, DNA-templated
DN44503_c5_g1_i1	1.058	6.32E-03	XP_015440178.1 PREDICTED: uncharacterized protein LOC107194969 [Dufourea novaeangliae]	0			F:GO:0005515	F:protein binding
DN43053_c7_g1_i1	0.981	5.00E-03	XP_018019523.1 PREDICTED: uncharacterized protein LOC108675989, partial [Hyalella azteca]	0			0	0
DN41792_c10_g1_i1	0.976	9.65E-03	ELU10999.1 hypothetical protein CAPTEDRAFT_176201 [Capitella teleta]	K01754	Amino acid metabolism-Glycine, serine and threonine metabolism and Valine, leucine and isoleucine biosynthesis		F:GO:0004794 ; P:GO:0006567	F:L-threonine ammonia-lyase activity; P:threonine catabolic process

Table A.1. continued

Transcript ID	Log₂FC	Adjusted p-value	Annotation	KO	KAAS Pathways	BRITE Hierarchies	GO IDs	GO Names
DN41287_c2_g1_i1	0.972	1.83E-03	XP_018022003.1 PREDICTED: uncharacterized protein LOC108678163 [Hyalella azteca]	0			0	0
DN43217_c11_g1_i1	0.875	5.17E-03	XP_018013070.1 PREDICTED: RNA-binding motif protein, X-linked 2-like [Hyalella azteca]	K13107		Protein families: genetic information processing-Spliceosome	F:GO:0003676	F:nucleic acid binding
DN40864_c0_g1_i1	0.867	1.03E-02	XP_018024774.1 PREDICTED: anionic trypsin-1-like [Hyalella azteca]	K01324	Immune system-Complement and coagulation cascades	Protein families: metabolism-Peptidases	F:GO:0004252 ; P:GO:0006508	F:serine-type endopeptidase activity; P:proteolysis
DN42006_c0_g1_i1	0.711	8.66E-03	XP_018023449.1 PREDICTED: uncharacterized protein LOC108679354 isoform X2 [Hyalella azteca]	K22762		Protein families: metabolism-Peptidases; Protein families: genetic information processing-Ubiquitin system	0	0
DN42659_c3_g2_i1	0.676	6.94E-03	XP_008476053.1 PREDICTED: transcription cofactor vestigial-like protein 4 [Diaphorina citri]	0			P:GO:0006355	P:regulation of transcription, DNA-templated

16°C vs. 18°C: under-expressed, DESeq2

Transcript ID	Log₂FC	Adjusted p-value	Annotation	KO	KAAS Pathways	BRITE Hierarchies	GO IDs	GO Names
DN20024_c0_g1_i1	-3.622	4.01E-05	EJY80286.1 VSP domain containing protein	0			0	0

			(macronuclear) [Oxytricha trifallax]				
DN39057_c0_g1_i1	-3.289	4.08E-04	CCW72337.1 unnamed protein product [Phytomonas sp. isolate Hart1]	0		0	0
DN40801_c5_g1_i1	-2.956	2.16E-03	KZP03403.1 hypothetical protein FIBSPDRAFT_768999, partial [Fibularhizoctonia sp. CBS 109695]	0		0	0
DN49660_c0_g3_i1	-2.944	5.03E-04	XP_006800759.1 PREDICTED: enoyl-CoA hydratase, mitochondrial-like [Neolamprologus brichardi]	K07511	Carbohydrate metabolism-Propanoate metabolism, Butanoate metabolism; Lipid metabolism- Fatty acid elongation, Fatty acid degradation; Amino acid metabolism-Valine, leucine and isoleucine degradation, Lysine degradation, Tryptophan metabolism; Metabolism of othe amino acids- beta-Alanine metabolism; Xenobiotics biodegradation and metabolism-Aminobenzoate	F:GO:0003824	F:catalytic activity

					degradation, Caprolactam degradation			
DN43737_c13_g14_i1	-2.936	9.88E-10	XP_015439268.1 PREDICTED: aconitate hydratase, mitochondrial-like [Dufourea novaeangliae]	K01681	Carbohydrate metabolism- Citrate cycle (TCA cycle), Glyoxylate and dicarboxylate metabolism; Energy metabolism- Carbon fixation pathways in prokaryotes		F:GO:0003994; P:GO:0006099; F:GO:0051539	F:aconitate hydratase activity; P:tricarboxylic acid cycle; F:4 iron, 4 sulfur cluster binding
DN37165_c1_g1_i1	-2.844	3.40E-03	XP_008297965.1 PREDICTED: tenascin-like [Stegastes partitus]	0			0	0
DN38763_c0_g1_i1	-2.699	1.25E-03	AWK77863.1 nonstructural polyprotein [Renmark bee virus 3]	0			0	0
DN28403_c0_g1_i1	-2.678	6.65E-03	CDW85334.1 UNKNOWN [Stylonychia lemnae]	0			0	0
DN46648_c0_g1_i1	-2.606	7.09E-03	XP_004024028.1 hypothetical protein IMG5_201690 [Ichthyophthirius multifiliis] EGR27144.1 hypothetical protein IMG5_201690	K11252		Protein families: genetic information processing-Chromosome and associated proteins; Protein families: signaling and	0	0

Table A.1. continued

			[Ichthyophthirius multifiliis]			cellular processes-Exosome		
DN45017_c0_g1_i1	-2.579	9.17E-03	XP_004032518.1 ubiquitin family protein, putative [Ichthyophthirius multifiliis] EGR30931.1 ubiquitin family protein, putative [Ichthyophthirius multifiliis]	K08770	Endocrine system-PPAR signaling pathway	Protein families: genetic information processing-Ubiquitin system	0	0
DN41202_c4_g1_i1	-2.519	1.28E-08	XP_018015969.1 PREDICTED: UNC93-like protein MFSD11 isoform X2 [Hyalella azteca]	0			0	0
DN42550_c5_g1_i1	-2.498	4.37E-04	PIK53963.1 hypothetical protein BSL78_09185 [Apostichopus japonicus]	K10873	Genetic Information Processing-Replication and repair- Homolgous recombination	Protein families: genetic information processing- DNA repair and recombination protein	P:GO:0000730; C:GO:0005634; P:GO:0045002	P:DNA recombinase assembly; C:nucleus; P:double-strand break repair via single-strand annealing
DN41202_c4_g2_i1	-2.437	1.07E-03	XP_018015969.1 PREDICTED: UNC93-like protein MFSD11 isoform X2 [Hyalella azteca]	0			0	0

Table A.1. continued

| DN49675_c0_g1_i1 | -2.410 | 1.46E-02 | XP_001448381.1 hypothetical protein [Paramecium tetraurelia strain d4-2] CAI38942.1 centrin-related-protein,putative [Paramecium tetraurelia] CAK80984.1 unnamed protein product [Paramecium tetraurelia] | K02183 | Environmental Information Processing- Signal transduction- RAS, Rap1, MAPK (plant), Apelin, Calcium, Phosphotidylinositol, cAMP, and cGMP-PKG signaling pathways; Cell cycle- Oocyte meiosis, Cellular senescence; Immune system- C-type lectin receptor signaling pathway; Endocrine system- LOTS OF SIGNALING including Melanogenesis; Circulatory system, Digestive system | Protein families: metabolism- Protein phosphatases and associated proteins; Protein families: genetic information processing- Membrane trafficking, Chromosome and associated proteins | F:GO:0005509 | F:calcium ion binding |
| DN38312_c2_g1_i1 | -2.335 | 2.25E-02 | BAK03331.1 predicted protein [Hordeum vulgare subsp. vulgare] | K04079 | Genetic Information Processing- Folding, sorting and degradation- Protein processing in endoplasmic reticulum; Signal transduction- P13K-Akt signaling pathway; Cell growth and death-Necroptosis; Immune system-Nod-like receptor | Protein families: metabolism- Protein phosphatases and associated proteins; Protein families: genetic information processing-Chaperones and folding catalysts, membrane trafficking, Proteasome, Mitochondrial biogenesis; Protein | F:GO:0005524 ; P:GO:0006457 ; F:GO:0051082 | F:ATP binding; P:protein folding; F:unfolded protein binding |

Table A.1. continued

					signaling pathway, Antigen processing and presentation, Th17 cell differentiation, IL-17 signaling pathway; Endocrine system	families: signaling and cellular processes- Exosome		
DN38763_c4_g1_i1	-2.295	2.41E-02	YP_009333533.1 hypothetical protein 1 [Beihai picorna-like virus 46] APG78911.1 hypothetical protein 1 [Beihai picorna-like virus 46]	0			0	0
DN44136_c16_g4_i1	-2.292	3.92E-03	YP_004563983.1 NADH dehydrogenase subunit 2 (mitochondrion) [Homarus americanus] ADP08205.1 NADH dehydrogenase subunit 2 (mitochondrion) [Homarus americanus]	K03879	Energy metabolism- Oxidative phosphorylation; Nervous system- Retrograde endocannabinoid signaling; Environmental adaptation- Thermogenesis	Protein families: genetic information processing- Mitochondrial biogenesis	0	0
DN35037_c2_g1_i1	-2.289	2.41E-02	XP_001012263.1 heat shock 70 kDa protein [Tetrahymena thermophila SB210] EAR92018.1 heat shock 70 kDa protein [Tetrahymena thermophila SB210]	K03283	Genetic Information Processing- Transcription- Spliceosome; Folding, sorting and degradation- Protein processing in endoplasmic reticulum; Signal transduction- MAPK signaling	Protein families: metabolism- Protein phosphatases and associated proteins, Spliceosome; Protein families: genetic information processing- Ribosome biogenesis, Chaperones and	0	0

Table A.1. continued

					pathway; Cellular Processes-Transport and catabolism-Endocytosis; Immune system-Antigen processing and presentation; Endocrine system; Aging- Longevity regulating pathway	folding catalysts, Membrane trafficking, Proteasome		
DN17549_c0_g1_i1	-2.277	2.15E-02	XP_018258600.1 hypothetical protein FOXG_22863 [Fusarium oxysporum f. sp. lycopersici 4287] KNB20555.1 hypothetical protein FOXG_22863 [Fusarium oxysporum f. sp. lycopersici 4287]	0			0	0
DN32452_c0_g1_i1	-2.253	2.91E-02	XP_001433506.1 hypothetical protein [Paramecium tetraurelia strain d4-2] CAK66109.1 unnamed protein product [Paramecium tetraurelia]	K07375	Cellular Processes-Transport and catabolism-Phagosome; Cellular community- Gap junction	Protein families: genetic information processing-Chromosome and associated proteins; Protein families: signaling and cellular processes-Cytoskeleton proteins, Exosome	0	0
DN44661_c12_g3_i1	-2.248	2.22E-02	XP_014606326.1 PREDICTED: uncharacterized protein LOC106787992 [Polistes canadensis] XP_014606327.1	0			0	0

Table A.1. continued

			PREDICTED: uncharacterized protein LOC106787992 [Polistes canadensis]					
DN38312_c1_g1_i1	-2.229	2.58E-02	BAK03331.1 predicted protein [Hordeum vulgare subsp. vulgare]	K04079	Genetic Information Processing- Folding, sorting and degradation- Protein processing in endoplasmic reticulum; Signal transduction- P13K-Akt signaling pathway; Cell growth and death- Necroptosis; Immune system- Nod-like receptor signaling pathwya, Antigen processing and presentation, Th17 cell differentiation, IL-17 signaling pathway; Endocrine system	Protein families: metabolism- Protein phosphatases and associated proteins; Protein families: genetic information processing- Chaperones and folding catalysts, membrane trafficking, Proteasome, Mitochondrial biogenesis; Protein families: signaling and cellular processes- Exosome	F:GO:0005524 ; P:GO:0006457 ; F:GO:0051082	F:ATP binding; P:protein folding; F:unfolded protein binding
DN48906_c0_g1_i1	-2.212	3.10E-02	XP_001454290.1 hypothetical protein [Paramecium tetraurelia strain d4-2] CAK86893.1 unnamed protein product [Paramecium tetraurelia]	K03263		Protein families: genetic information processing- Translation factors	F:GO:0003746 ; P:GO:0006452 ; F:GO:0043022 ; P:GO:0045901 ; P:GO:0045905	F:translation elongation factor activity; P:translational frameshifting; F:ribosome binding; P:positive regulation of translational elongation;

								P:positive regulation of translational termination
DN44614_c6_g1_i3	-2.140	7.57E-04	XP_015437916.1 PREDICTED: myosin heavy chain, muscle isoform X4 [Dufourea novaeangliae]	K17751	Circulatory system- Cardiac muscle contraction, Adrenergic signaling in cardiomyocytes		F:GO:0003774 ; F:GO:0005515 ; F:GO:0005524 ; C:GO:0016459	F:motor activity; F:protein binding; F:ATP binding; C:myosin complex
DN38312_c0_g1_i1	-2.095	4.57E-02	BAK03331.1 predicted protein [Hordeum vulgare subsp. vulgare]	K04079	Genetic Information Processing- Folding, sorting and degradation- Protein processing in endoplasmic reticulum; Signal transduction- P13K-Akt signaling pathway; Cell growth and death- Necroptosis; Immune system- Nod-like receptor signaling pathwya, Antigen processing and presentation, Th17 cell differentiation, IL-17 signaling pathway; Endocrine system	Protein families: metabolism- Protein phosphatases and associated proteins; Protein families: genetic information processing- Chaperones and folding catalysts, membrane trafficking, Proteasome, Mitochondrial biogenesis; Protein families: signaling and cellular processes- Exosome	F:GO:0005524 ; P:GO:0006457 ; F:GO:0051082	F:ATP binding; P:protein folding; F:unfolded protein binding

Table A.1. continued

DN39983_c2_g2_i1	-2.085	4.58E-02	WP_094890006.1 hypothetical protein, partial [Enterococcus faecium] OZS35839.1 hypothetical protein CG820_14625, partial [Enterococcus faecium]	0			0	0
DN44614_c6_g1_i2	-2.076	5.58E-04	XP_015437916.1 PREDICTED: myosin heavy chain, muscle isoform X4 [Dufourea novaeangliae]	K17751	Circulatory system-Cardiac muscle contraction, Adrenergic signaling in cardiomyocytes	Protein families: signaling and cellular processes-Cytroskeleton proteins	F:GO:0003774; F:GO:0005515; F:GO:0005524; C:GO:0016459	F:motor activity; F:protein binding; F:ATP binding; C:myosin complex
DN48617_c0_g1_i1	-2.066	4.34E-02	XP_001032881.1 hypothetical protein TTHERM_00486690 [Tetrahymena thermophila SB210] EAR85218.1 hypothetical protein TTHERM_00486690 (macronuclear) [Tetrahymena thermophila SB210]	0			0	0
DN33448_c0_g2_i1	-2.006	5.40E-02	BAK00005.1 predicted protein [Hordeum vulgare subsp. vulgare]	K11254		Protein families: genetic information processing-Chromosome and associated proteins	F:GO:0003677; F:GO:0046982	F:DNA binding; F:protein heterodimerization activity
DN30474_c0_g2_i2	-1.934	4.46E-03	AEC22817.1 hypothetical protein [Macrobrachium nipponense]	0			0	0

Table A.1. continued

DN43428_c5_g3_i1	-1.795	1.27E-02	XP_968467.1 PREDICTED: hexosaminidase D isoform X1 [Tribolium castaneum]	K14459	Glycan biosynthesis and metabolism- Various types of N-glycan biosynthesis, Other glycan degradation		P:GO:0005975; F:GO:0015929	P:carbohydrate metabolic process; F:hexosaminidase activity
DN1641_c0_g4_i1	-1.676	5.30E-02	AFS60116.1 selenoprotein M [Penaeus monodon]	0			0	0
DN42293_c6_g3_i1	-1.547	3.49E-02	XP_022777700.1 uncharacterized protein LOC111319140 [Stylophora pistillata]	0			F:GO:0005525	F:GTP binding
DN42033_c3_g1_i1	-1.459	1.73E-02	XP_015430000.1 PREDICTED: LOW QUALITY PROTEIN: disco-interacting protein 2 homolog A [Dufourea novaeangliae]	0			F:GO:0003824	F:catalytic activity
DN15357_c0_g1_i1	-1.381	3.60E-02	XP_022518617.1 zinc finger protein 239-like [Astyanax mexicanus]	K20796	Amino acid metabolism- Lysine degradation	Protein families: genetic information processing- Chromosome and associated proteins	F:GO:0003676	F:nucleic acid binding
DN33800_c0_g1_i1	-1.340	1.37E-02	AQW41379.1 selenium independent glutathione peroxidase [Penaeus monodon]	K00432	Lipid metabolism- Arachidonic acid metabolism; Metabolism of other amino acids- Glutathione metabolim; Endocrine system- Thyroid hormone synthesis		F:GO:0004602; P:GO:0006979; P:GO:0055114	F:glutathione peroxidase activity; P:response to oxidative stress; P:oxidation-reduction process

182

Table A.1. continued

DN36962_c0_g1_i1	-1.306	2.13E-02	XP_018018823.1 PREDICTED: uncharacterized protein LOC108675333 [Hyalella azteca]	0			0	0
DN42293_c5_g1_i1	-1.302	1.44E-02	XP_015282271.1 PREDICTED: uncharacterized protein LOC107123533 [Gekko japonicus]	0			F:GO:0005525	F:GTP binding
DN42293_c6_g1_i1	-1.267	4.84E-02	XP_022109304.1 uncharacterized protein LOC110989312 [Acanthaster planci]	0			0	0
DN43017_c5_g1_i1	-1.254		XP_015433474.1 PREDICTED: indole-3-acetaldehyde oxidase-like [Dufourea novaeangliae]	K00106	Nucleotide metabolism- Purine metabolism; Biosynthesis of other secondary metabolites- Caffeine metab; Xenobiotics biodegradation and metabolism- Drug metabolism- other enzymes; Cellular Processes-Peroxisome	Protein families: signaling and cellular processes-Exosome	F:GO:0005506; F:GO:0009055; F:GO:0051536; P:GO:0055114; F:GO:0071949	F:iron ion binding; F:electron transfer activity; F:iron-sulfur cluster binding; P:oxidation-reduction process; F:FAD binding
DN42183_c0_g2_i1	-1.169	2.04E-02	XP_002189391.2 PREDICTED: oxysterol-binding protein-related protein 11 [Taeniopygia guttata]	K20465		Protein families: genetic information processing-Membrane trafficking	0	0

Table A.1. continued

DN42089_c11_g2_i1	-1.168	4.77E-02	XP_018017640.1 PREDICTED: histone-lysine N-methyltransferase 2D-like [Hyalella azteca]	K06061	Environmental Information Processing- Signal transduction- Notch signaling pathway; Immune system- Th1 and Th2 cell differentiation		F:GO:0003713; P:GO:0007219; C:GO:0016607; P:GO:0045944	F:transcription coactivator activity; P:Notch signaling pathway; C:nuclear speck; P:positive regulation of transcription by RNA polymerase II
DN43640_c10_g1_i1	-1.119	6.27E-04	XP_015435958.1 PREDICTED: aldehyde dehydrogenase, mitochondrial [Dufourea novaeangliae]	K00128	Carbohydrate metabolism- Glycolysis/Gluconeogenesis, Ascorbate and aldrate metabolism, Pyruvate metabolism; Lipid metabolism- Fatty acid degradation, Glycerolipid metabolism, Sphingolipid metabolism; Amino acid metabolism- all categories within; Metabolism of other amino acids- beta-Alanine metabolism; Metabolism of terpenoids and polyketides- Insect hormone biosynthesis, Limonen and pinene		F:GO:0016620; P:GO:0055114	F:oxidoreductase activity, acting on the aldehyde or oxo group of donors, NAD or NADP as acceptor; P:oxidation-reduction process

					degradation; Xenobiotics biodegradation and metabolism- chloroalkane and chloroalkene degradation			
DN43557_c0_g1_i1	-1.111	3.46E-02	XP_018307258.1 PREDICTED: uncharacterized protein LOC108725004 [Trachymyrmex zeteki]	K00657	Amino acid metabolism- Arginine and proline metabolism; Cell growth and death- Ferroptosis		0	0
DN43379_c7_g1_i1	-1.098	4.15E-02	XP_018027669.1 PREDICTED: uncharacterized protein LOC108682923 [Hyalella azteca]	0			0	0
DN40754_c0_g1_i1	-1.085	5.01E-02	XP_015413423.1 PREDICTED: DNA mismatch repair protein Msh2 [Myotis davidii]	K08735	Genetic Information Processing- Replication and repair- Mismatch repair	Protein families: genetic information processing- DNA repair and recombination protein	F:GO:0005524; P:GO:0006298; F:GO:0030983; C:GO:0032300	F:ATP binding; P:mismatch repair; F:mismatched DNA binding; C:mismatch repair complex
DN39759_c0_g1_i1	-1.043	1.26E-02	XP_013387891.1 ankyrin repeat domain-containing protein 10 isoform X3 [Lingula anatina]	0			F:GO:0005515	F:protein binding

Table A.1. continued

DN44650_c4_g1_i1	-1.031	3.55E-02	XP_014349861.1 PREDICTED: uncharacterized protein LOC102358259 [Latimeria chalumnae]	0			0	0
DN41283_c3_g1_i1	-1.011	4.64E-02	XP_023717986.1 rab-like protein 2A [Cryptotermes secundus]	K07931		Protein families: signaling and cellular processes- Exosome	F:GO:0003924; F:GO:0005525	F:GTPase activity; F:GTP binding
DN42722_c18_g1_i1	-1.006	3.26E-02	EFX84425.1 hypothetical protein DAPPUDRAFT_230610 [Daphnia pulex]	0			0	0
DN43235_c9_g1_i1	-1.005	5.00E-03	AAH06165.3 Minichromosome maintenance complex component 2 [Homo sapiens]	MCM2; DNA replication licensing factor MCM2 [EC:3.6.4.12]	Genetic Information Processing- Replication and repair- DNA replication; Cell growth and death- Cell cycle, Cell cycle (yeast), Meiosis (yeast)	Protein families: genetic information processing- DNA replication proteins, Chromosome and associated proteins	F:GO:0003677; F:GO:0005524; C:GO:0005634; P:GO:0006270; C:GO:0042555; P:GO:1905775	F:DNA binding; F:ATP binding; C:nucleus; P:DNA replication initiation; C:MCM complex; P:negative regulation of DNA helicase activity
DN41520_c3_g1_i1	-1.000	2.49E-02	XP_018010881.1 PREDICTED: cyclin-Y-like [Hyalella azteca]	0			P:GO:0000079; F:GO:0019901	P:regulation of cyclin-dependent protein serine/threonine kinase activity; F:protein kinase binding

Table A.1. continued

DN43671_c15_g1_i1	-0.987	4.59E-02	AOE48155.1 hypothetical protein [Eumigus monticolus]	0				0	0
DN42238_c2_g1_i1	-0.964	5.30E-02	PSN50271.1 Transmembrane protein 161B [Blattella germanica]	0				0	0
DN41186_c0_g1_i1	-0.963	1.25E-02	ABI79454.2 alpha 2 macroglobulin [Litopenaeus vannamei]	K03910	Immune system-Complement and coagulation cascades	Protein families: genetic information processing-Membrane trafficking; Protein families: signaling and cellular processes- Exosome	F:GO:0004866; C:GO:0005615	F:endopeptidase inhibitor activity; C:extracellular space
DN44135_c11_g1_i1	-0.956	5.34E-02	XP_015375566.1 PREDICTED: 1,4-alpha-glucan-branching enzyme [Diuraphis noxia]	K00700	Carbohydrate metabolism- Starch and sucrose metabolism	Protein families: signaling and cellular processes-Exosome	F:GO:0003844; F:GO:0004553; P:GO:0005978; F:GO:0043169	F:1,4-alpha-glucan branching enzyme activity; F:hydrolase activity, hydrolyzing O-glycosyl compounds; P:glycogen biosynthetic process; F:cation binding
DN43557_c0_g2_i1	-0.943	4.15E-02	XP_023716377.1 N-acetyltransferase 9-like protein isoform X2 [Cryptotermes secundus] PNF24691.1 N-acetyltransferase 9-like	0			F:GO:0016747	F:transferase activity, transferring acyl groups other than amino-acyl groups

Table A.1. continued

			protein [Cryptotermes secundus]					
DN43912_c16_g1_i1	-0.935	5.04E-03	XP_025115894.1 LOW QUALITY PROTEIN: NAD-dependent protein deacylase sirtuin-5, mitochondrial-like [Pomacea canaliculata]	K11415		Protein families: genetic information processing- Chromosome and associated proteins	F:GO:0036054; F:GO:0036055; F:GO:0070403	F:protein-malonyllysine demalonylase activity; F:protein-succinyllysine desuccinylase activity; F:NAD+ binding
DN43713_c8_g1_i1	-0.918	6.94E-03	XP_025423397.1 bifunctional methylenetetrahydrofolate dehydrogenase/cyclohydrolase, mitochondrial [Sipha flava]	K13403	Metabolism of cofactors and vitamins- One carbon pool by folate		F:GO:0004488; P:GO:0055114	F:methylenetetrahydrofolate dehydrogenase (NADP+) activity; P:oxidation-reduction process
DN44303_c10_g1_i1	-0.914	3.93E-02	XP_018007934.1 PREDICTED: uncharacterized protein LOC108665670 [Hyalella azteca]	K00586		Protein families: genetic information processing- Translation factors	F:GO:0004164; P:GO:0017183	F:diphthine synthase activity; P:peptidyl-diphthamide biosynthetic process from peptidyl-histidine
DN44611_c14_g1_i1	-0.913	3.67E-03	ATP62320.1 L-type lectin [Litopenaeus vannamei]	K10082	Genetic Information Processing- Folding, sorting and degradation- Protein	Protein families: genetic information processing- Membrane	C:GO:0016020	C:membrane

188

Table A.1. continued

					processing in endoplasmic reticulum	trafficking; Protein families: signaling and cellualr processes- Lectins		
DN43905_c16_g1_i1	-0.907	7.74E-03	PZC85548.1 hypothetical protein B5X24_HaOG216656 [Helicoverpa armigera]	0			C:GO:0016021	C:integral component of membrane
DN44010_c7_g1_i1	-0.901	3.01E-02	XP_015435418.1 PREDICTED: LOW QUALITY PROTEIN: uncharacterized protein LOC107191011 [Dufourea novaeangliae]	K02649	Environmental Information Processing- Signal transduction- RAS, Rap1, ErbB, VEGF, Jak-STAT, TNF, HIF-1, FoxO, Phosphotidylinositol, Phospholipase D, Sphingolipid, cAMP, PI3K-Akt, AMPL, and mTOR signaling pathways; Cell growth and death- Apoptosis, Cellular senescence; Immune system- Platelet activation, Toll-like receptor signaling, C-type lectin receptor signaling, Natural killer mediated cytotoxicity, T cell receptor signaling, B cell	Protein families: genetic information processing- Membrane trafficking	F:GO:0005515 ; C:GO:0005942 ; F:GO:0035014 ; P:GO:0035556	F:protein binding; C:phosphatidyli nositol 3-kinase complex; F:phosphatidylin ositol 3-kinase regulator activity; P:intracellular signal transduction

189

Table A.1. continued

DN42366_c5_g1_i1	-0.890	8.05E-03	XP_018014164.1 PREDICTED: bestrophin-3-like [Hyalella azteca]	K22204		Protein families: signaling and cellular processes-Transporters	0	0
DN42829_c8_g1_i1	-0.872	3.67E-02	XP_015432876.1 PREDICTED: importin-7 [Dufourea novaeangliae]	K20223	Signal transduction-MAPK signaling pathway (fly)	Protein families: genetic information processing-Ribosome biogenesis	P:GO:0006886 ; F:GO:0008536	P:intracellular protein transport; F:Ran GTPase binding
DN44546_c7_g1_i1	-0.869	4.42E-02	XP_013419657.1 beta-1,4-mannosyl-glycoprotein 4-beta-N-acetylglucosaminyltransferase isoform X5 [Lingula anatina]	K00737	Glycan biosynhesis and metabolism- N-Glycan biosynthesis	Protein families: metabolism-Glycosyltransferases	F:GO:0003830 ; P:GO:0006487 ; C:GO:0016020	F:beta-1,4-mannosylglycoprotein 4-beta-N-acetylglucosaminyltransferase activity; P:protein N-linked glycosylation; C:membrane
DN1715_c0_g1_i1	-0.861	1.02E-02	ABG82044.1 ALG-2 interacting protein x [Penaeus monodon]	K12200	Cellular Processes-Transport and catabolism-Endocytosis	Protein families: genetic information processing-Membrane trafficking; Protein families: signaling and cellualr processes- Exosome	F:GO:0005515	F:protein binding
DN44089_c13_g1_i1	-0.841	1.85E-02	PSN46105.1 hypothetical protein C0J52_02270 [Blattella germanica]	0			F:GO:0005515 ; P:GO:0030433	F:protein binding; P:ubiquitin-dependent ERAD pathway

Table A.1. continued

DN44572_c9_g1_i1	-0.840	5.22E-02	XP_014282719.1 sestrin homolog isoform X5 [Halyomorpha halys]	K10141	Cell growth and death- p53 signaling pathway; Aging-Longevity regulating pathway		C:GO:0005634; P:GO:1901031	C:nucleus; P:regulation of response to reactive oxygen species
DN43411_c19_g1_i1	-0.836	1.86E-02	XP_023705243.1 RNA pseudouridylate synthase domain-containing protein 1-like isoform X1 [Cryptotermes secundus] XP_023705244.1 RNA pseudouridylate synthase domain-containing protein 1-like isoform X1 [Cryptotermes secundus] XP_023705246.1 RNA pseudouridylate synthase domain-containing protein 1-like isoform X1 [Cryptotermes secundus] PNF36000.1 hypothetical protein B7P43_G00576 [Cryptotermes secundus]	0			P:GO:0001522; F:GO:0003723; F:GO:0009982	P:pseudouridine synthesis; F:RNA binding; F:pseudouridine synthase activity
DN39939_c1_g2_i1	-0.828	2.94E-02	XP_015334841.1 PREDICTED: exportin-2 [Marmota marmota marmota]	K18423		Protein families: genetic information processing-Chromosome and associated proteins	P:GO:0006886; F:GO:0008536	P:intracellular protein transport; F:Ran GTPase binding
DN42844_c1_g3_i1	-0.821	3.52E-02	XP_018009539.1 PREDICTED: uncharacterized protein LOC108667068 [Hyalella azteca]	0			0	0

Table A.1. continued

DN43736_c0_g2_i1	-0.796	3.36E-02	AAW22143.1 SERCA [Panulirus argus] CAH10336.1 SERCA Ca(2+)-ATPase pump [Panulirus argus]	K05853	Signal transduction-Calcium signaling pathway; cGMP-PKG signaling pathway; Digestive system- Pancreatic secretion		F:GO:0005388 ; F:GO:0005524 ; C:GO:0016021 ; C:GO:0033017 ; P:GO:0070588	F:calcium-transporting ATPase activity; F:ATP binding; C:integral component of membrane; C:sarcoplasmic reticulum membrane; P:calcium ion transmembrane transport
DN43609_c11_g2_i2	-0.794	3.04E-02	XP_018024815.1 PREDICTED: uridine 5'-monophosphate synthase-like [Hyalella azteca]	K13421	Nucleotide metabolism-Pyrimidine metabolism; Xenobiotics biodegradation-Drug metabolism-other enzymes		F:GO:0004588 ; F:GO:0004590 ; P:GO:0006207 ; P:GO:0009116 ; P:GO:0044205	F:orotate phosphoribosyltransferase activity; F:orotidine-5'-phosphate decarboxylase activity; P:'de novo' pyrimidine nucleobase biosynthetic process; P:nucleoside metabolic process; P:'de novo' UMP biosynthetic process
DN44503_c3_g1_i1	-0.791	1.50E-02	KZS19314.1 Peroxisomal N-acetyl-spermine/spermidine oxidase [Daphnia magna]	0			F:GO:0016491 ; P:GO:0055114	F:oxidoreductase activity; P:oxidation-

Table A.1. continued

									reduction process
DN42525_c5_g1_i1	-0.783	2.55E-02	XP_015352751.1 PREDICTED: importin-11 isoform X1 [Marmota marmota marmota] XP_015352752.1 PREDICTED: importin-11 isoform X1 [Marmota marmota marmota]	0				P:GO:0006886; F:GO:0008536	P:intracellular protein transport; F:Ran GTPase binding
DN42667_c0_g1_i1	-0.744	4.09E-02	XP_019616894.1 PREDICTED: GPI ethanolamine phosphate transferase 3-like [Branchiostoma belcheri]	K05288	Glycan biosynhesis and metabolism-Glycosylphosphatidylinositol (GPI) anchor biosynthesis			P:GO:0006506; F:GO:0051377	P:GPI anchor biosynthetic process; F:mannose-ethanolamine phosphotransferase activity
DN43506_c9_g1_i1	-0.737	1.21E-02	EFX86991.1 hypothetical protein DAPPUDRAFT_97204 [Daphnia pulex]	K14548	Genetic Information Processing-Translation-Ribosome biogenesis in eukaryotes	Protein families: genetic information processing-Ribosome biogenesis		F:GO:0005515	F:protein binding
DN42572_c11_g1_i1	-0.733	4.50E-02	XP_021934314.1 histone-lysine N-methyltransferase SMYD3 [Zootermopsis nevadensis] KDR23505.1 SET and MYND domain-containing protein 3 [Zootermopsis nevadensis]	K11426		Protein families: genetic information processing-Chromosome and associated proteins		F:GO:0005515	F:protein binding

Table A.1. continued

DN43282_c8_g2_i1	-0.692	4.84E-02	ACD13595.1 mitotic checkpoint protein [Penaeus monodon]	K02180	Cell growth and death- Cell cycle, Cell cycle (yeast)	Protein families: genetic information processing- Spliceosome; Chromosome and associated proteins	F:GO:0005515	F:protein binding
DN40629_c0_g1_i1	-0.688	6.94E-03	XP_018025798.1 PREDICTED: serine palmitoyltransferase 1-like [Hyalella azteca]	K00654	Lipid metabolism- Sphingolipid metabolism; Environmental Information Processing- Signal transduction- Sphingolipid signaling pathway; Cellular Processes- Transport and catabolism- Autophagy (yeast)	Protein families: metabolism- Amino acid related enzymes	F:GO:0003824; P:GO:0009058; F:GO:0030170	F:catalytic activity; P:biosynthetic process; F:pyridoxal phosphate binding
DN39729_c0_g1_i1	-0.686	4.16E-02	XP_019621706.1 PREDICTED: LOW QUALITY PROTEIN: iduronate 2-sulfatase-like [Branchiostoma belcheri]	K01136	Glycan biosynhesis and metabolism- Glycosyaminoglycan degradation; Cellular Processes- Lysosome		F:GO:0004423	F:iduronate-2-sulfatase activity
DN43172_c9_g1_i1	-0.685	2.90E-02	ATU31747.1 Calcium-activated chloride channel regulator 2, partial [Procambarus clarkii]	0			0	0
DN43319_c2_g2_i1	-0.680	2.23E-02	XP_003397184.1 calcium/calmodulin-dependent protein kinase type 1 isoform X2 [Bombus terrestris] XP_003488206.1	K08794	Signal transduction- Calcium signaling pathway; Endocrine system- Oxytocin signaling pathway, Aldosterone	Protein families: metabolism- Protein kinases	F:GO:0005515	F:protein binding

Table A.1. continued

			calcium/calmodulin-dependent protein kinase type 1 isoform X2 [Bombus impatiens]		synthesis and secretion			
DN43509_c9_g1_i1	-0.678	1.85E-02	XP_018026731.1 PREDICTED: X-ray repair cross-complementing protein 5-like [Hyalella azteca]	K10885	Genetic Information Processing-Replication and repair- Non-homolgous end-joining	Protein families: genetic information processing- DNA repair and recombination protein	P:GO:0000723 ; F:GO:0003684 ; F:GO:0004003 ; P:GO:0006303 ; P:GO:0006310 ; F:GO:0042162 ; C:GO:0043564	P:telomere maintenance; F:damaged DNA binding; F:ATP-dependent DNA helicase activity; P:double-strand break repair via nonhomologous end joining; P:DNA recombination; F:telomeric DNA binding; C:Ku70:Ku80 complex
DN42664_c6_g1_i1	-0.676	2.24E-02	XP_018013390.1 PREDICTED: RNA polymerase II-associated protein 1-like [Hyalella azteca]	K20826		Protein families: genetic information processing-Transcription machinery	P:GO:0006366	P:transcription by RNA polymerase II
DN43340_c9_g1_i1	-0.669	4.63E-02	XP_015604384.1 ADP-ribosylation factor-binding protein GGA1 isoform X2 [Cephus cinctus]	K12404	Cellular Processes-Lysosome	Protein families: genetic information processing-Membrane trafficking	C:GO:0005622 ; P:GO:0006886 ; P:GO:0016192	C:intracellular; P:intracellular protein transport; P:vesicle-mediated transport

Table A.1. continued

DN43843_c13_g1_i1	-0.659	4.61E-02	XP_015354902.1 PREDICTED: myotubularin-related protein 9 [Marmota marmota marmota]	K18084		Protein families: metabolism- Protein phosphatases and associated proteins	0	0
DN41791_c0_g1_i1	-0.659	3.90E-02	XP_023333559.1 SET and MYND domain-containing protein 4-like [Eurytemora affinis]	0			F:GO:0005515	F:protein binding
DN42705_c11_g1_i1	-0.611	2.32E-02	XP_003699563.1 PREDICTED: transcription initiation factor IIA subunit 2 [Megachile rotundata]	K03123	Genetic Information Processing-Transcription- Basal transcription factors	Protein families: genetic information processing-Transcription machinery	C:GO:0005672 ; P:GO:0006367	C:transcription factor TFIIA complex; P:transcription initiation from RNA polymerase II promoter
DN43142_c9_g1_i1	-0.584	1.56E-02	XP_022249137.1 sphingomyelin phosphodiesterase 4-like isoform X2 [Limulus polyphemus]	K12353	Lipid metabolism-Sphingolipid metabolism		F:GO:0050290	F:sphingomyelin phosphodiesterase D activity
DN40556_c1_g1_i1	-0.551	4.68E-02	XP_015429929.1 PREDICTED: ubiquitin carboxyl-terminal hydrolase 14 [Dufourea novaeangliae]	K11843		Protein families: metabolism-Peptidases; Protein families: genetic information processing-Ubiquitin system	F:GO:0005515 ; P:GO:0016579 ; F:GO:0036459	F:protein binding; P:protein deubiquitination ; F:thiol-dependent ubiquitinyl hydrolase activity

Table A.1. continued

DN42011_c22_g1_i1	-0.544	3.59E-02	XP_023706027.1 transmembrane protein 11 homolog, mitochondrial [Cryptotermes secundus]	0				P:GO:0007005; C:GO:0031305	P:mitochondrion organization; C:integral component of mitochondrial inner membrane
DN43605_c6_g1_i1	-0.520	1.75E-02	EFX78317.1 GST-N-Metaxin-like protein [Daphnia pulex]	0				0	0
DN44386_c20_g1_i1	-0. 511	2.72E-02	XP_013191358.1 PREDICTED: vacuolar-sorting protein SNF8 [Amyelois transitella]	K12188	Cellular Processes-Transport and catabolism-Endocytosis	Protein families: genetic information processing-Membrane trafficking; Protein families: signaling and cellular processes- Exosome		C:GO:0000814; P:GO:0071985	C:ESCRT II complex; P:multivesicular body sorting pathway
DN43586_c8_g1_i1	-0.494	3.18E-02	XP_017889657.1 PREDICTED: U1 small nuclear ribonucleoprotein A [Ceratina calcarata]	0				F:GO:0003676	F:nucleic acid binding

18°C vs. 22°C: over-expressed, DESeq2

Transcript ID	Log$_2$FC	Adjusted p-value	Annotation	KO	KAAS Pathways	BRITE Hierarchies	GO IDs	GO Names
DN20024_c0_g1_i1	3.572	1.94E-04	EJY80286.1 VSP domain containing protein (macronuclear) [Oxytricha trifallax]	0			0	0
DN39057_c0_g1_i1	3.170	2.67E-03	CCW72337.1 unnamed protein product	0			0	0

Table A.1. continued

			[Phytomonas sp. isolate Hart1]					
DN37165_c1_g1_i1	3.164	2.67E-03	XP_008297965.1 PREDICTED: tenascin-like [Stegastes partitus]	0			0	0
DN40801_c5_g1_i1	2.863	1.13E-02	KZP03403.1 hypothetical protein FIBSPDRAFT_768999, partial [Fibularhizoctonia sp. CBS 109695]	0			0	0
DN14111_c0_g1_i1	2.753	6.32E-03	XP_013189132.1 PREDICTED: uncharacterized protein LOC106133808, partial [Amyelois transitella]	0			0	0
DN40801_c1_g1_i1	2.732	2.17E-02	CDW75723.1 UNKNOWN [Stylonychia lemnae]	0			0	0
DN45017_c0_g1_i1	2.698	2.74E-02	XP_004032518.1 ubiquitin family protein, putative [Ichthyophthirius multifiliis] EGR30931.1 ubiquitin family protein, putative [Ichthyophthirius multifiliis]	K08770	Endocrine system-PPAR signaling pathway	Protein families: genetic information processing-Ubiquitin system	0	0
DN46648_c0_g1_i1	2.658	2.86E-02	XP_004024028.1 hypothetical protein IMG5_201690 [Ichthyophthirius multifiliis] EGR27144.1 hypothetical protein IMG5_201690	K11252		Protein families: genetic information processing-Chromosome and associated proteins; Protein families: signaling and	0	0

Table A.1. continued

			[Ichthyophthirius multifiliis]				cellular processes-Exosome		
DN32452_c0_g1_i1	2.546	4.46E-02	XP_001433506.1 hypothetical protein [Paramecium tetraurelia strain d4-2] CAK66109.1 unnamed protein product [Paramecium tetraurelia]	K07375	Cellular Processes-Transport and catabolism-Phagosome; Cellular community- gap junction		Protein families: genetic information processing-Chromosome and associated proteins; Protein families: signaling and cellular processes-Cytoskeleton proteins, Exosome	0	0
DN48553_c0_g1_i1	2.494	4.46E-02	AVD68958.1 obstructor F [Cherax quadricarinatus]	0				C:GO:0005576 ; P:GO:0006030 ; F:GO:0008061	C:extracellular region; P:chitin metabolic process; F:chitin binding
DN17549_c0_g1_i1	2.478	4.68E-02	XP_018258600.1 hypothetical protein FOXG_22863 [Fusarium oxysporum f. sp. lycopersici 4287] KNB20555.1 hypothetical protein FOXG_22863 [Fusarium oxysporum f. sp. lycopersici 4287]	0				0	0
DN30852_c0_g1_i1	2.355	4.02E-03	XP_003436050.1 AGAP002186-PB [Anopheles gambiae str. PEST] EGK96211.1 AGAP002186-PB	K20053			Protein families: genetic information processing-Membrane trafficking	F:GO:0005509 ; F:GO:0005515	F:calcium ion binding; F:protein binding

Table A.1. continued

			[Anopheles gambiae str. PEST]					
DN44335_c12_g1_i1	2.278	3.83E-02	WP_110883463.1 hypothetical protein [Gammaproteobacteria bacterium 2W06] PYZ99375.1 hypothetical protein A6K26_009605 [Gammaproteobacteria bacterium 2W06]	0			F:GO:0005515	F:protein binding
DN44335_c9_g2_i1	2.007	1.76E-02	WP_110883463.1 hypothetical protein [Gammaproteobacteria bacterium 2W06] PYZ99375.1 hypothetical protein A6K26_009605 [Gammaproteobacteria bacterium 2W06]	K06777		Protein families: metabolism- Protein phosphotases and associated proteins	F:GO:0005515	F:protein binding
DN42329_c8_g1_i1	1.988	4.46E-02	XP_018013994.1 PREDICTED: spondin-2-like [Hyalella azteca]	0			0	0
DN41548_c0_g1_i1	1.482	3.36E-02	XP_018022073.1 PREDICTED: uncharacterized protein LOC108678215 [Hyalella azteca]	K08145		Protein families: signaling and cellular processes- Transporters	C:GO:0016021; F:GO:0022857; P:GO:0055085	C:integral component of membrane; F:transmembrane transporter activity; P:transmembrane transport

Table A.1. continued

18°C vs. 22°C: under-expressed, DESeq2

Transcript ID	Log₂FC	Adjusted p-value	Annotation	KO	KAAS Pathways	BRITE Hierarchies	GO IDs	GO Names
DN44253_c4_g1_i2	-3.143	2.85E-03	P84293.1 RecName: Full=Hemocyanin subunit 2; AltName: Full=CaeSS2	K00505	Amino acid metabolism-Tyrosine metabolism; Biosynthesis of other secondary metabolites-Isoquinoline alkaloid biosynthesis, Betalain biosynthesis; Endocrine system-Melanogenesis		0	0
DN43047_c4_g2_i1	-3.075	3.57E-04	XP_018011013.1 PREDICTED: uncharacterized protein LOC108668336 [Hyalella azteca]	0			C:GO:0005576 ; P:GO:0006030 ; F:GO:0008061	C:extracellular region; P:chitin metabolic process; F:chitin binding
DN44253_c4_g1_i1	-3.049	4.33E-03	Q6KF81.1 RecName: Full=Pseudohemocyanin-2; Flags: Precursor CAB38043.1 pseudo-hemocyanin, partial [Homarus americanus]	0			0	0

Table A.1. continued

DN36928_c0_g2_i1	-2.637	6.03E-03	XP_015349413.1 PREDICTED: methylmalonate-semialdehyde dehydrogenase [acylating], mitochondrial isoform X1 [Marmota marmota marmota]	K00140	Carbohydrate metabolism-Propanoate metabolism, Inositol phosphate metabolism; Amino acid metabolism-Valine, leucine and isoleucine degradation; Metabolism of other amino acids- beta-Alanine metabolism		F:GO:0004491; P:GO:0055114	F:methylmalonate-semialdehyde dehydrogenase (acylating) activity; P:oxidation-reduction process
DN44464_c1_g2_i1	-2.505	4.46E-02	XP_018021257.1 PREDICTED: ubiquitin-conjugating enzyme E2 Q2-like [Hyalella azteca]	K10582	Genetic Information Processing- Folding, sorting and degradation-Ubiquitin mediated proteolysis	Protein families: genetic information processing-Ubiquitin system	0	0
DN44105_c8_g1_i2	-2.455	2.74E-02	ATU31745.1 calpain-B-like protein, partial [Procambarus clarkii]	K08585		Protein families: metabolism-Peptidases	F:GO:0004198; C:GO:0005622; P:GO:0006508	F:calcium-dependent cysteine-type endopeptidase activity; C:intracellular; P:proteolysis
DN37507_c2_g1_i1	-2.423	3.82E-02	XP_015840144.1 PREDICTED: RNA-directed DNA polymerase from mobile element jockey-like, partial [Tribolium castaneum]	0			0	0

Table A.1. continued

DN42874_c10_g1_i1	-2.344	2.76E-03	ABW77320.1 clottable protein 2 [Penaeus monodon]	0			F:GO:0005319 ; P:GO:0006869	F:lipid transporter activity; P:lipid transport
DN44302_c1_g5_i1	-1.710	7.90E-04	XP_006816303.1 PREDICTED: VWFA and cache domain-containing protein 1-like, partial [Saccoglossus kowalevskii]	0			0	0
DN44146_c12_g3_i1	-1.636	5.05E-02	XP_018027696.1 PREDICTED: uncharacterized protein LOC108682943 isoform X1 [Hyalella azteca]	0			0	0
DN44302_c1_g4_i1	-1.566	3.73E-02	XP_013390170.1 VWFA and cache domain-containing protein 1-like [Lingula anatina]	0			0	0
DN41941_c1_g1_i1	-1.524	5.03E-02	XP_018026550.1 PREDICTED: phytanoyl-CoA dioxygenase domain-containing protein 1 homolog [Hyalella azteca]	0			0	0
DN44146_c12_g2_i1	-1.446	2.13E-02	XP_018027698.1 PREDICTED: uncharacterized protein LOC108682944 [Hyalella azteca] XP_018027699.1 PREDICTED: uncharacterized protein LOC108682944 [Hyalella azteca]	0			0	0

Table A.1. continued

DN40922_c0_g1_i1	-1.337	1.91E-03	XP_018015412.1 PREDICTED: organic cation transporter protein-like [Hyalella azteca]	K08202		Protein families: signaling and cellular processes-Transporters	C:GO:0016021; F:GO:0022857; P:GO:0055085	C:integral component of membrane; F:transmembrane transporter activity; P:transmembrane transport
DN43449_c21_g1_i1	-0.990	4.74E-02	XP_020605164.1 calcium-responsive transcription factor-like isoform X1 [Orbicella faveolata]	0			0	0
DN42866_c15_g1_i1	-0.821	2.88E-02	XP_018019065.1 PREDICTED: uncharacterized protein LOC108675555 isoform X3 [Hyalella azteca]	0			0	0
DN42618_c14_g1_i1	-0.573	7.75E-03	XP_012339503.1 PREDICTED: C-Myc-binding protein isoform X3 [Apis florea] XP_016769903.1 PREDICTED: C-Myc-binding protein isoform X4 [Apis mellifera] XP_016919615.1 PREDICTED: C-Myc-binding protein isoform X3 [Apis cerana] XP_016919616.1 PREDICTED: C-Myc-binding protein isoform X3 [Apis cerana]	0			F:GO:0003713; P:GO:0006355	F:transcription coactivator activity; P:regulation of transcription, DNA-templated

BIOGRAPHY OF THE AUTHOR

Amalia M. Harrington was born in Ann Arbor, Michigan, on March 14, 1988. She was raised in Ann Arbor and graduated from Huron High School in 2006. She attended the University of San Diego and graduated *summa cum laude* in 2010 with a Bachelor of Arts degree in Marine Science. After working as a lab technician for a year, Amalia joined Dr. Kevin Hovel's Marine Conservation Ecology Lab at San Diego State University as a master's student, where she studied the habitat use behaviors and antipredator strategies of juvenile California spiny lobster. She completed her Master of Science degree in Biology in summer 2014, after which she taught *Introduction to Oceanography* at San Diego City College as an Adjunct Instructor and worked as a Scientific Aid at the California Department of Fish and Wildlife. Amalia moved to Maine and entered the Marine Biology graduate program in the University of Maine's School of Marine Sciences in fall 2015. She then joined Dr. Heather Hamlin's lab in fall 2016 where she has focused on understanding how predicted changes in climate will impact the physiology of the American lobster. Amalia is a candidate for the Doctor of Philosophy degree in Marine Biology from the University of Maine in May 2019.